TEXTE
75/2013

Measurement of Fine and Ultrafine Particles from Office Devices during Printing in order to Develop a Test Method for the Blue Angel Ecolabel for Office-Based Printing Devices

Umwelt
Bundes
Amt
Für Mensch und Umwelt

| TEXTE | 75/2013

ENVIRONMENTAL RESEARCH OF THE
FEDERAL MINISTRY OF THE ENVIRONMENT,
NATURE CONSERVATION AND NUCLEAR SAFETY

Project No. (FKZ) 3708 95 301
Report No. (UBA-FB) 001743/E

Measurement of Fine and Ultrafine Particles from Office Devices during Printing in order to Develop a Test Method for the Blue Angel Ecolabel for Office-Based Printing Devices

by

Dr. Mathias Barthel
Dr. Stefan Seeger
Dipl.-Ing. Monika Rothhardt
Dr. Olaf Wilke
Dr. Wolfgang Horn
Elevtheria Juritsch
Dr. Oliver Hahn
Dr. Oliver Jann
Bundesanstalt für Materialforschung und –prüfung (BAM), Germany

On behalf of the Federal Environment Agency (Germany)

UMWELTBUNDESAMT

ISSN 1862-4804

Study performed by: Bundesanstalt für Materialforschung und –prüfung (BAM)
Fabeckstr. 44-46
12203 Berlin, Germany

Study completed in: August 2011

Publisher: Federal Environment Agency (Umweltbundesamt)
Wörlitzer Platz 1
06844 Dessau-Roßlau
Germany
Phone: +49-340-2103-0
Fax: +49-340-2103 2285
Email: info@umweltbundesamt.de
Internet: http://www.umweltbundesamt.de
http://fuer-mensch-und-umwelt.de/

Edited by: Section III 1.3 Eco-design, Environmental Labelling, Environmentally Friendly Procurement
Dr. Jörn-Uwe Thurner

Dessau-Roßlau, August 2013

Report Cover Sheet

1. Report No. UBA-FB

2.

3.

4. Report Title
Measurement of Fine and Ultrafine Particles from Office Devices during Printing in order to Develop a Test Method for the Blue Angel Ecolabel for Office-Based Printing Devices

5. Autor(s), Family Name(s), First Name(s)
Dr. Barthel, Mathias
Dr. Seeger, Stefan
Dipl.-Ing. Rothhardt, Monika
Dr. Wilke, Olaf,
Dr. Horn, Wolfgang
Juritsch, Elevtheria
Dr. Hahn, Oliver,
Dr. Jann, Oliver

6. Performing Organisation (Name, Address)

Bundesanstalt für Materialforschung und -prüfung (BAM)
Federal Institute for Materials Research and Testing (BAM)
Subdivision 4.2
Fabeckstrasse 44-46
D 12200 Berlin, Germany

7. Sponsoring Agency (Name, Address)

Umweltbundesamt, Postfach 14 06, 06813 Dessau-Roßlau

15. Supplementary Notes

8. Report Date
2011-08-31

9. Publication Date

10. UFOPLAN-Ref. No.
3708 95 301

11. No. of Pages
182 + supplemet pages

12. No. of Reference
67 + supplement references

13. No. of Tables, Diagrams
31

14. No. of figures
94 + supplement figures

16. Abstract

The continuous public debate on possible adverse health effects of fine (FP) and ultrafine particle (UFP) emissions from laser printing devices induced the German Federal Environment Agency (UBA) to initiate a research project aimed at developing a test method for particle counting under standard conditions in environmental test chambers. Chemical analysis of the aerosols was another project objective. As an outcome, the quantification of particle emissions was integrated into the test scheme Annex S-M (testing of chemical emissions) of the existing German standard RAL UZ-122 for awarding the German Blue Angel ecolabel to laser printing devices, as well as into the harmonised international test standards ECMA-328 and ISO/IEC 28360. The procedure for aerosol measurement was successfully tested in an international round robin. After approval of these modifications by RAL, the German RAL UZ-122 guideline considered quantitative criteria related to fine and ultrafine particle emissions as well as a respective test procedure for product testing and awarding the Blue Angel ecolabel. As a result of the secondary aim of the project, some particle sources within laser printing devices were identified by the coupling of analytical methods. The identified source contributions, the analysis of the chemical composition of the particles and their size distributions add to the knowledge on these emissions and may enhance the environmental risk assessment in comparison with other aerosol sources.

17. Keywords
office machines, laser printing devices, particle emissions

8. Price

19

20.

List of Contents

List of Figures

Supplementary figures to Chapter 4.1

Supplementary figures to Chapter 4.2

List of Tables

Additional Tables to Chapter 4.1

Preamble

The research project was commissioned by the Federal Environment Agency and supported by means of the Environmental Research Programme as a project for the development of the award criteria for the “Blue Angel” ecolabel for office-based laser printing devices. The project objective was to investigate office devices with a laser printing function, i.e. printers, copiers and faxes and multifunctional devices which are generally referred to in this report as laser printing devices or abbreviated as LPD. Laser printing devices use a laser to create a static electrical charge pattern, which attracts toner onto paper. The toner is then fused by heat to produce black and white or colour prints on paper and other media based on the xerographic principle. Printers, based on other operating principles, such as Inkjet printers were not part of this research project. The studies presented in this report were preceded by two research projects carried out by the BAM Division 4.2 whose results have been published under the numbers 71/03 and 35/08 of the UBA text series. The 2003 report discussed important fundamentals for indoor air quality, test chamber emission measurement and assessment of emissions, and made theoretical considerations for understanding the concentration profiles observed in test chamber measurements. The 2008 report presents the results of investigations conducted on laser printing devices over the period from 2004 to 2007. These were used to revise the test procedure for measuring emissions from hardcopy devices with respect to awarding the “Blue Angel” ecolabel for office devices. The research project on which this report is based focuses on the measurement of particulate emissions in the area of fine and ultrafine particles from laser printing devices. Against the backdrop of a public debate about possible hazards related to these emissions, UBA has commissioned BAM to develop a measurement method for these emissions, to expand the existing awarding criteria for the "Blue Angel" ecolabel by the aspect of particle emissions and to physically and chemically analyse particulate emissions. The resulting awarding criteria will be submitted to RAL later this year. Emission characteristics of laser printing devices, conclusions on awarding criteria and interim results of the project were discussed in three sessions of a project-related expert group.

The members of the expert group included representatives of German testing institutes accredited to RAL-UZ 114, of ECMA, BITKOM and the Federal Environment Agency. The names of all members of this expert group are listed in the Appendix. The members of the expert group have provided helpful guidance to the project, which is gratefully acknowledged.

1 Introduction

1.1 Background and Objectives

In order to improve indoor air quality, it is necessary to reduce gaseous or particulate air pollution. A prerequisite is the identification of sources, including a quantitative, physical and material description of their emissions. Some of the major emission sources of volatile organic compounds (VOC) are furnishing materials, building products, furniture and office equipment. Numerous sources of fine and ultrafine particles (e.g. combustion processes: fireplace, candles, smoking, food preparation) also contribute to a deterioration of indoor air quality (for a review see e.g. Afsari et al. 2005 [1]). The mortality from respiratory and cardiovascular disease increases with increasing particulate concentration, and is generally higher from the finer PM2.5 dust fraction than by the coarser PM10 fraction.[2] Epidemiological studies[3,4] into air pollution by aerosols have provided evidence of a particular activity of ultrafine particles in humans. Indoors, in workplaces and in general in the environment, fine and ultrafine particles are therefore considered potentially hazardous to health. [5,6,7,8]

---

[1] Afshari A., Matson U., Ekberg L. E.: Characterization of indoor sources of fine and ultrafine particles: A study conducted in a full-scale chamber, Indoor Air (2005) 15 p141–150

[2] Rödelsperger K., Brückel B., Podhorsky S., Schneider J.: Abschlussbericht zum Projekt F 2075 „Charakterisierung ultrafeiner Teilchen für den Arbeitsschutz – Teil 2“ im Auftrag der Bundesanstalt für Arbeitsschutz und Arbeitsmedizin (2009)

[3] Wichmann H. E., Heinrich J., Peters A.: Gesundheitliche Wirkungen von Feinstaub. In: Wichmann H. E., Schlipköter H. W., Fülgraff F. (Hrsg.) „Fortschritte in der Umweltmedizin“.Ecomed-Verl.-Ges. (2002)

[4] Wichmann H. E.: Epidemiologie ultrafeiner Teilchen. BIA-Report. St. Augustin. HVBG (2003) p53-86

[5] Abt E., Suh H., Allen G. und Koutrakis P.: Characterization of Indoor Particle Sources. Environ. Health Perspect. (2000) 108 (1) p35–44

[6] Ibald-Mulli A., Wichmann H.-E., Kreyling W. and A. Peters, A.: Journal of Aerosol Medicine (2002) 15(2) p189-201

[7] Bundesgesundheitsblatt - Gesundheitsforsch - Gesundheitsschutz (2008) Springer Medizin Verlag

[8] M Politis M. et. al.: Global NEST Journal, (2008) Vol. 10, No 3, p439-452

Aerosol emissions from office devices, or from laser printing devices in the strictest sense of this study, have been described for several years in a number of papers.[9,10,11,12,13,14] At the same time, clues and evidence for potential impairment to the health of exposed people are being sought.[15,16,17,18,19,20] Self-help organisations and suppliers of retrofit protective equipment claim – with various arguments – a

---

[9] Bake D., Moriske H.-J., Untersuchungen zur Freisetzung feiner und ultrafeiner Partikel beim Betrieb von Laserdruck-Geräten, Umweltbundesamt UBA, (2006)

[10] Seeger S., Wilke O., Bücker M., Jann O.: Time- and Size-Resolved Characterization of Particle Emissions from Office Machines. Proc. Int. Conf. Healthy Buildings (2006), Lisboa, Portugal, Vol. II p447-450

[11] Wilke O., Jann O., Brödner D., Schneider U., Krocker CH., Kalus S., Seeger S., Bücker M.: Prüfung von Emissionen aus Bürogeräten während der Druckphase zur Weiterentwicklung des Umweltzeichens Blauer Engel für Laserdrucker und Multifunktionsgeräte unter besonderer Berücksichtigung der Sicherung guter Innenraumluftqualität, Forschungsbericht: Umweltforschungsplan des Bundesministeriums für Umwelt, Naturschutz und Reaktorsicherheit - Förderkennzeichen (UFOPLAN) 204 95 373 / UBA-FB 001159 - Abschlussbericht 35 (2008) 8, p1-164; Hrsg.: Umweltbundesamt (UBA) ISSN 1862-4804

[12] Schripp, Wensing, Uhde, Salthammer, He, Morawska: Evaluation of Ultrafine Particle Emissions from Laser Printers Using Emission Test Chambers Environ. Sci. Technol. 42, (2009) p4338–4343

[13] Schripp, Mulakampilly, Delius, Uhde, Wensing, Salthammer, Kreuzig, Bahadir, Wang, Morawska: Comparison of ultrafine particle release from hardcopy devices in emission test. Gefahrstoffe - Reinhaltung der Luft 69(3) (2009) p71-76

[14] Morawska, He, Johnson, Jayaratne, Salthammer, Wang, Uhde, Bostrom, Modini, Ayoko, Mcgarry, Wensing: An Investigation into the Characteristics and Formation Mechanisms of Particles Originating from the Operation of Laser Printers. Environ. Sci. Technol. 43 (2009) p1015–1022

[15] Gallardo M., Romero P., Sanchez-Quevedo M. C., Lopez-Caballero J. J.: Siderosilicosis due to photocopier toner dust, The Lancet Vol. 334 (1994)

[16] Smola, Georg & Hohensee, Gesundheitsgefahren durch Laserdrucker. Gefahrstoffe - Reinhaltung der Luft 62, (2002) p295-301

[17] Siegmann, S., Jansing, P.-J.: Innenraumbelastung durch Laserdrucker und Fotokopiergeräte, Prakt. Arb. Med 2: 6-11 (2005)

[18] Kagi N. et al.: Indoor air quality for chemical and ultrafine particle contaminants from printer Building and Environment 42 (2007) p1949–1954

[19] Mersch-Sundermann et. al.: Evaluierung möglicher Beziehungen zwischen Emissionen aus Büromaschinen, insbesondere aus Fotokopierern und Laserdruckern, und Gesundheitsbeeinträchtigungen bzw. Gesundheitsschäden bei exponierten Büroangestellten, Abschlussbericht Projekt UFO-Plan FKZ 705 62 449, Bundesinstitut für Risikobewertung (BfR), Berlin, (2007)

[20] Presseerklärung BfR 07/2008 vom 18.04.2008, BfR schließt gesundheitliche Beeinträchtigungen durch Emissionen aus Büromaschinen nicht aus, BfR 2008, http://www.bfr.bund.de/cd/11029, siehe auch: Gesundheitliche Bewertung Nr. 014/2008 des BfR vom 31. März 2008

relationship between particulate emissions from laser printing devices and health impairment, including occupational disability, of people exposed to them.[21]

A comparative analysis of the literature with regard to significant data and findings for evaluating particle emissions from laser printing devices is hindered by the following aspects:

- Measurement conditions are poorly documented, not comparable or not transferable.
- Test scenarios and conditions vary from in-situ measurements in copy centres and offices to standardised tests in emission test chambers.
- Aerosol measurement techniques and quantities used (mass- or number-based) are not uniform or not comparable.
- Type, construction materials and age of office devices and toner materials used vary. The available literature covers a total of at least 15 years of development history of laser printing technology.
- Many studies deal with a few devices as individual cases, only a few are devoted to systematic comparisons of dissimilar laser device pools.

However, a few important facts were known when the project started: [9,10,11,12,13, 14]

- Laser printers emit aerosols in the border area between ultrafine and fine particles. Maximum particle diameters of the number-based particle size distributions are usually between 5 and 300 nm.
- Toner particles with diameters > 1 µm, as they are available as powder in the toner cartridges, do not contribute practically to the number of emitted particles. The occasional rumoured scenario of a massive direct release of toner powder as "toner dust" during normal operation is not in agreement with the results of relevant aerosol emission measurements.

Against this backdrop, UBA initiated the research project reported here to look into the nature of particulate emissions and update the award criteria RAL-UZ-122 of the Blue Angel ecolabel for office devices in this regard. The award criteria of the Blue Angel

---

[21] Stelting H.-J.: Krank durch Toner – Erfahrungen mit einer Nanopathologie, Umweltmed Forsch Prax 11 (5) (2006) p329 – 337

ecolabel (RAL-UZ) are being regularly updated. Labelling of office-based printing devices with the Blue Angel has been possible since 1996. The use of the label is voluntary and must be applied for by the holder at RAL (German Institute for Quality Assurance and Certification e.V.). Specific requirements stipulated in the award criteria with which it must comply. For printers the award criteria RAL-UZ-85 was formerly valid, RAL-UZ-62 for copiers and RAL-UZ-114 for multi-functional devices. The award criteria were published in 2003 together with a new test method and were valid until end of 2006. From June 2006, new award criteria for office devices with print function (RAL-UZ-122) and an updated test method with adjusted allowable emission rates were introduced which aggregated and replaced the old award criteria from January 2007. Standard ECMA-328, first published in 2001 by the ECMA (European Computer Manufacturer Association), which also contained the determination of emissions from electronic devices, was harmonised with RAL-UZ-122 from 2006. The resulting standard ECMA-328, 2nd Edition, was used as a template for the ISO/IEC Standard 28360 from September 2007.

The currently valid award criteria deal with the material emissions TVOC, ozone, benzene, styrene and gravimetrically measurable dust. A more precise detection of ultrafine and fine particle emissions requires a metrological and methodological improvement. For the current study, key findings of a BAM research project were used (UBA research report, Wilke et al. 2008):

- The comparable detection of emissions of fine and ultrafine particles from office devices requires a special test method with specified conditions. This is a prerequisite to set limiting requirements in the context of the Blue Angel ecolabel and to check their compliance.
- The first comparative studies on particle emission behaviour of laser printing devices under standardised test conditions in emission test chambers appeared to make feasible the integration of particle emission measurement into the award criteria UZ 122 to supplement the existing test procedure. A separate test did not appear necessary.

1.2 Objectives

Based upon this project the following main topics have been set:

a) Detailed characterisation of particulate emissions from laser printing devices:

- Chemical characterisation of particulate emissions from office devices and identification of their sources.
- Physical characterisation of particulate emissions from office devices during the prepress and printing phase in terms of size distribution, mass and number concentrations, dynamics and dispersal behaviour.
- Comparative measurements to determine the emission behaviour of various brands currently available on the market to assess the relevance of particulate emissions.
- Investigation of the ageing behaviour of printing devices in terms of particulate emissions by repeated measurements on selected devices, which also form a reference pool.

b) Further development of test standards for the measurement of particulate emissions:

- Clarification of the influence of methodological factors on particle measurements using different aerosol devices and in emission test chambers of different sizes and types
- Comparison of printers with different emission behaviour
- Comparison of different methods of data analysis
- Developing a proposal for the integration of particle emission measurement in the current award criteria RAL-UZ 122 and a proposal for appropriate measurands
- Integration of the characterisation of particulate emissions in emission test chambers into ECMA-328 and ISO 28 360

c) Quality assurance:

- Establishment of a reference pool of selected printing devices. This will create an additional way to confirm the reliability of test results and facilitate comparative measurements with other measuring institutes.
- Designing comparative measurements with other measuring institutes.

2 Methods and Equipment

2.1 Emission Test Chambers

Emission test chambers enable the reproducible measurement of substances emitted from a material into the air under standardised and to a large extent constant test conditions. Studies within this project used 1 m³ and 5 m³ emission test chambers with the same standard environmental conditions (T = 23 °C and 50 % relative humidity). In order to determine the emission behaviour of volatile organic compounds in small concentrations down to the lower µg m^{-3} range, the emission test chambers must not only satisfy the usual climate parameters, air exchange rate and air flow velocity, but also a number of further specialist requirements. In particular:

- Extremely inert chamber walls of glass or polished high-grade steel to minimise wall effects
- Efficient air mixing
- Minimise sealant materials capable of causing intrinsic emissions and adsorption and desorption effects
- Ability to clean the chamber, for example through baking
- High-purity air and water supply with low VOC and dust content

These requirements are equally fulfilled by both chambers. In addition, the precise and virtually background-free measurement of particle number concentration to determine FP and UFP emissions from about 5 nm particle diameter raises prerequisites on the blank value of the particle number concentration and thus on the quality of high-purity air supply.

The reason for choosing extremely inert chamber wall materials is to keep adsorption effects on them to a minimum so that pollutant concentration in the air is not influenced by so-called wall effects. In addition to influencing pollutant or particle concentration in the air during emission measurements, wall effects can impair subsequent investigations in the form of memory effects from the preceding measurements.

Both test chambers were equipped with the same high-purity air supply system. High-purity air was provided by an oil-free compressor in which a downstream cleaning unit removed moisture, VOC, dust and fine and ultrafine particles from the compressed air. The cleaning unit (Ultrafilter Oilfreepac) consists of a pre-filter (dust and aerosol separation), air drying (heatless dryer - silica gel with automatic regeneration), activated carbon cartridge for VOC absorption and a fine filter and an postfilter (submicrofilter < 0.01 µm, degree of separation 99.99999 %) to retain both FP and UFP from the ambient air and abraded activated carbon particles. Various humidification principles were used in the two chambers. High-purity water was used for humidification which was obtained from desalinated water. In the case of 1 m³ chambers the water was sent through a postcleaning unit (EASYpure UV D 7402) for further desalination and removal of possible organic compounds. An overview of the parameters in the emission test chambers is given in Table 1.

Table 1: Parameters of the emission test chambers used

Parameter	Unit	1 m³ chamber	5 m³ chamber
Volume (V_c)	m³	1.00	4.98
Test space dimensions (W, H, D)	mm	750, 750, 1778	2400, 1700, 1220
Wall material		High-grade steel, polished	
Temperature (T)	°C	23 ± 2	
Relative humidity (R. H.)	%	50 ± 5	
Air exchange rate (n)	h^{-1}	(1 – 4) ± 5 %	(1 – 2) ± 5 %
Air flow velocity	$m\ s^{-1}$	0.1 – 0.3	0.1 – 0.3
Air supply		High-purity air	

1 m³ chamber

A standard VOC emission test chamber from the firm Vötsch Industrietechnik GmbH was used as the 1 m³ emission test chamber in this project. It conforms to DIN ISO 16000-9 and has been extensively reported in the literature.[22] The interior test space is made of high-grade steel with low surface roughness and no joints. The test space fan used for air circulation is driven from the outside using a magnetic clutch. Air conditioning in the chamber is performed using a thermally regulated blanket and condensation point humidification. Contacts and openings in the chamber wall enable

---

[22] Meyer U., Möhle K., Eyerer P., et al.: Entwicklung, Bau und Inbetriebnahme einer 1 m³-Bauteilmesskammer zur Bestimmung von Emissionen aus Endprodukten. Staub - Reinhaltung der Luft 54 (1994) p137 - 142

electrical connections and the entry of sensor cables. A slight overpressure in the test space prevents contamination from entering the chamber. To regenerate the chamber a heating system is available which eliminates memory effects through thermal desorption at up to 240 °C (baking). The surface of the walls and fittings, which in principle are capable of adsorption of semivolatile compounds, is approximately 7 m².

Detail view: test chamber with a printer, door open.

Figure 1: 1 m³ emission test chamber, complete measurement station

<u>5 m³ chamber</u>

The 5 m³ chamber shown in Figure 2 enables large devices to be tested. It conforms to DIN ISO 16000-9 and was used for comparing measurements in the 1 m³ chambers to investigate the influence of the chamber size on the characteristics of particle emissions from laser printing devices.

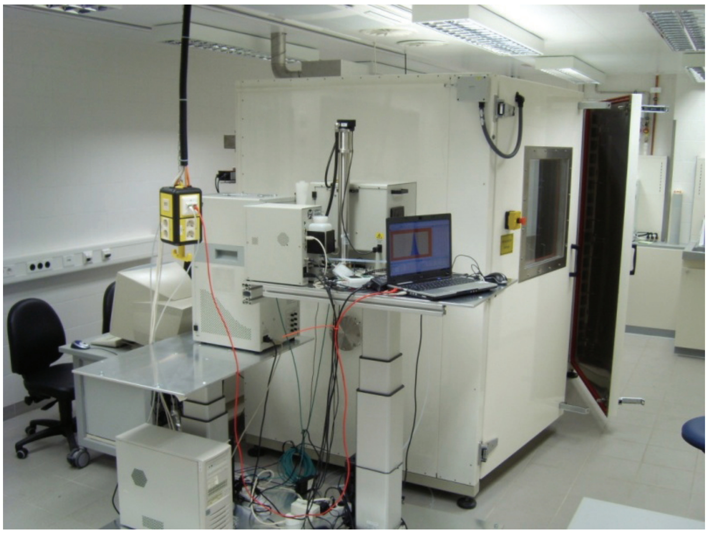

Figure 2: 5 m³ emission test chamber with double door, complete measuring station

The emission test chamber was manufactured by TIRA Umweltsimulation GmbH. The interior test space is made of high-grade steel with low surface roughness and no joints. Humidification and dehumidification of the chamber is achieved via a saturated steam supply and dry air flow. The temperature is controlled via a thermally regulated blanket with a water-flow plate heat exchanger and electrical heating elements. Contacts and openings in the chamber wall enable electrical connections to be made and entry of sensor cables into the test space. A slight overpressure in the test space prevents contamination from entering the chamber. Air circulation takes place through the high-purity air supply. If required, a mobile air circulation module can also be operated in the test space. The air circulation module consists of an electrically driven fan in a stainless steel housing which is steplessly variable from the outside. No increase in the background to FP/UFP was found due to operation of the fan module. To regenerate the chamber, a controllable electric baking module is fitted in the test space which can reach a maximum temperature of 300°C.

2.2 Climate measurement

Climate measurements were carried out using factory-calibrated devices. Climate sensors combined with dataloggers of various types from the ALMEMO Company were used as external measurement instruments. This enabled continuous measurements at different measuring points.

Measurement accuracy of climate sensors

Moisture sensor Type FH A 646-R	
Range of measurement	5 % to 98 % R. H.
Maximum linearity deviation	± 2 % R. H.
Operational temperature	- 30 °C to +100 °C
Nominal temperature	25 °C ± 3 K
Temperature sensor	NTC Type N
Accuracy	0 °C to 70 °C ± 0.1 K
Air pressure sensor Type FD A 612 MA	
Range of measurement	0 mbar to 1050 mbar
Accuracy	± 0.5 % (typical ± 0.1 % of end value)
Operational temperature	25 °C ± 3 K

2.3 Measurement of Dust, Fine and Ultrafine Particles

The gravimetric method has so far been used as a conventional method for determining dust emission rate within the award guideline UZ-122 of the Blue Angel for office devices with printing function. This method is primarily effective for fine dust > 1 µm particle diameter. Dust emissions from office laser printing devices as gravimetrically determined at BAM in an earlier UFOPLAN research project were very low. None of 30 different desktop printing devices and 27 freestanding printers exceeded the limiting value of 4 mg/h. 51 out of 57 devices emitted even less than ¼ of this threshold.[10]

If ultrafine, fine and possibly even coarse particles occur together in an aerosol, the ultrafine particles in particular cannot be quantitatively detected gravimetrically due to their low contribution to the total mass of particles – definitely not with the accuracy and distinction sharpness required for an award criterion. The total mass in an aerosol consisting of UFP only may be too little to be measured gravimetrically; the required deposition on a carrier medium (filter, impactor substrate) must also be performed with a high and known efficiency. The gravimetric method is not continuous and cannot detect rapid changes over time. Thus gravimetry does not represent an appropriate method to quantify the relative dominant fraction of UFP and FP emitted from laser printing devices.

The methods for measuring a time-dependent FP/UFP concentration can be grossly different with regard to their operating principles:[23]

- Counting of scattered light pulses caused by particles
- Measuring the electric charge carried by particles

They differ from each other in terms of particle size range, the detectable particle number concentrations and time resolution. In addition to particle counters, particle spectrometers are used in which particle count and size classification are combined. Thus the measurement of number-based size distributions is possible. Particle spectrometers also differ in size resolution, i.e. the number and range of the particle size classes. In this research project, different aerosol measurement instruments, to be described below, were used to determine the suitable devices for the quantification of FP/UFP emissions from office devices.

2.3.1 Aerosol Measuring Instruments

Here only a brief description of the operation and performance will be given. Detailed descriptions can be found in the literature[23] or manufacturer's information.

Laser Particle Counter (OPC, Optical Particle Counter)

A 1.108 type OPC from Grimm Labortechnik was used. The particles contained in the air pass through a measurement chamber at a specified flow rate (1.5 l/min) and are irradiated with monochromatic laser light. By analysing the scattered laser light, the scattered light diameter of each particle is determined and recorded in one of 15 size classes. The midpoints of the size classes are: 0.3, 0.4, 0.5, 0.65, 0.8, 1, 1.6, 2, 3, 4, 5, 7.5, 10, 15 and 20 µm. By measuring the frequency of particles in the size classes in rapid succession – i.e. typically every 6 seconds – snapshots of the number-based particle size distribution are created in an aerosol. The maximum measurable number concentration is 2×10^3 particles/cm³.

---

[23] Baron P., Willeke K.: Aerosol Measurement – Principles, Techniques and Applications, 2nd Edition Wiley Interscience, (2005)

Scanning Mobility Particle Sizer (SMPS)

The type 3936 particle spectrometer from TSI Inc. used in this study, classifies particles according to their electrical mobility in an electric field. A polydisperse aerosol is drawn at a constant flow rate (0.3 or 1.5 l/min). By irradiation with radioactive β-emitters (Kr-85), a specified bipolar electrical charge distribution is generated in the aerosol at the device entry. The polydisperse particles are conducted in a laminar air flow at a constant velocity through the size classifier (DEMC, differential electrical mobility classifier). In DEMC – depending on the field direction – either positively or negatively charged particles make a radial drift towards a central electrode in a radially symmetrical electric field which is perpendicular to the flow direction. Thus, the particle trajectories are influenced so that, depending on the electric field strength, a particle fraction with a specified electrical mobility is selectively directed through an exit opening to a particle counter. A periodic change of field strength enables the scanning of up to about 100 logarithmically distributed particle size classes one after the other (up to 32 size channels per decade) in minutes. A separate condensation particle counter (CPC, see below) is usually used as a counting unit in SMPS. Especially in very rapidly changing aerosols, the slow scanning speed is a disadvantage: very fast processes can scarcely be detected. The fact that particles of different size classes are never measured collectively, rather sequentially, i.e. at different times, can lead to a distortion between measured and true particle size distribution. The particle size range of a SMPS is variable and is typically between a few nm and 1 µm. The measurement range of the number concentrations depends on the separate particle counter used.

Fast Particle Spectrometer

At BAM, two device variants from the TSI Inc. company are available which can be described as fast mobility particle sizer (FMPS, Type 3091) and Engine Exhaust Particle Sizer (EEPS, Type 3090). These devices combine size classification of particles according to their electrical mobility with particle counting via measurement of the electric charge transported on electrodes. At the device inlet, a unipolar electrical charge distribution is generated in the aerosol via a two-stage ionizer (corona charger). The aerosol is then directed in a laminar flow rate of 10 l/min through a column. In the column, 22 ring electrodes are arranged concentrically around cylindrical central electrodes staggered above each other. Each of the ring electrodes separates particles with a specific electrical mobility. This is achieved by appropriate electric field strengths between the ring and central electrodes. The aerosol passes through the column so quickly that all stages are deposited almost simultaneously. From the individual measurement signals a number-based size distribution is calculated in 32 logarithmically distributed size channels.

Condensation Particle Counter (CPC)[23]

CPCs are used as particle counters and are not able to classify particles by size. A similar technique as in OPCs is used. Larger particles from about 250 nm in diameter can be optically counted directly when passing a laser detection sensor. Smaller particles cannot be directly counted in this way because of the very limited scattered light signal. To achieve a high counting efficiency over a wide size range for UFP and small FP, the aerosol in a CPC is first passed through a zone of saturated vapour (saturator). As condensation nuclei, smaller particles in particular increase rapidly by the addition of condensed liquid to a few µm in diameter. Then this size fraction can also be optically measured. When using a CPC as a counting unit in a SMPS, control software ensures that the data from size classifications in the DEMC and concentration measurement in the CPC are attributed correctly. CPCs as stand-alone devices can measure the total time-dependent concentration of an aerosol integrally within a type-dependent particle size range. Water (W-CPCs), butanol (B-CPCs) or isopropyl alcohol (I-CPCs) are used as working fluids. In this study, W-CPCs and B-CPCs from different manufacturers were compared. CPCs measure in the lower concentration range in the so-called single-count mode (SC). At medium concentrations the test signal is continuously corrected and at high concentrations, CPCs switch over to the so-called photometric mode (PM), in which no single scattered signals are recorded, but a sum signal is evaluated.

Table 2: Parameters of the aerosol measurement devices used

Measurement device	**SMPS**	**EEPS** **FMPS**	**OPC**	**CPCs**		
Manufacturer / type	TSI 3936	TSI 3090 TSI 3091	Grimm 1.108	Grimm 5.414	TSI 3785	TSI 3775
Work liquid	-	-	-	Butanol	Water	Butanol
Test flow rate [l/min]	as CPC	10	1.2	0.3 (0.6)	1	1.5 (0.3)
Size range approximate data [nm]	5 - ≤1000	5.6 - 560	300 - 20000	4 - >3000	5 - >3000	4 - >3000
Size resolution [class / decade]	32	16	15	-	-	-
Concentration range [1/cm³]	1 – 10E8	min. 5E3 max. 1.5E8 channel-dependent (EEPS)	< 2E6	SC 0 – 1E5 PM 1E5 -	SC 0 – 10E4 PM 1E4 – 1E7	SC 0 – 5E4 PM 5E4 – 1E7
Measurement error	as CPC	N/A	N/A	SC: ±10 % PM: ±20 %	SC: ±10 % PM: N/A	SC: ±10 % PM: ±20 %
Measurement frequency / scanning time [seconds]	≤ 120	0.1 (EEPS) 1 (FMPS)	6	1	1	1

SC: Single Count Mode, PM: Photometric Mode

2.3.2 Methods and Tools of Qualitative Analysis

Samples for qualitative analysis methods were generated in the 1 m^3 emission test chamber in accordance with the procedure described in Annex S-M. In each case, it was printed using the monochromatic mode on standard paper (80 g/m^2, water content: 3.8 - 5.6 %, manufacturer: X'tensa). In the case of XRF measurements, the allocation of the substrates was carried out in two successive 10-minute printing processes to achieve an improved signal-to-noise ratio. The particle number concentration vs. time curves and climate parameters, power consumption of the LPD and temperature of the printed paper were always recorded.

Cascade Impactor

In addition to the particulate emissions tested in this study, laser printers emit VOCs and SVOCs. This fact raises special conditions on the experimental procedure, since certain sampling techniques let the emitted gaseous VOCs and SVOCs condense on the substrates. In these cases it is not possible to distinguish whether an identified compound was emitted in gaseous or particulate form. In contrast, the sampling technique used here enables this distinction with the help of a cascade impactor. Due to the geometry of the cascade impactor used in this study (DLPI 10, Dekati, Finland), particles are separated exclusively, while gaseous emissions follow the streamlines and cannot condense on the substrates.

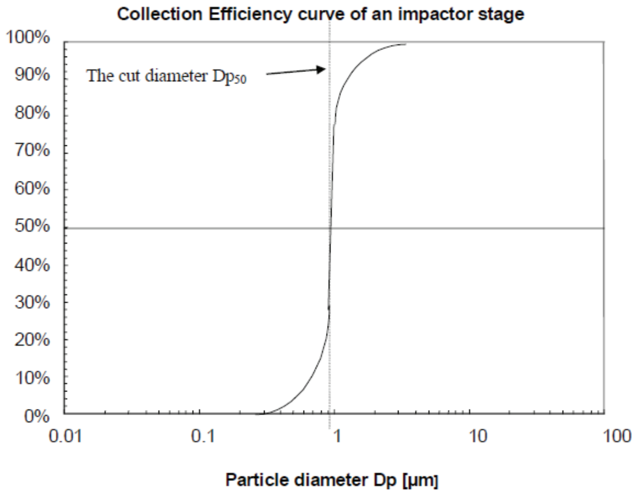

Figure 3: Schematic illustration of the separation efficiency of a cascade impactor stage with a cut point of 1 µm

Figure 3 shows a typical separation efficiency curve for a cascade impactor stage with a cut point of 1 µm. Depending on the subsequent analysis method, the cascade impactor was fitted with different substrates of high-purity aluminium or polycarbonate film to minimise background signals.

The sampling takes place using a vane-type rotary pump wherein the flow rate is adjusted by means of a ball valve and a pressure gauge to 10 l/min. The resulting cut points for the 13 cascade impactor stages are displayed in Table 3:

Table 3: Cut points of cascade impactor stages for a flow rate of 10 l/min

Cascade impactor stage	**13**	**12**	**11**	**10**	**9**	**8**	**7**	**6**	**5**	**4**	**3**	**2**	**1**
Cut point d_{50} (µm)	10	7	4.3	2.7	1.8	1.1	0.65	0.40	0.27	0.16	0.10	0.06	0.03

Micro X-Ray Fluorescence Spectroscopy (µXRF)

The aerosol samples as well as toner, paper and plastic samples from the vicinity of the laser printer fuser unit were analysed by means of a mobile energy dispersive micro-X-ray spectrometer (ArtTAX®, Bruker Nano GmbH, previously Röntec GmbH, Berlin, Germany). The device consists of an air-cooled low-power molybdenum tube, a polycapillary X-ray optics (diameter of the investigated sample area: 100 µm), an electro-thermally cooled XFlash detector and a CCD camera with alignment laser for sample adjustment. The optional helium purging of the excitation and detection beam paths for the detection of light elements has not been used in order to prevent inadvertent removal of the deposited particles. In this operating mode the design enables the detection of elements with $Z > 13$

The silicon drift detector has an energy resolution of 160 eV for the Mn-K_α line at a count rate of 10 kcps. It has an active surface area of 30 mm^2 and consists of an 8-µm thick DuraBeryllium window. The angle geometry between the primary beam, sample and the detector is 0°/40° relative to the normal of the sample surface. All measurements were performed by a 30 W low-power molybdenum tube (50 kV, 600 µA) and a measuring time of 60 s (live time) to minimise the risk of radiation damage to the sample.

In the present study, for each cascade impactor stage with analysable particle amounts, 4 spectra were taken via a deposition spot and then averaged. The XRF spectra obtained as such within an energy range up to 30 keV reflect an average element composition of the deposited particles. In contrast to individual particle analysis, accidental contamination being incorrectly attributed to the particle emissions will be avoided.

Gas Chromatography/Mass Spectrometry (GC-MS)

To ensure background-free sampling using a cascade impactor is attained, impurities in the substrates used must be excluded. In the case of GC-MS analysis, high-purity aluminium substrates were used. Previous studies have shown that contaminants in the form of phthalates and siloxanes from the manufacturing process or storage in plastic containers play a role here. To eliminate these impurities the substrates were initially treated in acetone for 15 min. in an ultrasonic bath and then baked for 30 minutes at 320 °C. The treated substrates are free of volatile organic contaminants.

The analysis of aerosol samples was performed using a thermodesorption GC-MS unit equipped with a cold feed system. The aluminum substrates were transferred in glass sorbent tubes stage-wise from the cascade impactor and held by stainless steel frit in the appropriate position. The sorbent tubes and the stainless steel frit were previously cleaned in acetone for 10 minutes in an ultrasonic bath and then baked as per DIN ISO 16000-6 for 10 minutes at 320 °C under a helium purge gas at a flow rate of 100 ml/min. The sample application was carried out using the thermodesorption unit

(Gerstel TDS 3) at an initial temperature of 40 °C (3 minutes) followed by heating with a temperature gradient of 60 °C/min to a temperature of 200 °C which was held for 7.5 minutes.

The GC oven temperature programme was started at an initial temperature of 40 °C (holding time 1 minute) which enabled an optimum separation of the components. This is followed by heating at a gradient of 15 °C/min to 310 °C (holding time 15 minutes) and finally, another heating at a gradient of 5 °C/min to a temperature of 320 °C which is held for another 5 minutes. The total running time of the temperature program using an Rxi-5MS column (30 m x 0.25 mm x 1 µm) was 41 minutes.

Individual plastic samples, the paper used and toner samples were extracted by thermal extraction, first in glass sorbent tubes filled with Tenax TA and stainless steel frit and then delivered to the TD-GC-MS. For thermal extraction a temperature of 180 °C was selected to simulate the minimum temperature in the vicinity of the fuser unit. The sample application and GC analysis was carried out in analogy of the analysis of aerosol samples.

For the detection of brominated compounds in the plastic samples, a modified procedure was used. The plastic samples were first extracted for 30 minutes in toluene in an ultrasonic bath. In the gas chromatographic analysis, a DB-5MS column (30 m x 0.25 mm x 0.25 µm) was used. The temperature programme applied was started for 0.2 minutes at a temperature of 110 °C followed by heating to 200 °C at a temperature gradient of 30 °C/min. Further heating to 300 °C was performed with a reduced gradient of 20 °C/min and the final temperature of 300 °C was held constant for 15 minutes.

The detection of brominated compounds in the printer aerosols was performed by means of a wet chemical extraction of the substrates using dichloromethane. Samples were applied via a cold feed system (Gerstel KAS 4) and the temperature programme was started at a temperature of 60 °C (0.1 min). Heating to 280 °C followed (3 min) and then to 345 °C (3 min) with a temperature gradient of 600 °C/min. A DB5-MS column (10 m x 0.25 mm x 0.25 µm) in conjunction with the GC-MS unit (GC: Agilent 6890; MS: Agilent 5975C) was used. The oven temperature programme started at an initial temperature of 70 °C (1 min) followed by heating to 300 °C with a gradient of 20 °C/min

(7.5 min) and then to 345 °C (2 min). Mass spectrometric detection was performed by electron impact ionisation and the unit was operated in SCAN/SIM mode.[24]

Thermoconditioner

To examine the volatility of the emitted particles and to quantify the potential solid contributions to the aerosol, particle concentration measurements using a butanol-based CPC (*TSI 3775*) and an upstream rotating disk diluter with a thermoconditioner (*TSI/Matter 379020A-30*) were carried out at room temperature and 400 °C. The use of a rotating disk diluter before the thermoconditioner ensured that vaporised volatile elements did not recondense during cooling in the path to the CPC. Examples of heating the aerosol, with and without prior dilution are shown schematically in Figure 4.

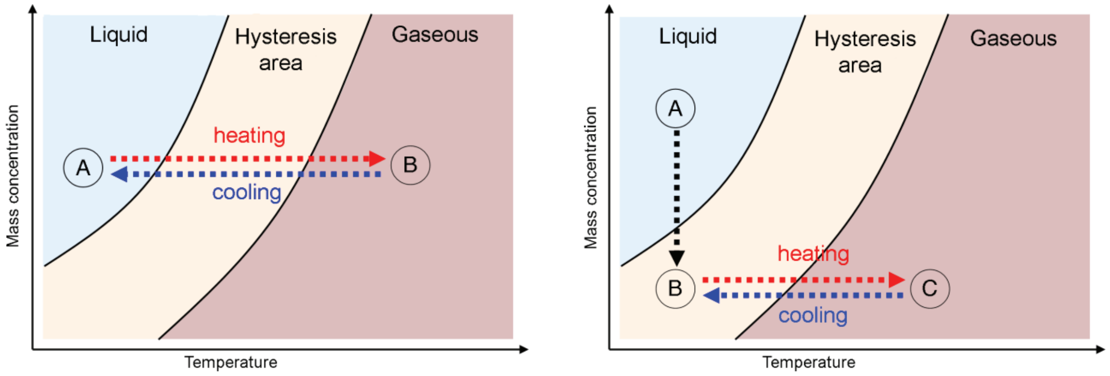

Figure 4: Schematic illustration of the phase transitions of the vaporisable ultrafine particles when using the thermoconditioner.

Due to a lack of precise knowledge about mass concentrations of the organic compounds to be vaporised, no comment can be made about the necessary dilution. The presence of case B can be confirmed for this investigation after conducting a temperature series.

The rotating disk diluter was operated in the measurements at room temperature with a dilution factor of 125 to ensure the operation of the CPC in single counter mode. The measurements at 400 °C were carried out using a dilution factor of 13 to remain above the detection limit of CPC at low particle concentrations.

---

[24] Written information: Mechlinski A.; PiCA Prüfinstitut Chemische Analytik GmbH, Berlin (2011)

3 Selection and Properties of the Investigated Office Devices

3.1 Selection of Office Devices

At the first meeting of the project's expert group on 27.02.2009, the Federal Association for Information Technology, Telecommunication and New Media (BITKOM) presented a list which contained 82 LPD (laser printer devices) from 13 manufacturers. The list contained both monochrome and colour multifunction devices (printing, scanning, faxing, copying) and printers with a very wide performance range (see Figure 5). The terms of the UFOPLAN project required a selection to be made.

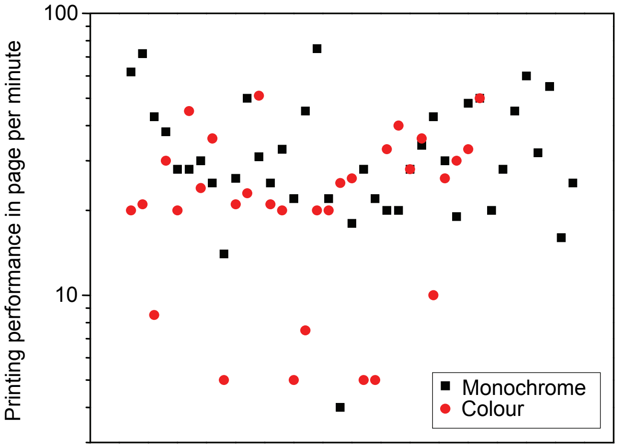

Figure 5: Overview of the printing performance of the BITKOM device list

For the project, a pool of 10 LPD was selected, hereafter referred to as BAM pool. Figure 6 shows the relative performance distribution, measured as printing speed for monochrome and colour LPD of the BITKOM list. Within this project it was not possible to create a representative selection of the entire performance range, instead, the BAM pool was formed from LPD with a printing performance of up to 34 pages per minute. The printing performances of the LPD from the BAM pool are shown as vertical bars in the diagrams of Figure 6. The BAM pool represents more than 50 % of the performance spectrum of the BITKOM list for both printing modes.

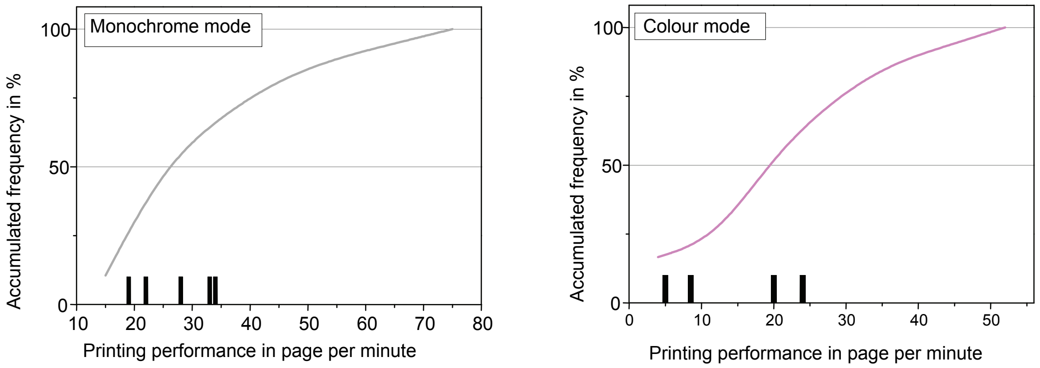

Figure 6: Overview of the printing performance for monochrome and colour office devices of the BITKOM list. Black bars indicate the devices of the BAM pool.

3.2 Device Properties

The technical data of the LPD are summarized in the table below.

Table 4: Technical data of the BAM pool

LPD	**Type**	**Manu-facturer**	**Volume** (m³)	**Printing speed** Pages/minute Colour	Monochrome	**Type of ventilation**
1	Printer	A	0.09	20	20	N/A.
2	MFD	B	0.09	5	24	N/A.
3	Printer	C	0.04	-	25	Blower
4	Printer	A	0.05	-	32	Suction
5	Printer	D	0.04	-	18	Blower
6	Printer	E	0.05	7.5	7.5	N/A.
7	Printer	B	0.08	-	33	Blower
8	Printer	F	0.09	21	21	Blower
9	Printer	G	0.03	-	23	Blower
10	MFD	A	0.11	-	21	Blower

MFD: multifunction device; A, B, C, D, E, F, G: manufacturer code

The individual devices have small to medium volumes and meet all the requirements of UZ-122 for tests in a 1 m³ chamber. The *blower* type ventilation indicates air actively expelled by a fan from at least one housing opening. Accordingly, the *suction* type ventilation includes at least one housing opening where air is actively drawn in by a fan. Devices marked with N/A do not exhibit active ventilation from the outside during operation. It should be emphasised at this point that LPD do not necessarily need active ventilation. [25]

The imaging components in LPD, particularly the fuser units and the toner systems used differ greatly depending on manufacturer and device type. The fuser unit has the task of thermally fixing the toner onto the paper. Development over the last 10 years has been aimed primarily at energy conservation. This was mainly achieved in the fuser units which can consume up to 70 % of the electrical energy. By optimising the heating elements and materials, and by minimising the mass to be heated, it was possible to significantly reduce the fuser temperatures, the required heating times and the energy required. These modifications also required an adjustment to the toner systems, in particular a reduction of the melting points.

The pool devices were procured starting in spring 2009. Seven manufacturers were represented in the pool. It can therefore be assumed that the pool represents various new fuser technologies and toner systems. Within the project, no individual analysis of the fuser technologies in the pool devices was performed because of concerns that the necessary manipulations of the LPD may have had a massive impact on their error-free operation and the reproducibility of the emissions. Relevant detailed information from the manufacturers was not available in the project. Reference is made at this point to the appropriate literature [26] for an attribution of toner materials and fuser technologies to manufacturers and LPD types.

A second pool of LPD exists from earlier research projects in BAM, [11] hereafter referred to as Pool-2. These devices, collected from the year 2005 on, also have small to medium volumes and comparable technical data. Some particle emission results from Pool-2 are used below for comparison.

---

[25] See e.g.: www.fujixerox.co.jp/eng/company/headline/2007/0201_ene_save.html

[26] Final report on Task 1 “definition” for the EuP Preparatory Studies on Imaging Equipment (Lot 4), Chapter 6.2, Fraunhofer Institute for Reliability and Microintegration IZM, Berlin (2007)

4 Investigations and Results

4.1 Qualitative Analysis

Airborne particulate emissions from the devices were separated from the aerosol using a cascade impactor and thus made accessible to qualitative analysis (see Figure 7). The use of the 13-stage cascade impactor with depositable particle diameters of 30 nm to 10 µm made size-dependent chemical composition investigations possible.

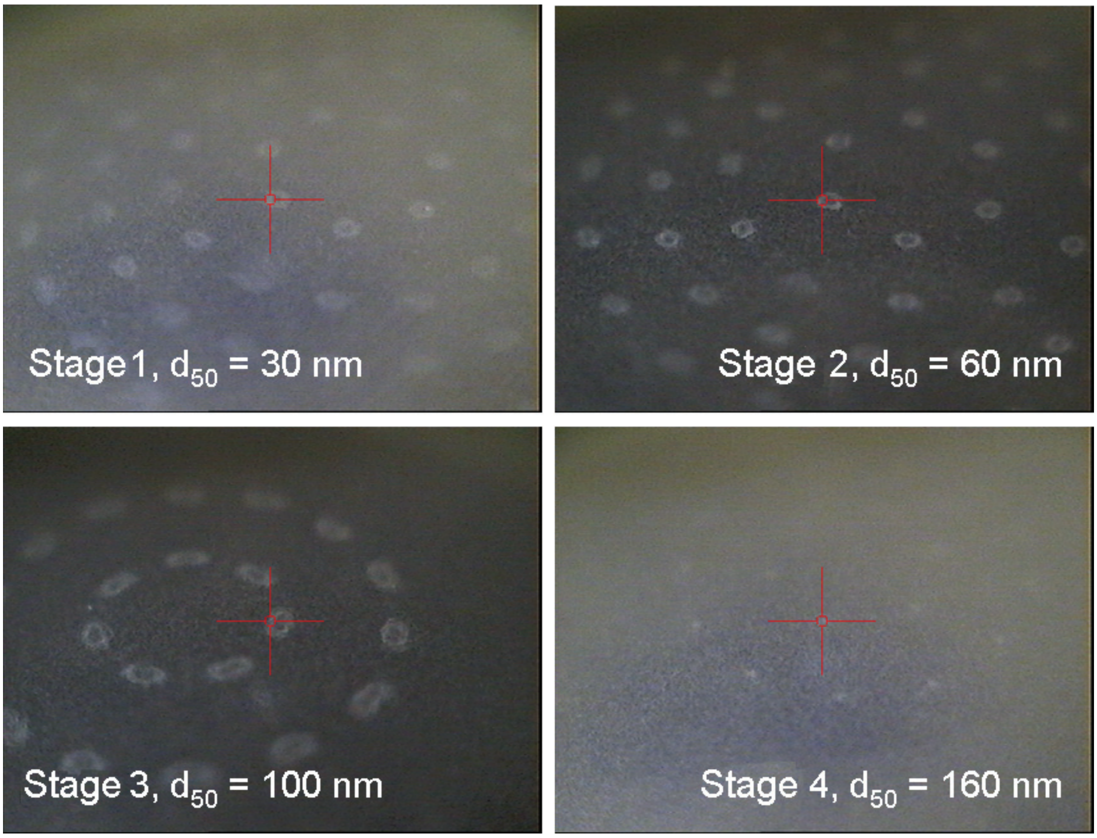

Figure 7: Typical impaction pattern of the deposited particles on the cascade impactor stages 1 to 4 of the example of LPD 8.

The qualitative analysis of the deposited fine and ultrafine particles was performed using the combination of two techniques: micro X-ray fluorescence spectroscopy (µXRF) and thermodesorption gas chromatography-mass spectrometry (TD-GC-MS). The application of XRF ensures the detection of the elemental composition including non-volatile components that are not able to be detected by the TD-GC-MS. Furthermore, this method provides information on substituted organic compounds, whose substituents have atomic numbers $Z \geq 13$. Elements with $Z < 13$ cannot be detected by the method used here, which excludes the detection of organic compounds without the corresponding substituents.

Volatile organic compounds can be split and optionally identified using TD-GC-MS analysis. The combination of the two analytical methods thus ensures that a comprehensive picture of the chemical composition of the particulate emissions is obtained.

Contributions of gaseous emissions to the XRF and GC-MS signals can be excluded, as non-particulate emissions cannot be deposited in the cascade impactor. The analysis of chamber blank values also enables the unique attribution of the identified aerosol components to the particulate emissions from the laser printers.

It must be emphasised that the method only provides information about the qualitative composition of the particles. The results obtained do not allow any quantitative conclusions about the concentrations of individual compounds to be drawn.

4.1.1 XRF Analysis

LPD Aerosoles

For qualitative analysis of the emitted particles, printing was always performed in the monochrome mode. Various studies have shown that the majority of particles emitted from laser printers are re-condensates of semivolatile organic compounds (SVOCs) handelt.[13,27 ,28] With the help of XRF analysis, the relatively small contributions of mainly solid inorganic compounds to the particulate emissions can be detected. It should be noted that only the elemental composition of the particles examined can be derived from the XRF signals. No information about the actual state of bonding or the existence of ionic compounds can be obtained.

In addition, evidence of appropriately substituted organic compounds such as brominated hydrocarbons can be obtained.

---

[27] He C., Morawska L., Wang H., Jayaratne R., McGarry P., Johnson G. R., Bostrom T., Gonthier J., Authemayou S. and Ayoko G.: Quantification of the relationship between fuser roller temperature and laser printer emissions. J. Aerosol. Sci. 41 (2010) p523 – 530

[28] Wensing M., Schripp T., Uhde E., Salthammer T.: Ultra-fine particles release from hardcopy devices: Sources, real-room measurements and efficiency of filter accessories. Sci. Total Environ. (2008) p407, 418 – 427

The proof of elements that indicate the presence of inorganic compounds, allows conclusions to be drawn about solid particles in the printer aerosols. The presence of inorganic solid particles in printer aerosols has been discussed in the literature, however, it has not been possible to quantify the number of solid particles.[13] The extent to which inorganic particles play a role can be determined by measuring the particle number concentration after evaporation of volatile components at 400 °C (see Section 4.2.3).

In the energy range up to 30 keV, the following elements were identified by XRF on the substrates using the size-selective deposition of particles: silicon (Si), sulfur (S), chlorine (Cl), calcium (Ca), titanium (Ti), chromium (Cr) , iron (Fe), bromine (Br) and traces of nickel (Ni) and zinc (Zn). The said elements were primarily detectable on the cascade impactor stages at cut points of 60-160 nm. Ca is the most abundant detectable element and constitutes the only aerosol component in LPD 1, 3, 4, 5 and 10 that can be detected using the XRF method. Metals such as Fe, Cr, Ni and Zn are found in 4 out of 10 devices (LPD 2, 7, 8 and 9). Br could be clearly detected in the aerosols of 2 devices (LPD 7 and 9), while Si and Cl occurred in 3 devices (LPD 7, 8 and 9). S was found in detectable amounts only in LPD 7 and Ti in LPD 8 and 9.

LPD 6 is a low emitter – there were no analysable particle depositions detected on the impactor substrates.

The elements detected in the present work that can be unambiguously attributed to the printer aerosols are summarised in Table 5. Where possible, the individual elements are attributed to the assumed sources such as paper materials (blue), toner (green) and structural components (yellow) involved in the printing process. A detailed derivation and discussion of this attribution will be made in a subsequent section. The corresponding XRF spectra are shown in Figures 8.1 to 8.10. The spectra of the stages 1 to 4 from the aerosol of LPD 7 are shown as examples in Figure 8.

Table 5: Size-resolved results of XRF analysis of deposited particles from the LPD tested.

d50 (nm)	30	60	100	160	270
LPD 1			Ca*		
LPD 2		Ca* Cr Fe Ni*			
LPD 3		Ca*			
LPD 4				Ca*	
LPD 5	Ca	Ca	Ca*		
LPD 6					
LPD 7		Si* S* Ca Br*	Si S Cl Ca Cr* Fe* Zn* Br	Si S Cl* Ca Zn* Br	
LPD 8			Si	Si Ca	Si Cl* Ca Ti* Fe
LPD 9		Cl* Fe Br*	Si Cl* Ca Ti* Fe Br	Ca Ti* Fe* Br*	
LPD 10		Ca*	Ca	Ca*	

* Detectable element in traces; empty cells: concentration below detection limit
Attributed to sources: paper (blue), toner (green), structural components (yellow)

In previous studies by Morawska et al., Ca, C, Fe, Ti, Si and Mg were found. Of these, the contributions of Ti and Si were mainly attributed to the chamber air contaminants.[14]

It was not possible in Morawska's study to distinguish between impurities in the chamber air and particles to be attributed to the printer aerosols due to the sampling technique, the passive deposition on transmission electron microscopy (TEM) grids and the subsequent analysis of individual particles by energy dispersive X-ray fluorescence analysis (EDX).

In contrast, the analysis of the total particles deposited and comparison with the corresponding blank samples used in the current study allowed the elements detected to be directly attributed to the printer aerosols.

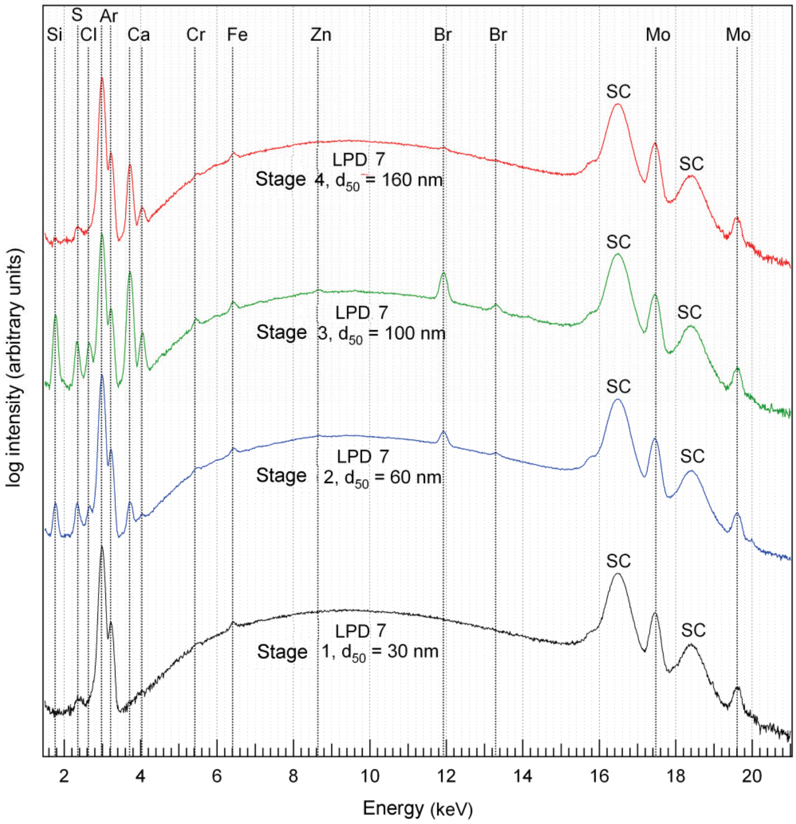

Argon (Ar) is attributed to the room air. Scatter signals are marked with SC.

Figure 8: XRF spectra of the deposited particles of LPD 7 with an attribution of the detected elements.

In the BITKOM study, the elements Al, Cl, Ca, Co, Cr, Cu, Fe, K, Mg, Mn, Na, Ni, P, S, Si, Ti and Zn were found.[29] Sampling using filters and subsequent SEM/EDX analysis of single particles in this case only enables limited conclusions to be drawn about the origin of the particles. There is no final opinion on whether the detected elements are directly related to printer aerosols.

Summing up, analysable quantities of particles were separated in the present studies in the particle size range from less than 30 nm to above 270 nm. Essentially, the approximate determination of the particle size distribution by the cut points of the cascade impactor stages is in good agreement with the particle size distributions determined with the help of EEPS. The XRF analysis only failed to provide findings at

---

[29] Wensing M., Delius W., Fauck C., Omelan A., Petersen J., Schripp T., Uhde E., Salthammer T.: Measurement and characterization of UFP emissions from hardcopy devices in operation. BITKOM WKI UFP Project Final Report (2010), unpublished

the small particle sizes (cascade impactor stage 1, d_{50} = 30 nm), except for LPD 5, while almost all printers exhibited visible particle depositions at this stage (see Figure 7). It is assumed that the particles on stage 1 of the cascade impactor are mainly organic compounds which are not readily detectable by the XRF analysis used here without appropriate substituents. These compounds are the subject of the GC-MS analysis (see Section 4.1.2).

Furthermore, it is surprising that some printers emit particles with diameters of 160 nm plus leading XRF signals able to be evaluated, while this size range hardly plays a role in the number-based particle size distributions. This is attributed to the fact that a small number of particles with a relatively large diameter and a correspondingly high mass lead to signals above the detection limit of the XRF spectrometer. The measurements of the fine particles using OPC (see Section 4.3) confirm the presence of particles in this size range, although their number is of minor importance compared to the ultrafine particles.

XRF Analysis Potential Particle Sources

The emergence of fine and ultrafine particles from laser printers is primarily attributed to the thermal processes. In order to draw conclusions about the emergence mechanisms and chiefly the sources of the particles, potentially relevant materials were investigated in this study. Thus an investigation was directed towards the paper used, the respective toner and some structural components of the printer which are exposed to distinctive heat effects due to the lack of space within the unit. These in particular include plastic components which are used near the fuser unit and may be exposed to temperatures of about 130 – 210 °C. [28]

Toner and Paper

The analysis of four black toner examples led to the identification of Si, Sn, Ca, Ti, V, Cr, Mn, Fe, Ni and Zn as essential ingredients. An overview is shown in Table 6.

The most intensive signal was by far always to be attributed to iron. This is primarily due to the fact that in addition to polymers, other pigments and other additives, Fe(III) oxide (Fe_2O_3) is the main component of toner powder. Si signals indicate the use of nanoscale Si oxides to improve the flow characteristics and charge stability.

Sometimes silicon-titanium mixed oxides are also used,[30] which explains the occurrence of Ti signals.

It is believed that various transition metals such as Ti, V, Cr, Mn, Ni and Zn, may be added to the toner for catalytic reasons in order to promote polymerisation in the fixing step.[31]

Table 6: XRF results of four toner samples tested

	XRF results of toner samples
LPD 3	Si, Sn, Ca, Ti, V, Cr, Mn, Fe
LPD 5	Si, Sn, Ca, Ti, V, Cr, Mn, Fe, Ni, Zn
LPD 7	Ca, Ti, V, Cr, Mn, Fe, Zn
LPD 9	Si, Ca, Ti, Cr, Fe

The EDX analysis of toner samples by Morawska et al. detected mainly Fe, some Ti and Sr and small amounts of Al and Si.[14] The differences in the results are probably primarily due to the fact that the toner samples come from different manufacturers.

In the XRF measurement of the paper batch used, the elements Ca, Ti, Fe and Sr and small amounts of Cl were detected.[32] More detailed measurements also have found these elements in office paper where, in addition, some Mn, Y, Ba, La and Ce were found. The differences can be traced back to the differences in detection sensitivity and to the different manufacturers of office paper.

The main component of the elemental composition in the energy range studied is Ca. This is consistent with the findings of other studies and can be explained by the use of calcium carbonate $CaCO_3$ as a mineral filler. [33] The presence of Ti is at least partially attributed to the use of Ti(IV) oxide TiO_2 as a white pigment. Since the compounds

---

[30] http//:www.aerosil.com/product/aerosil/en/Pages/default.aspx

[31] Rožić M., Rožmarić Mačefat M., Oreščanin V.: Elemental analysis of ashes of office papers by EDXRF spetrometry. Nucl. Instrum Meth. B 229 (2005) p117 – 122

[32] Spence L. D., Baker A. T., Byrne J. P.: Characterization of document paper using elemental compositions determined by inductively coupled plasma mass spectrometry. J. Anal. Atom. Spectrom. 15 (2000) p 813 – 819

[33] Manso M., Carvalho M. L.: Elemental identification of document paper by X-ray fluorescence spectrometry. J. Anal. Atom. Spectrom. *22 (*2007) p164 – 170

$CaCO_3$ and TiO_2 are not used as high-purity compounds in the context of papermaking, the occurrence of the further elements may be explained by the presence of impurities.[31]

The XRF spectra of an example toner (LPD 7), of paper samples and the blank value of an unused polycarbonate film are plotted in Figure 9.

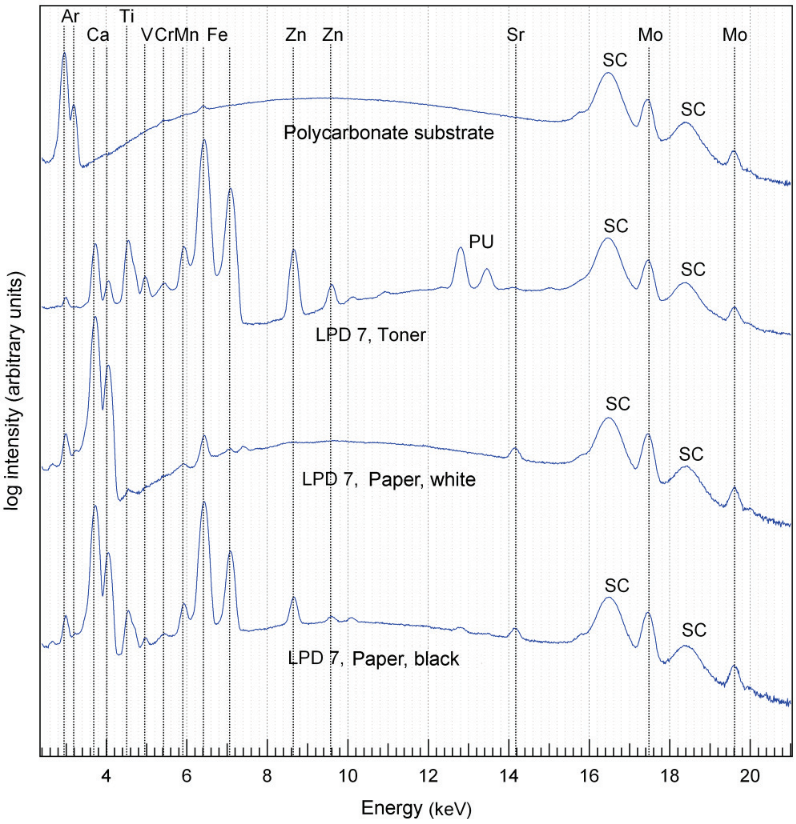

Figure 9: XRF spectra of a toner sample from LPD 7, paper samples and a polycarbonate substrate

The paper sample of the black printed paper reflects, as expected, in addition to the elemental composition of the white paper, the elements of the toner. The blank value of the unused polycarbonate substrate exhibits weak signals at the energies of Fe and Cr, which are experimentally related and were considered in the evaluation of the XRF spectra.

Structural Components

High temperatures near the fuser unit and the lack of space within the laser printer raise special demands on the materials used, particularly regarding flammability of plastic parts. Short codes by the manufacturers or suppliers enable an identification of the plastics used and the added flame retardants. The short codes are however not always available or are sometimes not accessible due to the design.

The plastic housing materials of the fuser unit mainly consist of glass fibre reinforced polyesters (PBT, PET), acrylonitrile butadiene styrene (ABS) or polycarbonate (PC). Polybrominated aromatic hydrocarbons (FR (16), FR (17)) have been used as flame retardants in the first place, but also halogen-free organic phosphorus compounds (FR (40)). Table 7 shows an overview of the flame retardants used in accordance with the labelling by the manufacturers according to ISO 1043-4.

Table 7: Short codes of the stated fire retardants and their significance

Flame retardants	Description
FR (16)	Aromatic brominated compounds excluding brominated diphenyl ether and biphenyls
FR (17)	Aromatic brominated compounds excluding brominated diphenyl ether and biphenyls in combination with antimony compounds
FR (40)	Halogen-free organic phosphorous compound

According to RAL-UZ122, halogen-containing polymers and additives of organic halogen compounds are not permitted as flame retardants in the plastics of the housing and housing parts. However, "special plastic parts that are installed in the immediate vicinity of heating and fixing units" are exempt from this rule, but these must not contain any PBB (polybrominated biphenyls), PBDE (polybrominated diphenyl ethers) or chlorinated paraffins.[34]

In a study using GC-MS analysis, Wensing et al. detected trixylyl phosphate, an organic phosphorus compound used as a flame retardant in a printer aerosol.[28] However, it was not possible to unambiguously distinguish between gaseous and particulate emissions because of the sampling technique. Although relevant XRF signals and labels indicated the use of organic phosphorus compounds in the plastic components of the tested printers, no phosphorus signals were observed in the printer aerosol samples in the present study.

---

[34] Vergabegrundlage für Umweltzeichen, Bürogeräte mit Druckfunktion (Drucker, Kopierer, Multifunktionsgeräte) RAL-UZ 122, Ausgabe Juni (2006)

Figures 10.1 to 10.10 in the Appendix show XRF spectra of various plastic parts that were found in parts exposed to heat in the printers, especially in the immediate vicinity of the fuser unit. Figure 10 gives an example of the spectra of the structural components of LPD 7. The results of the components tested and their short codes are summarised in Table 8. The findings with respect to the elements Si, P, Br and Sb are listed here as these elements are of particular interest with regard to particulate emissions from laser printers. The elemental composition of the structural components is not discussed in detail at this point.

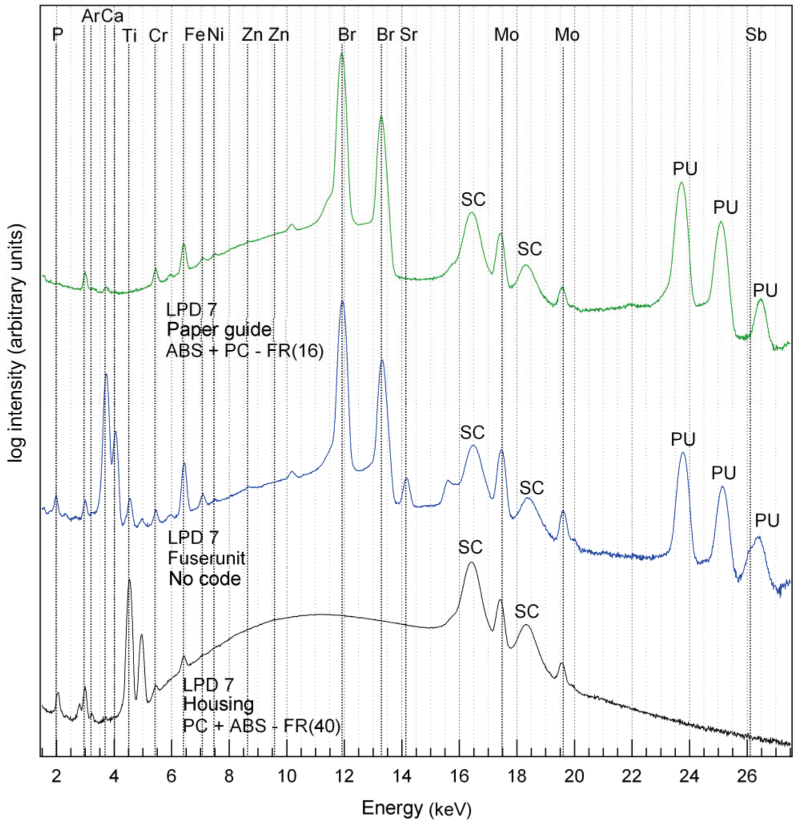

Attribution of the elements was performed with the help of the *Kα* lines of the relevant element. Scatter signals are marked with SC and sum peaks with PU.

Figure 10: XRF spectra of the structural components of LPD 7.

Table 8: Results of XRF analysis of structural components in the vicinity of the fuser unit with corresponding short codes

	Designation/short code	**XRF results**
LPD 1	Fuser unit Part 1/PBT-GF30-FR(17) Fuser unit Part 2/PBT-GF30-FR(17)	Br, Sb Br, Sb
LPD 2	Fuser unit Part 1/no code Fuser unit Part 2/no code Fuser unit Part 3/PET-(GF+MD)40-FR(17) Fuser unit lubricant	P, Br, Sb P, Br, Sb P, Br, Sb -
LPD 3	Fuser unit bottom/no code Fuser unit top/no code	Si, P P, Br*
LPD 4	Fuser unit Part 1/no code Fuser unit Part 2/PC+ABS-FR(40)	Si, P, Br* P, Br*
LPD 5	Fuser unit/PET-GF40-FR(17)	P, Br, Sb
LPD 6	Fuser unit/PBT-GF30-FR(17) PS†, next to fuser unit/PC+ABS-FR(40)	P*, Br, Sb P, Br*
LPD 7	Fuser unit/no code External housing/PC+ABS-FR(40) Guide member/ABS+PC-FR(16)	P, Br, Sb P Br, Sb
LPD 8	Fuser unit/PET-(GF+MD)40-FR(17) Fuser unit flap/PBT-I-GF30-FR(17) Fuser unit lubricant	P, Br, Sb Br, Sb Br, Sb
LPD 9	Fuser unit/PET-(GF+MD)40-FR(17) External housing/no code Paper output guide member/no code Pressure roller/no code	P, Br, Sb - - -
LPD 10	Fuser unit/no code Paper output guide member/PC+SAN-(MS+TD)20FR	P, Br, Sb Si

*Element detected in trace amounts only
† Plastic structure

In six out of ten laser printers tested, the use of brominated flame retardants was clearly stated by the short codes, while in the other cases the XRF spectra indicated the presence of brominated compounds. All devices tested thus had at least one structural component in a thermally exposed area whose XRF spectrum indicates the presence brominated flame retardants. Except for LPD 3 and LPD 4, where bromine was detectable only in traces, bromine signals at 11.92 and 13.29 keV, respectively were the dominant signals. In eight out of the ten printers tested, antimony signals were also observed at energies of 26.11 and 26.36 keV ($K\alpha$). The signals are partially overlapped by the Br sum peaks but can be clearly distinguished from the Br ($K\beta/K\beta$) sum peak (see Figure 11).

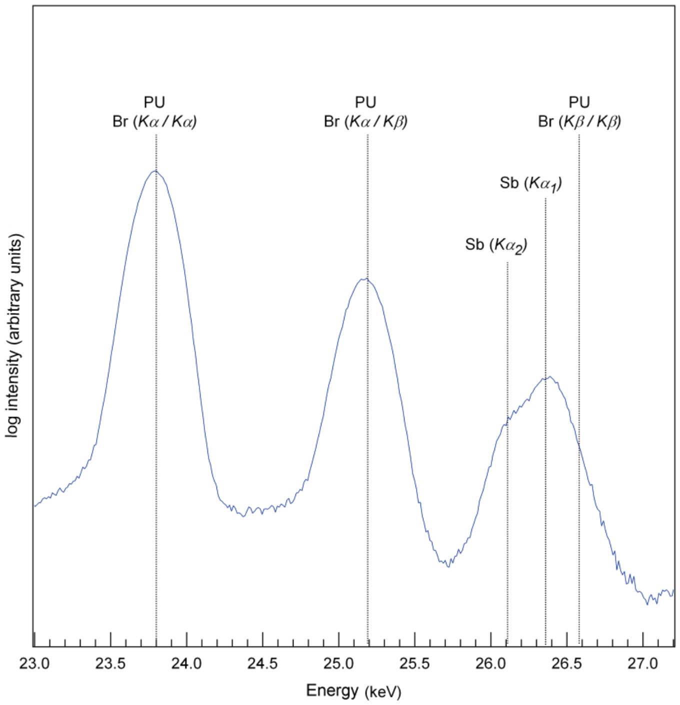

Antimony can be unambiguously identified based on the partly overlapping signals at 26.11 and 26.36 keV.

Figure 11: Br sum peaks (PU) of the Br-Kα and Br-Kβ lines as well as Sb-Kα lines.

The presence of Sb signals indicates the use of antimony(III) oxide Sb_2O_3 – which is not always declared by the relevant short codes – which is used to improve the flame-retardant effect of brominated flame retardants. The actual flame retardant compound is $SbBr_3$, which is produced during heating of Sb_2O_3 in the presence of brominated flame retardants.

Due to the relatively high vapour pressure of $SbBr_3$ at the elevated temperatures near the fuser unit, a contribution of $SbBr_3$ to the particulate emissions would be conceivable. However, although antimony signals were indeed observed in structural components, but not in the aerosol, possible contribution of $SbBr_3$ to the aerosol can be excluded.

The laser printer pressure roller ensures that the paper is pressed with a constant pressure against the fuser roller when passing through the fuser unit. This component was only available for analysis in the case of LPD 9. Although this element is exposed to high temperatures, no indicators of flame retardants such as Br or P were detected.

In all laser printers except for LPD 1, components are installed whose XRF spectra in combination with the corresponding short codes indicate the use of organic phosphorus compounds as flame retardants. Unlike the study by Wensing et al., these contributions were not detected in the aerosol within the present study.[28]

Attributing the elements detected to their potential sources

Based on the findings about elemental composition of toner and paper, a large part of the elements found in the printer aerosols are attributed to these sources.

The elements Si, Cr, Fe, Ni and Zn can be found in the toner and in the individual printer aerosols. These elements are therefore attributed to the toner as the main source. In the case of Si, contributions of siloxanes play a role (see Section 4.1.2). Attributing Fe to the toner is supported by the findings of Morawska et al.[14]

Ca was detected in the aerosol of all printers except the low-emitter LPD 6. The presence of Ca is attributed to the paper since this contains $CaCO_3$ as an essential inorganic component and paper dust represents a plausible mechanism of particle formation in this context. This attribution is further consistent with the findings of Morawska et al.[14]

Titanium occurs in both the paper and in the toner and thus cannot be unambiguously attributed to either of the two sources. In contrast, Cl can be found exclusively in the paper.

The attribution to the various sources is highlighted in Table 5 in colour. On the basis of the detection of Br-containing compounds in the structural components of the laser printers and the relevant codes, it is assumed that the Br fractions of the aerosols can be attributed to this source. This attribution is supported by the GC-MS results (see Section 4.1.2). It should be noted that bromine can be detected with the aid of the XRF method used here very efficiently, so that even small amounts can lead to qualitative indications of Br-containing compounds. From the results presented no quantitative comments about the contribution of Br-containing compounds to the aerosol can be made.

4.1.2 GC-MS Analysis

To identify semivolatile volatile organic compounds that make up the majority of particulate emissions from laser printing devices, a thermodesorption GC-MS analysis has been carried out for each stage of the cascade impactor which contained a visible particle deposition. Furthermore in analogy to the procedure for the XRF analysis, paper, toner and structural components were analysed. To obtain as complete a picture of the SVOCs involved in particle generation as possible, different GC methods were applied (see Chapter 2.4).

Printer Aerosol

As part of the GC-MS analysis of deposited particles from the printer aerosols, compounds from the substance classes of alkanes, alkenes, siloxanes, phthalates and esters or waxes were detected. Table 9 displays an overview of the occurrence of different classes of substances in the 10 devices tested. The overview does not include the size-dependent information on particle composition obtained by the cascade impactor. Size-resolved results can be found in Figures 12.1 to 12.10 and Tables 10.1 to 10.10. Figures 12 and 14 show examples of size-resolved chromatograms of LPD 2 and LPD 5; the associated tabular listings can be found in Tables 10 and 11.

Table 9: Results of the GC-MS analysis of the engaged cascade impactor stages of the ten laser printers tested

LPD	**GC-MS results**					
1	Alkanes	Alkene		Phthalates	Esters/waxes	
2	Alkanes		Siloxanes	Phthalates	Esters/waxes	Alcohols
3	Alkanes	Alkenes	Siloxanes	Phthalates	Esters/waxes	Aromatic compound
4	Alkanes		Siloxanes	Phthalates	Esters/waxes	
5	Alkanes				Esters/waxes	
6						
7	Alkanes			Phthalates	Esters/waxes	Acetic acid ester
8			Siloxanes	Phthalates	Esters/waxes	
9	Alkanes	Alkenes	Siloxanes	Phthalates	Esters/waxes	
10	Alkanes	Alkene				

In all aerosol samples, with the exception of LPD 6, semivolatile organic compounds were detected. LPD 6 is a low-emitter. In this case, there were no analysable particle depositions available. With regard to the observed SVOCs, an unambiguous identification of the compounds is only possible in individual cases. This is mainly due to the strong fragmentation of the molecules. Because of the absence of molecular ion signals, frequently only an attribution to a substance class can be made using specific fragments. In almost all printer aerosols except for LPD 8, significant amounts of alkanes were detected. With The alkanes were waxy hydrocarbons with chain lengths of C_{20} - C_{36}. The attribution is done using the retention times of the relevant alkane standards. It should be noted that the retention times of identical compounds may vary when comparing different printers. This is due to changes in the GC-MS analysis method and has been taken into account in the attribution.

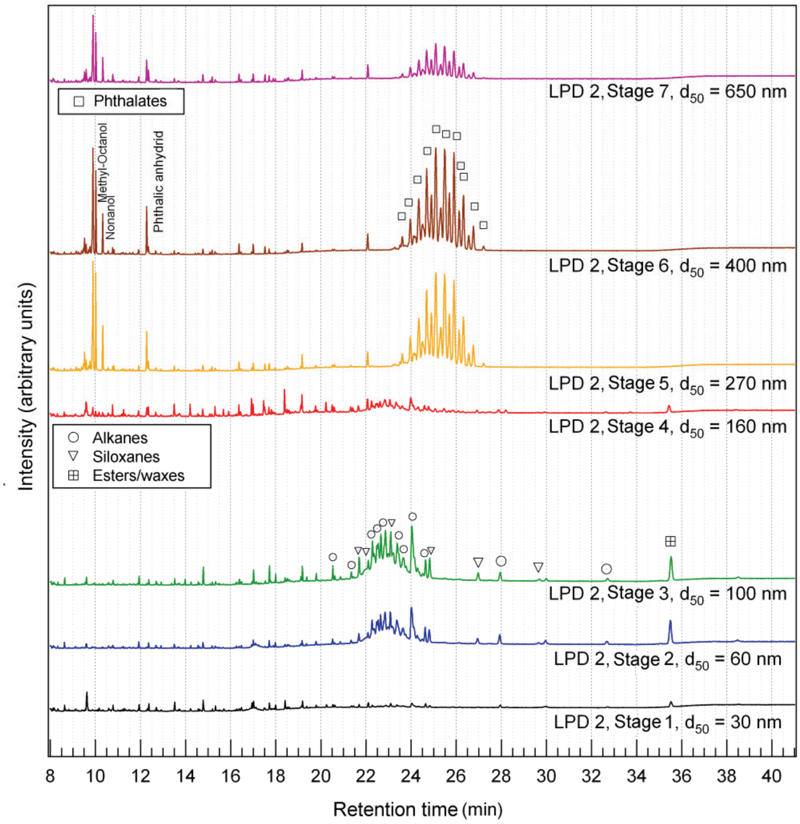

The cascade impactor stages are shown where analysable quantities of particles were deposited: here the stages 1 to 7 with cut points d_{50} = 30 – 650 nm

Figure 12: GC-MS results of the deposited aerosol of LPD 2

Long-chain alkenes can be found in the aerosols of LPD 1, 3, 9 and 10. Octadecene (LPD 9) and docosene (LPD 1 and 9) can be unambiguously identified.

Siloxanes were found in the aerosol in five of the tested printers, LPD 2, 3, 4, 8 and 9,. Cyclic and linear siloxanes can be distinguished based on the fragments occurring. Typical mass fragments of higher homologous siloxanes include m/Z = 295, 355, 369 and 429. While the fragments m/Z = 355 and 429 can be observed in abundance among cyclic siloxanes, these fragments occur among the linear siloxanes with only a relatively low intensity. Accordingly, ions with m/Z = 295 and 369 in cyclic siloxanes occur at a low intensity.[35]

In the present cases the proportion of cyclic siloxanes is greater than that of other components, but an unambiguous identification of the ring size is difficult because of the absence of the molecular peak. Contributions of siloxanes to emissions from LPD have been described in other studies.[14,36,37] In the search of potential sources for particle production, the siloxanes could not be attributed to any of the analysed components. As discussed in the section of the XRF analysis of the structural components, lubricants near the fuser unit were analysed by XRF in two cases (LPD 2 and 8), but Si content has not been detected. Despite the negative findings, it is believed that the origin of the siloxanes is mainly in their use as temperature-resistant lubricants, particularly since the thermally exposed areas are not easily accessible for analysis.

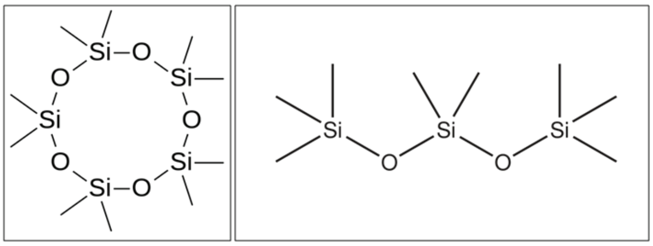

Figure 13: Structural formulas of decamethylcyclopentasiloxane (D5, left) and octamethyltrisiloxane (L3, right) as examples of a cyclic and linear siloxane

Certain siloxanes are also used as plastic additives in polycarbonates and rubber mixtures.[38] Taking into account the contribution of Si to the XRF spectra of the

---

[35] Pickering G.R., Olliff C.J., Rutt K.J.: The Mass Spectrometric Behaviour of Dimethylcyclosiloxanes, Org. Mass Spectrom. 10 (1975) p1035 – 1045

[36] Wilke O., Seeger S., Bresch H., Brödner D., Juritsch E., Jann, O.: Sampling and characterisation of ultrafine particles released from laser printers. Proceedings of the 11th International Conference on Indoor Air and Climate. Copenhagen, (2008), ID 239

[37] Wensing M., Delius W., Omelan A.; Uhde E., Salthammer T., He C., Wang, H., Mortawska L.: Ultra-fine particles (UFP) from laser printers: chemical and physical charaterization. Proceedings of Healthy Buildings, Syracuse (2009), ID 171

[38] Wypych G.: Handbook of Plasticizers, ChemTec Publishing (2004)

structural components, a contribution to this class of substances from plastic parts is also conceivable.

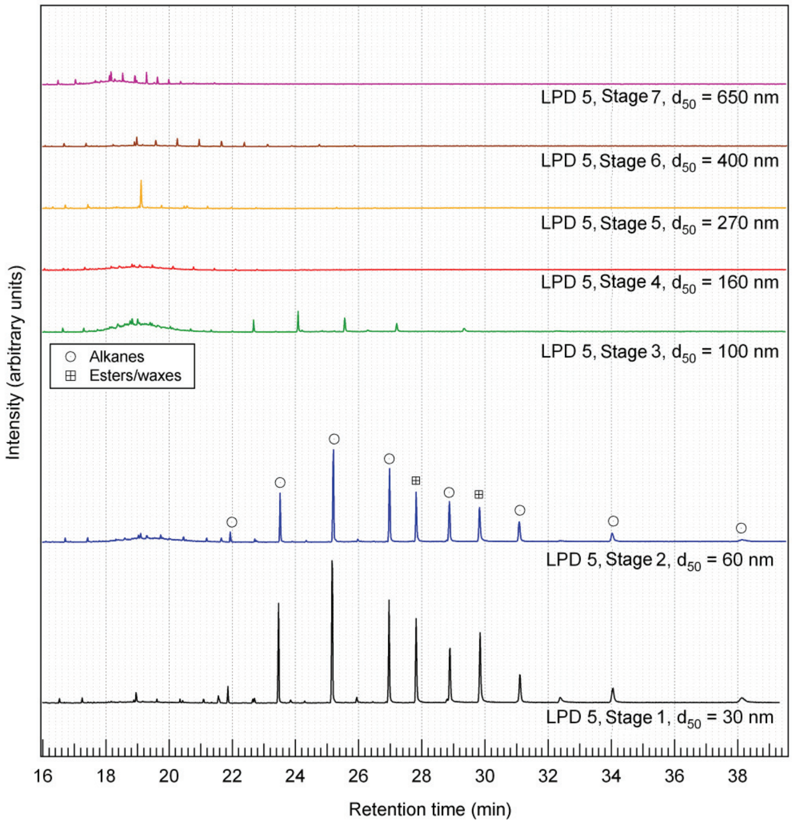

The cascade impactor stages are shown where analysable quantities of particles were deposited: stages 1 to 7 with cut points d_{50} = 30 – 650 nm.

Figure 14: GC-MS-Ergebnisse des deponierten Aerosols von LPD 5. GC-MS results of the aerosol deposited from LPD 5

Phthalic acid esters (phthalates, compare Figure 15) play a role in the printer aerosol of seven of the devices (LPD 1, 2, 3, 4, 7, 8 and 9). The occurrence of phthalates is believed to be associated with the use as plasticisers in plastics. The gaseous emissions of phthalates from indoor building materials have been the object of many investigations.[39,40,41] A strong temperature dependence of the emissions was observed

---

[39] Wilke O., Jann O.: Bestimmung von Weichmacheremissionen aus unterschiedlichen Materialien in Messkammern, Tagungsband 4. Freiberger Polymertag, Forschungsinstitut für Leder- und Kunstledertechnologie, Freiberg, G/1-G/11; (1999)

[40] Wilke O., Jann O., Brödner D.: VOC- und SVOC-Emissionen aus Fuhbodenaufbauten und den dafür verwendeten Materialien. Gefahrst Reinhalt Luft 63 (2003) p92 – 98

which makes the emission of phthalates plausible given the high temperatures during the printing process. While mainly compounds such as di(2-ethylhexyl) phthalate (DEHP), di-n-butyl phthalate (DBP) and benzyl butyl phthalate (BBP) with boiling points of 340 to 370 °C play a role in the gaseous phase, more semivolatile higher homologous phthalates were also observed in the particulate emissions, with the exception of DEHP which was detected in the aerosol of LPD 4. Indeed, di-iso-nonyl phthalates were clearly identified in the case of LPD 2.

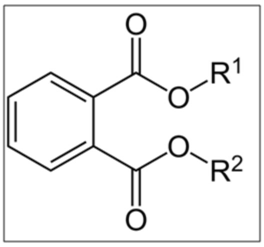

Figure 15: General structural formula of an o-phthalic acid ester

With the exception of the aerosol of LPD 10 and the aerosol of low-emitter LPD 6, long-chain hydrocarbons with an ester group can be detected in all aerosols. Esters of long-chain fatty acids with long-chain alcohols, by definition, are also known as waxes. The detection of these compounds in the paper provides a clear attribution to this source. A comparison of the retention times of the observed waxes with those of the alkane standards and an electron impact ionisation analysis of the occurring fragments enables conclusions to be drawn on the chain length of the alkyl residue. Accordingly, there are esters with more than 20 carbon atoms.

In addition, in certain printer aerosols, compounds were found which are characteristic of the device. These include alcohols, acetic acid esters and not clearly identifiable aromatic hydrocarbon compounds.

The findings partially coincide with the results of other studies. In investigations into particulate emissions carried out under the BITKOM studies, mainly long-chain alkanes between C_{21} and C_{48} and siloxanes were detected. Here, too, both cyclic and linear siloxanes were found. In two of the 26 tested devices, organic phosphorus compounds were identified.[29] Due to the sampling technique, it cannot be unmistakeably decided

---

[41] Wensing M., Uhde, E., Salthammer T.: Plastics additives in the indoor environment – flame retardants and plasticizers. Sci. Total Environ. 339 (2005) p19 – 40

whether the detected compounds are attributable to the ultrafine particulate emissions or if they were emitted in gaseous form.

Typical VOCs detected in previous studies, for instance by Wilke et al.[11], in connection with gaseous emissions from LPD include 1-butanol, benzene, ethylbenzene, styrene, xylene, toluene, phenol, cyclohexane and heptane. In a study by Morawska et al., ethylbenzene, o,m,p-xylene, styrene, pentadecane (C_{15} alkane), hexadecane (C_{16} alkane), heptadecane (C_{17} alkane) and dimethyl phthalate were found and they are all considered as possible constituents of particulate emissions.[14] The compounds mentioned were not detected in the present work and it is assumed that they do not play any or only a minor role in particle production, as co-condensates for example. This is mainly due to the fact that the relatively volatile VOCs do not, or only to a minor extent, condense under these conditions and contribute to particle production. Because of the separation characteristics of the cascade impactor used, compounds in mainly gaseous form cannot be detected. Evidence of longer-chain alkanes ($> C_{20}$) in the aerosols of the devices tested suggests that compounds with higher boiling points increasingly contribute to aerosol production.

Table 10: GC-MS results of aerosol samples of LPD 2 compared to toner and paper

The chemical composition is classified according to particle diameters of cascade impactor stages (d_{50}: cut point of the stages).

Aerosol				**Toner**	**Paper**
Stage 2 – 3 (d_{50} = 60 – 100 nm)		**Stages 5 – 7 (d_{50} = 270 – 650 nm)**			
RT (min)	**Compound**	**RT (min)**	**Compound**	**Compound**	**Compound**
20.5	C_{24} alkane	10.0	Methyl octanol	C_{24} alkane	
21.4	C_{25} alkane	10.3	n-nonanol		
21.7	Siloxane	12.3	Phthalic acid anhydrid		
22.1	Siloxane	23.6 – 27.2	Isononyl phthalates		
22.3	C_{26} alkane			C_{26} alkane	
22.7	C_{26} alkane				
22.9	C_{26} alkane				
23.1	Siloxane				
23.4	C_{27} alkane			C_{27} alkane	
23.6	C_{27} alkane				
24.0	C_{27} alkane				
24.6	C_{28} alkane			C_{28} alkane	
24.8	Siloxane				
27.0	Siloxane				
27.9	C_{30} alkane			C_{30} alkane	
29.7	Siloxane				
32.7	C_{32} alkane				
35.5	Esters/waxes				Esters/waxes

Considering the size-resolved GC-MS results, it is obvious that the chemical composition of particles varies with the particle diameter in some of the devices. For example, in LPD 2 on stages 2 and 3, corresponding to cut points of 60 to 100 nm, particles with an identical chemical composition consisting primarily of alkanes, siloxanes, and esters/waxes were found. On stages 5 – 7, according to cut points of 270 – 650 nm, mainly isononyl phthalates (see Figure 12 and Table 10) can be detected. Similar dependence of the chemical composition on the particle size was observed in devices LPD 1, LPD 3 and LPD 4.

In contrast to this, the devices LPD 5, LPD 7, LPD 8, LPD 9 and LPD 10 (see Figure 14 and Table 11) exhibited a substantially homogeneous chemical composition on the affected cascade impactor stages.

Table 11: GC-MS results of aerosol samples of LPD 5 compared to toner and paper

The chemical composition is classified according to particle diameters of cascade impactor stages (d_{50}: cut point of the stages).

Aerosol LPD 5		**Toner LPD 5**	**Paper**
Stufen 1 – 3 (d_{50} = 30 – 100 nm)			
RT (min)	**Compound**	**Compound**	**Compound**
21.9	C_{20} alkane	C_{20} alkane	
23.5	C_{22} alkane	C_{22} alkane	
25.2	C_{24} alkane	C_{24} alkane	
27.0	C_{26} alkane	C_{26} alkane	
27.8	Esters/waxes		Esters/waxes
28.9	C_{28} alkane	C_{28} alkane	
29.8	Esters/waxes		Esters/waxes
31.1	C_{30} alkane	C_{30} alkane	
34.0	C_{32} alkane	C_{32} alkane	
38.1	C_{34} alkane		

Polybrominated Aromatic Hydrocarbons

Polybrominated aromatic hydrocarbons are used as flame retardant additives in plastics. Emissions from this class of electronic devices have been extensively investigated.[42,43,44] Due to the boiling point range, a large proportion of these compounds ranked among the SVOCs and they are therefore considered as potential components of the particulate emissions in question.

Based on the results from the XRF analysis, which suggest that brominated compounds contribute to the particulate printer emissions from LPD 7 and LPD 9, further GC-MS analysis of the aerosols in these devices was performed. Since

---

[42] Maddalena R. L., McKone, T. E., Destaillats H., Russell, M. Hodgson A. T., Perino C.: Quantifying pollutant emissions from office equipment. Final report, Lawrence Berkeley National Laboratory, Berkeley, CA, (2009)

[43] Destaillats H., Maddalena R. L., Singer B. C., Hodgson A. T., McKone, T. E.: Indoor pollutants emitted by office equipment: A review of reported data and information needs. Atmos. Environ. 42 (2008) p1317 – 1388

[44] Kemmlein S., Hahn O., Jann O.: Emissions of organophosphate and brominated flame retardants from selected consumer products and building materials. Atmos. Environ. 37 (2003) p5485 – 5493

brominated compounds cannot be detected by the standard GC-MS method, a modified method has been used (see Section 2.4.3).

The targeted study of aerosols from LPD 7 and LPD 9 in terms of brominated compounds provided no results for LPD 7, while traces of a hexabrominated compound were detected in LPD 9. Figure 16 shows the corresponding mass spectrum.

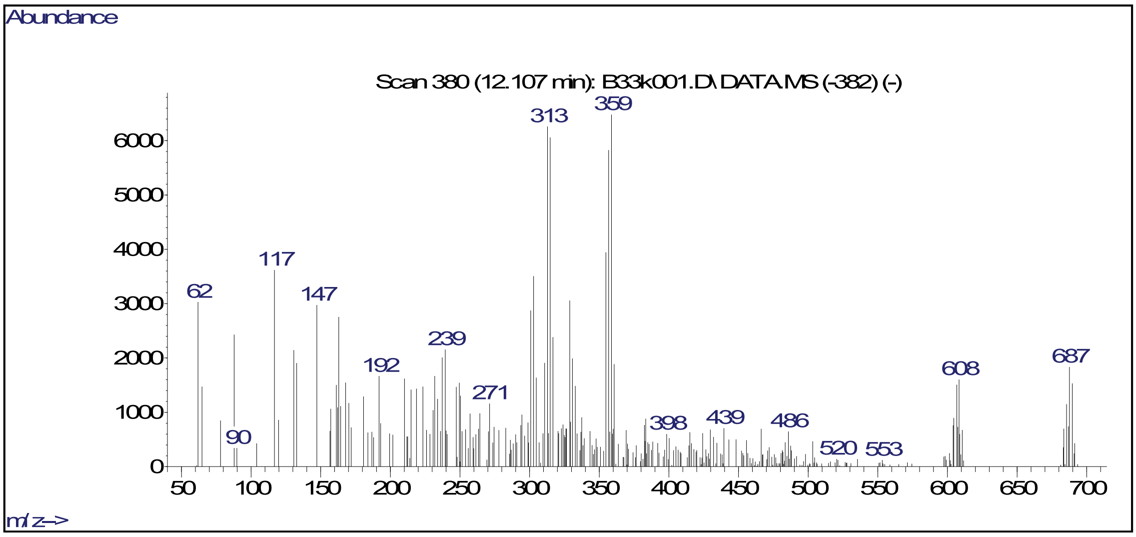

Figure 16: Mass spectrum of a hexabrominated compound that was found in trace amounts in the aerosol of LPD 9

A comparison with the NIST database[45] revealed a relatively poor agreement of 37 % with the mass spectrum of 1,1'-[1,2ethanediylbis(oxy)]bis[2,4,6-tribromo]-benzene (CAS: 37853-59-1) (BTBPE). The corresponding structural formula is shown in Figure 17. The poor fit can be understood considering the low signal intensity and the resulting low signal-to-noise ratio.

---

[45] NIST Standard Reference Database 1A, The NIST Mass Spectrometry Data Center, (2008)

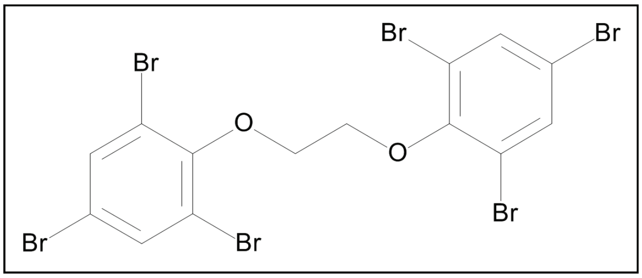

Figure 17: Structural formula of 1,1'-[1,2ethanediylbis(oxy)]bis[2,4,6-tribromo]-benzene (CAS: 37853-59-1) BTBPE).

The results obtained suggest that BTBPE is present in traces in the aerosol of LPD 9. The question of whether the Br signals of the XRF spectra can be explained by the relatively low concentrations of the hexabrominated compound cannot be conclusively clarified.

It is assumed that other bromine-containing contributions may play a role, in particular because despite of a positive Br finding in the XRF measurements in the aerosol of LPD 7, gas chromatography failed to provide any proof of detection for brominated compounds.

BTBPE is widely used as a flame retardant in various plastics and as a synergist with Sb_2O_3. A large part of the compound changes into the gas phase at temperatures around 240 °C and is fragmented at 340 °C primarily to 2,4,6-tribromophenol and vinyl tribromophenylether.[46,47,48]

As discussed in more detail in the section on GC-MS analysis of the structural components, BTBPE could not be identified as part of the plastic in the vicinity of the fuser unit of LPD 9. The fact that 2,4,6-tribromophenol was detected in the corresponding materials may result from the original BTBPE being fragmented during

---

[46] Covaci A., Harrad S., Abdallah M. A.-E., Ali N., Law R. J., Herzke D., de Wit C. A.: Novel brominated flame retardants: A review of their analysis, environmental fate and behaviour. Environ. Int. 37 (2011) p532 – 556

[47] Balabanovich A. I., Luda M. P., Camino G., Hornung A.: Thermal decomposition behavior of 1,2-bis-(2,4,6-tribromophenoxy)ethane. J. Anal. Appl. Pyrol. 67 (2003) p95 – 107

[48] Balabanovich A. I., Luda M. P., Operti L.: GC/MS Identification of Pyrolysis Products from 1,2-bis-(2,4,6-tribromophenoxy)ethane. Journal of Fire Sciences 22 (2004) p269 – 292

analysis. Another possible explanation is that BTBPE found in the aerosol has arisen from brominated precursor compounds under the effect of heat.

GC-MS Analysis of Potential Particle Sources

For the analysis of the materials involved in the printing process, a thermoextraction of volatile components was initially performed which were then analysed by gas chromatography. In contrast to wet chemical extraction methods, those compounds which can be evaporated under the influence of heat are analysed by thermoextraction, and thus may contribute to aerosol production during the printing process. The extraction temperature of 180 °C was chosen so that the thermal conditions in the vicinity of the fuser unit were simulated.

Toner and Paper

The analysis of toner samples showed that the volatile components are mainly composed of long-chain sometimes branched alkanes and alkenes, esters, and aromatic hydrocarbons, not always clearly identifiable. Table 12 shows an overview of the results of the GC-MS analysis of the toner samples. Examples are introduced in Figures 18 and 19: the chromatograms of the toner of LPD 3 and LPD 6, while the other devices can be found in Figures 18.1 to 18.10.

Table 12: Results of GC-MS analysis of toner samples after thermoextraction at 180 °C

Toner sample of LPD:	GC-MS results
1	Benzenedicarboxyl acid ester, aromatic compounds, 1-heptacosanol, alkanes (C_{21} – C_{35})
2	Styrene, propenoic acid ester, benzaldehyde, 1-dodecene, 1-chloro dodecane, benzophenone, alkanes (C_{16} – C_{32})
3	Phenol, acetophenone, biphenyl, alkanes (C_{15} – C_{34}), benzoic acid ester, aromatic compounds
4	Aromatic compound, benzene propanoic acid ester, alkanes (C_{29} – C_{36})
5	1-Octanol, phenoxypropanol, aromatic compounds, alkanes (C_{20} – C_{32})
6	Styrene, aromatic compounds, alkanes (C_{24} – C_{35})
7	2-Allylphenol, benzenedicarboxyl acid ester, terephthalic acid ester, alkanes (C_{22} – C_{28})
8	1-Tridecene, cyclododecane, ether, C_{21} alkane, propenoic acid ester, squalane, C_{24} alkene
9	Cyclohexadecane, hexadecane acid, aromatic compound, propenoic acid ester, C_{27} alkane, squalene, cholesterol
10	Acetophenone, butenoic acid ester, aromatic compounds, alkanes (C_{29} – C_{35})

In the case of toner samples, the temperature of 180 °C during thermoextraction may lead to polymerisation and other side reactions. Accordingly, the detected compounds do not necessarily reflect the composition of the toner but give evidence of compounds that are emitted from the printer and potentially contribute to particle production. It is assumed for some of the compounds extracted from the toner samples that they do not contribute to particle production because of their relatively low boiling points.

It is noticeable that the toner of the low-emitter LPD 6 (see Figure 19) has a chemical composition comparable with the toners of the other devices. Thus alkanes with chain lengths of C_{24} – C_{35} are there which can be found both in the toner of other devices and make up a large part of particulate emissions. This suggests that the composition of the toner is not the determining factor for the low particulate emission rate of LPD 6.

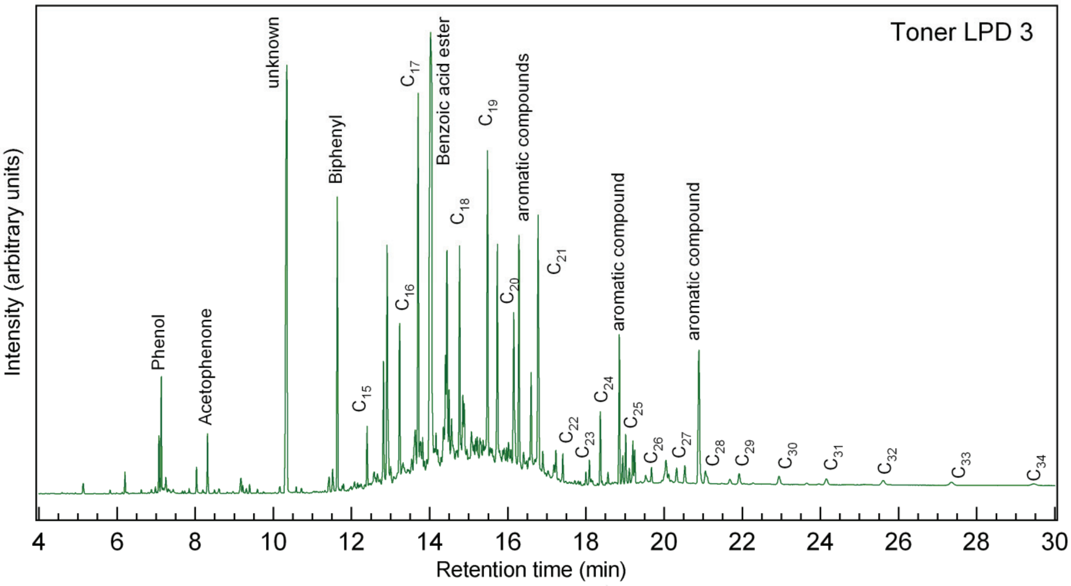

Figure 18: GC chromatogram of the toner (black) of LPD 3 with the identifiable substances attributed

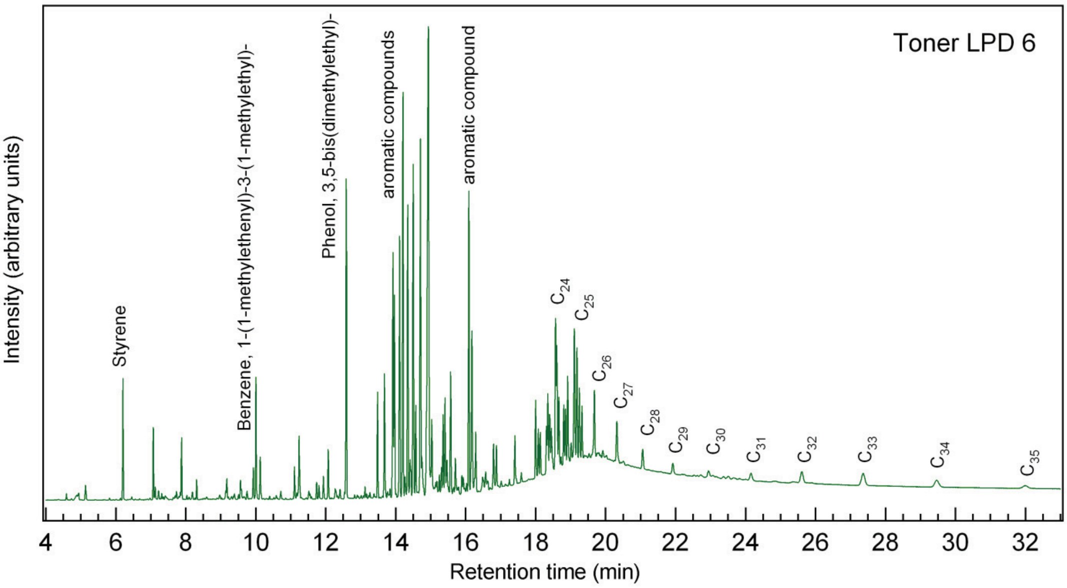

Figure 19: GC chromatogram of the toner (black) of LPD 6 with assignment of the identifiable substances

In the analysis of the paper used, retention times of 31.1, 35.7 and 41.8 minutes indicated certain compounds which were present virtually in all printer aerosols with the exception of LPD 6 and LPD 10 (see Figure 20). All three have the characteristic fragments with mass numbers 239, 255, 267 and 283. The fragments with m/Z = 239 and 255 occur as relatively concentrated.

Due to the mass difference of Δm = 28 between the mass fragments of 239 and 267 and 255 and 283, one can conclude the loss of a CO group. This can occur through a McLafferty rearrangement and explains the mass numbers of the fragments observed. The compounds cannot be unambiguously identified, but it is suspected that they are esters with long-chain alkyl residues. A comparison of retention times with those of the alkane standards suggests a total number of carbon atoms > 20.

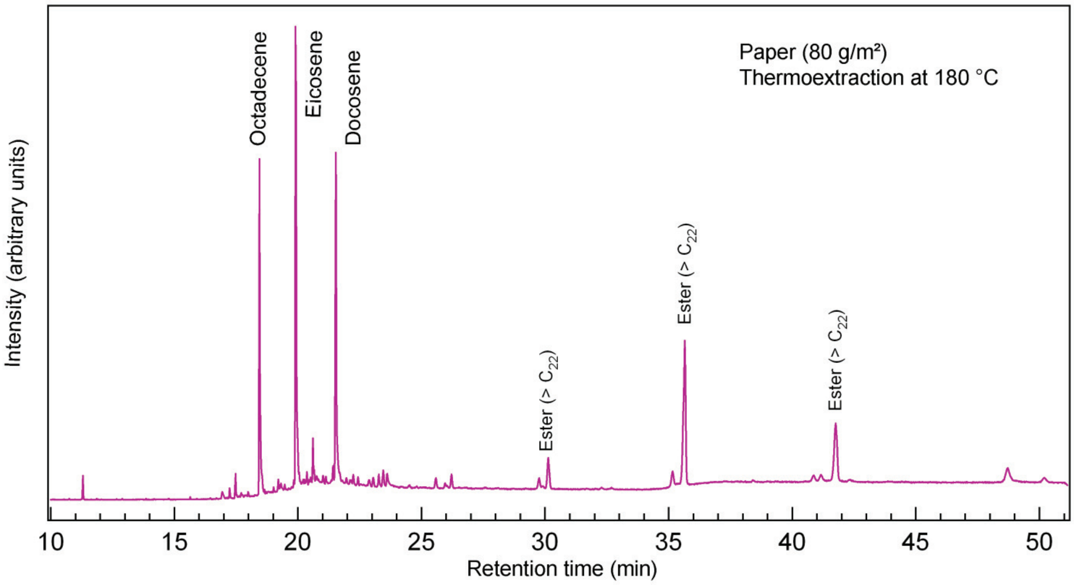

Figure 20: Chromatogram of a sample of the paper used after thermoextraction at 180 °C

Furthermore, the alkenes octadecene (C_{18}, RT = 18.5 min), eicosene (C_{20}, RT = 19.9 min) and docosene (C_{22}, RT = 21.5 min) were detected as volatile constituents of paper. Alkenes are produced as products of ester pyrolysis, but the thermoextraction temperature of 180 °C is too low to assume that pyrolysis of the esters detected during sample extraction took place. It is believed that the observed alkenes are products of papermaking. Docosene was found in the aerosol of two of the printers, LPD 1 and LPD 9, while octadecene was detected in the aerosol of LPD 9.

Structural Components

The analysis of structural components of a laser printer turns out to be very expensive due to the great variety of materials. For this reason, plastics from heat-exposed areas were analysed in isolated cases only.

Based on the examples of LPD 4 and LPD 7, plastic samples taken from the area of the fuser unit were studied. In the case of LPD 4, the analysis of the plastic sample from the fuser unit housing detected an oxaspirodion and triphenyl phosphate as plastic components (see Figure 21). Neither compound was detected in the aerosol.

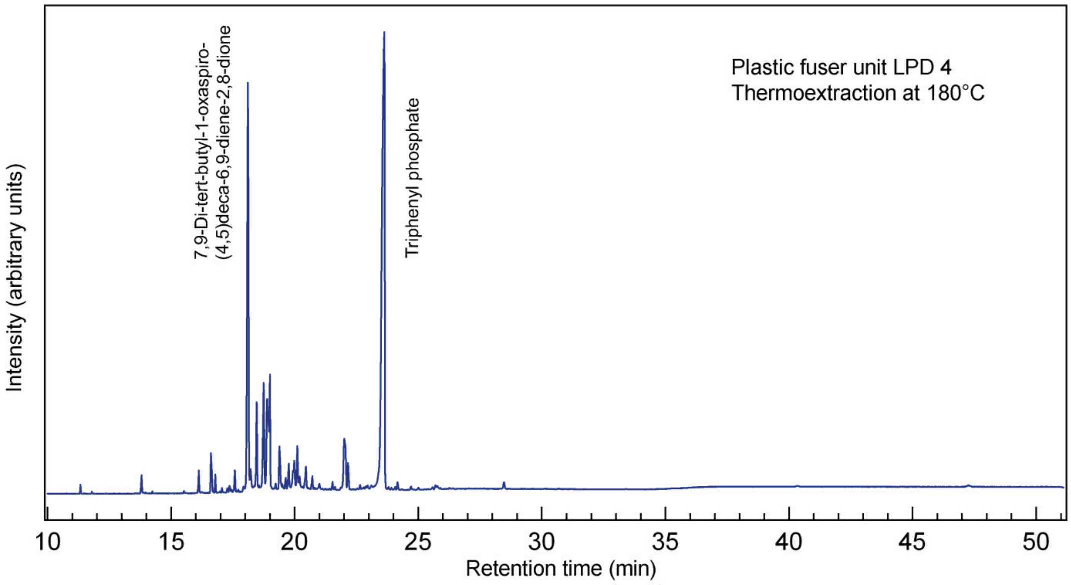

Figure 21: Chromatogram of a plastic sample from around the fuser unit of LPD 4 after thermoextraction at 180 °C

The detection of triphenyl phosphate confirms Wensing et al.'s assumption that organophosphorus compounds observed in certain printer aerosols may stem from structural components near the fuser. This result is consistent with the short code FR (40) indicating the presence of organophosphorus flame retardants. However, in the case of LPD 4, triphenyl phosphate was not detected in the aerosol.

Since plastic parts in the vicinity of the fuser unit are suspected to be the prime sources of brominated compounds, these materials were analysed by two separate methods in the affected devices LPD 7 and LPD 9.

The RoHS (Restriction of the use of certain Hazardous Substances in Electrical and Electronic Equipment) has already restricted the use of brominated flame retardants in electrical and electronic components since July 2006.[49] In particular, the addition of polybrominated biphenyls (PBBs) and polybrominated diphenyl ethers (PBDEs) is strictly regulated. Thus, the use of deca-BDE in electrical and electronic applications

---

[49] Directive 2002/95/EC of the European Parliament and of the council of 27 January 2003 on the restriction of the use of certain hazardous substances in electrical and electronic equipment (2003)

has been banned in the EU since July 2008[50] and certain compositions of the commercial mixtures of penta-BDE and octa-BDE are on the list of "Persistent Organic Pollutants" of the Stockholm Convention.[51] These restrictions have resulted in development of "new" polybrominated flame retardants or using them more extensively.[52] As Table 8 shows, certain structural components near the fuser unit of some devices have short codes that indicate the use of brominated flame retardants. The regulated polybrominated diphenyl ethers (see Figure 22) and polybrominated biphenyls (see Figure 23) are excluded.

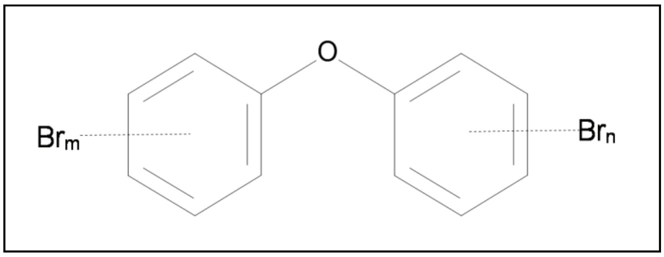

Figure 22: General structural formula of a polybrominated diphenyl ether with (m + n) bromine atoms

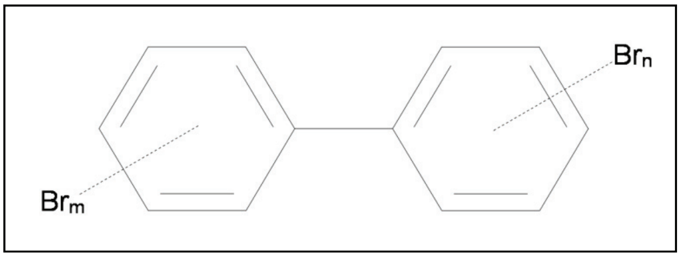

Figure 23: General structural formula of a polybrominated biphenyl with (m + n) bromine atoms

---

[50] European Court of Justice, Cases C-14/06 and C-295/06, Judgement of the Court, 1 April 2008, Directive 2002/95/EC and Commission Decision 2005/717/EC; 2008http:// curia.europa.eu. accessed July 2010

[51] Ashton M., Kantai T., Kohler P.M., Roemer-Mahler A., Templeton J.: Summary of the Fourth Conference of the Parties to the Stockholm Convention on Persistent Organic Pollutants: 4–8 May (2009), http://chm.pops.int/Programmes/NewPOPs/The9newPOPs/tabid/672/language/en-US/Default.aspx.

[52] Covaci A.., Harrad S., Abdallah M. A.-E., Ali N., Law R. J., Herzke D., de Wit C. A.: Novel brominated flame retardants: A review of their analysis, environmental fate and behaviour. Environ. Int. 37 (2011) p532 – 556

According to the codes, PBBs or PBDEs were detected in the plastic samples of fuser units of LPD 7 and LPD 9.

The compounds 2,4,6-tribromophenol (bromol), traces of tetrabromobisphenol A and two other brominated aromatic compounds were identified. A clear identification of these aromatics was not possible for lack of an appropriate molecule signal. The fragmentation pattern, however, indicates isomers of tetrabromoxylene. Based on the available data, it was not possible to unambiguously clarify whether or not the monocyclic compounds are fragments of an originally larger brominated molecule. In the course of the analysis, a fragmentation would be conceivable.

An overview of the results is presented in Table 13 and the corresponding chromatograms are shown in Figures 24, 25 and 26.

Table 13: Compounds found in plastic samples taken from near the fuser unit of LPD 7 and LPD 9

Device	**Component**	**Short code**	**GC-MS results**	
			RT (min)	**Compound**
LPD 7	Fuser unit	No code	3.525	Brominated aromatic compound
			4.592	Brominated aromatic compound
	Paper guide	ABS+PC-FR(16)	4.392	2,4,6-tribromophenol (bromol)
LPD 9	Fuser unit	PET-(GF+MD)40-FR(17)	9.092	2,4,6-tribromophenol (bromol)
			14.033	Tetrabromobisphenol A*

* Compound detectable in traces only

The findings are consistent with the results of the XRF analysis. In the corresponding plastic samples, the XRF spectrum has a dominant Br signal in each case. Where available, the short codes of the plastic components are consistent with the finding.

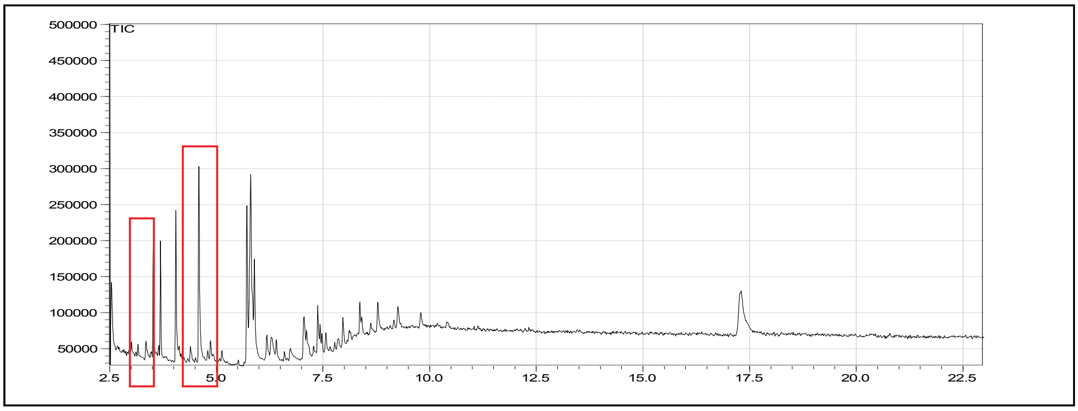

Two brominated aromatic compounds, non identifiable in greater detail, are indicated in red. Retention times: 3.53 and 4.59 min.

Figure 24: GC-MS spectrum of a plastic sample (fuser unit, LPD 7).

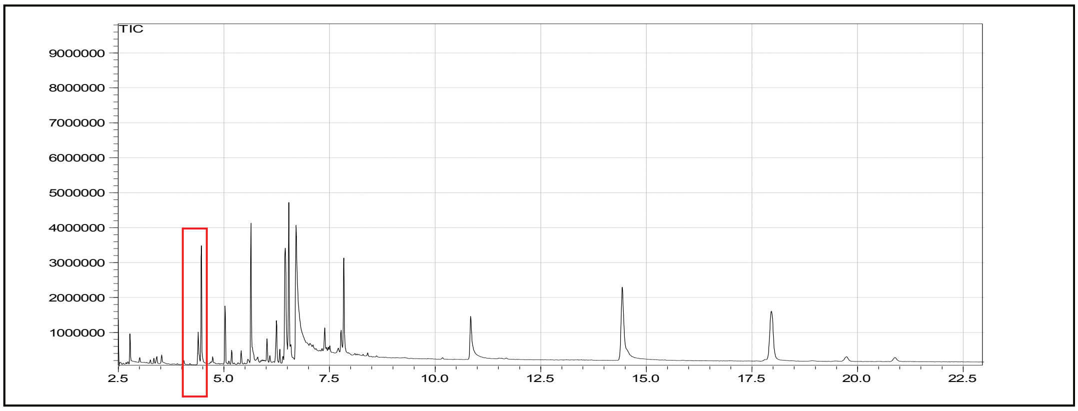

2,4,6-Tribromophenol (bromol) is indicated in red.

Figure 25: GC-MS spectrum of a plastic sample (Paper guide, LPD 7).

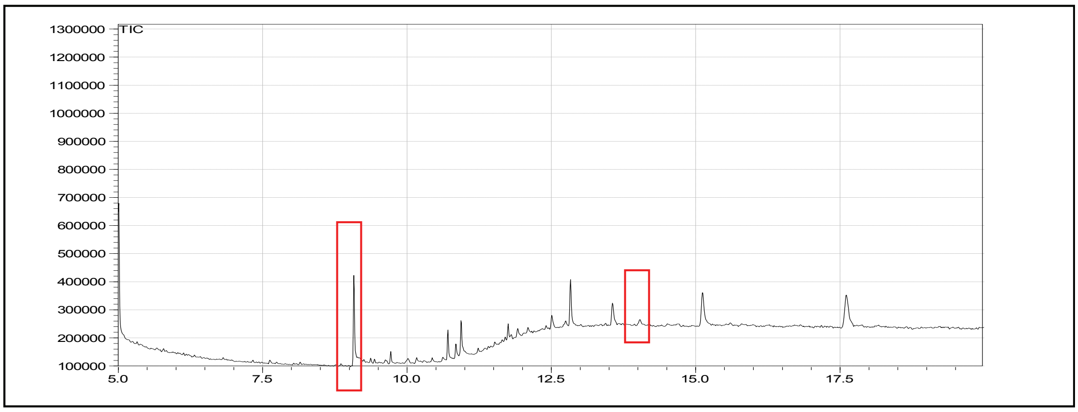

2,4,6-Tribromophenol (bromol) and tetrabromobisphenol A are indicated in red. Retention times: 9.09 and 14.03 min.

Figure 26: GC-MS spectrum of a plastic sample (fuser unit, LPD 9).

Another analysis of the plastic parts which included the fuser unit of the devices LPD 7 and LPD 9 provided evidence of a brominated compound in both cases whose mass spectrum is illustrated in Figure 27.

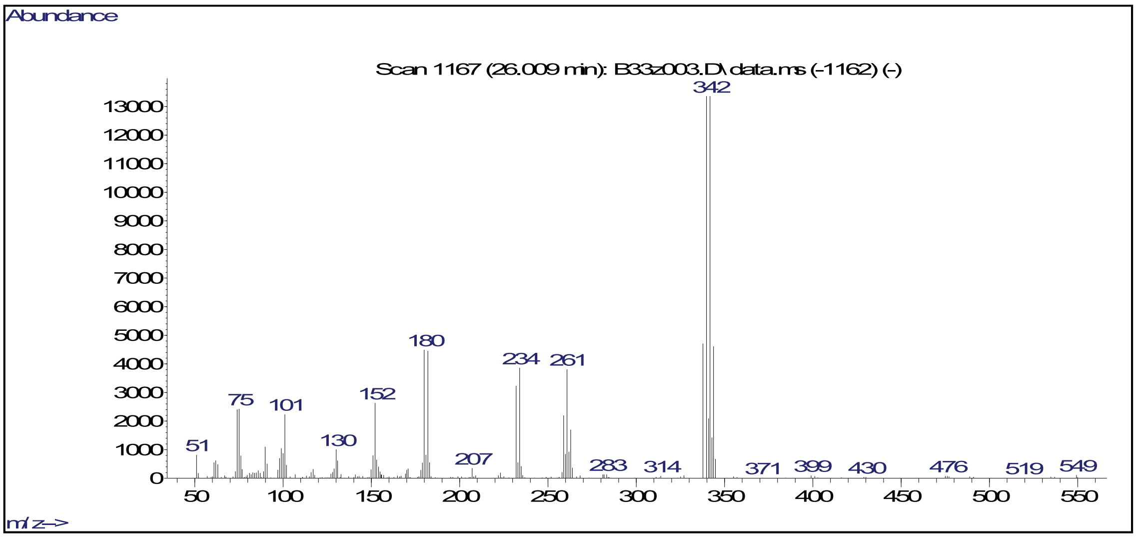

Figure 27: Mass spectrum of the brominated compound in the plastic housing of the fuser units of LPD 7 and LPD 9.

The compound co-elutes with 4-bromobiphenyl among the selected compounds, but this does not allow a conclusive assessment of the structure. From the mass fragments formed, the presence of three bromine atoms can be derived and it is believed an aromatic compound as a structural element. Since a mixture of common polybrominated diphenyl ethers and biphenyls, and other brominated compounds such as tetrabromobisphenol A, pentabromophenol, hexabromobenzene and tetrabromo-xylene was used as a reference standard and no match found, these compounds can be excluded.

Attribution of the Detected Aerosol Components to Potential Sources

According to the results, the long-chain alkanes detected in the aerosol can be mainly assigned to contributions from the toner. Furthermore, the long-chain esters observed can be attributed to paper, like the alkenes octadecene and docosene.

No constituents of the aerosols in the plastic parts were detected using the standard GC-MS method. It is noteworthy that only a small proportion of the materials used was analysed by gas chromatography.

The findings from the analysis of brominated compounds suggest that the compound detected in the aerosol of LPD 9 is connected to the brominated compounds of the structural components. In the case of the aerosol of LPD 7, which also yielded Br signals in the XRF analysis, gas chromatography failed to detect any brominated compound.

It is also assumed that the source of the siloxanes in the printer aerosol should be considered in the use of this class of compounds as thermally stable lubricants. In addition, phthalates are attributed to contributions from plastic parts, but the analysis of potential sources provided no evidence for the latter two attributions.

The example of LPD 4 illustrated in Figure 28 shows the comparison of the established compounds of the aerosol, the plastic from around the fuser unit, the toner and the paper used.

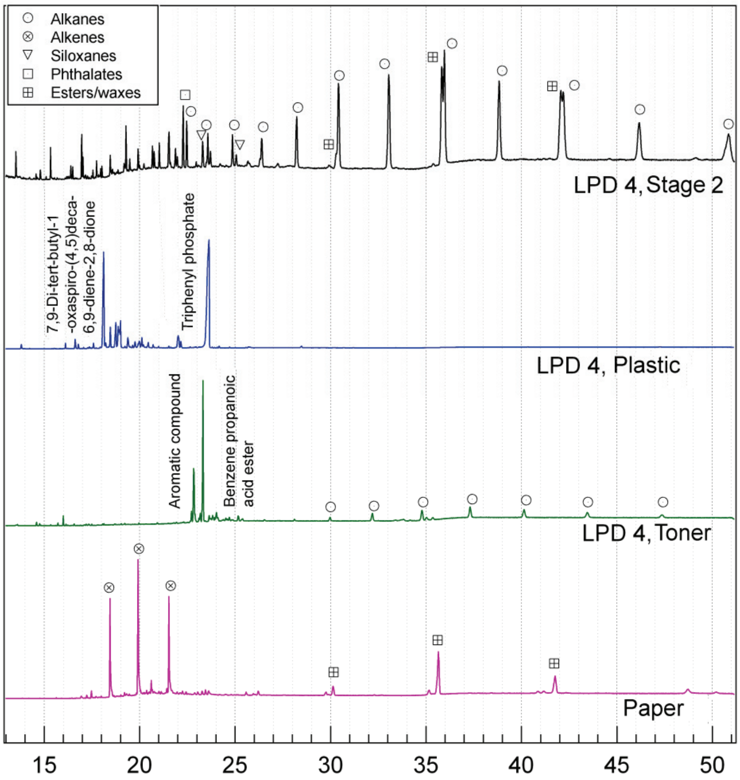

Figure 28: GC-MS results of the printer aerosol and potential sources of particles involved in the printing process (example of LPD 4)

4.1.3 Studies into the Volatility of Particles

Particulate emissions from laser printers were tested using two examples from the device pool in terms of volatility or in terms of potential solid particle content. For this purpose, two devices were chosen whose qualitative aerosol analysis suggested different fractions of solid particles. A positive calcium finding in the XRF results was considered an indication of solid particles, since the calcium contents in the aerosol are mainly attributed to solid calcium carbonate $CaCO_3$, used in paper production.

XRF results of the deposited particles from LPD 4 have shown that there were only traces of calcium in a particle size range around 160 nm. In contrast, the XRF analysis of LPD 7 shows a significant contribution by calcium on the stages with cut points 60, 100 and 160 nm as well as contributions from silicon, iron, chromium and zinc which can also be considered as contributions to a solid particle fraction.

A butanol CPC was equipped with an upstream combination of a rotation thinner and a thermoconditioner. Particle emission measurements were performed in each case when the thermoconditioner was operating at room temperature and at 400 °C. The total particle numbers TP were calculated for the two temperatures from the data according to the procedure of the RAL-UZ-122, Annex S-M. A brief heating of the aerosol in the thermoconditioner to temperatures around 400 °C leads to the evaporation of a large part of the particulate emissions since these are predominantly semi-volatile organic compounds. The number concentration vs. time curves at room temperature or 400 °C for the devices LPD 4 and LPD 7 are shown in Figures 29 and 30. The results for *TP* are summarised in Table 14.

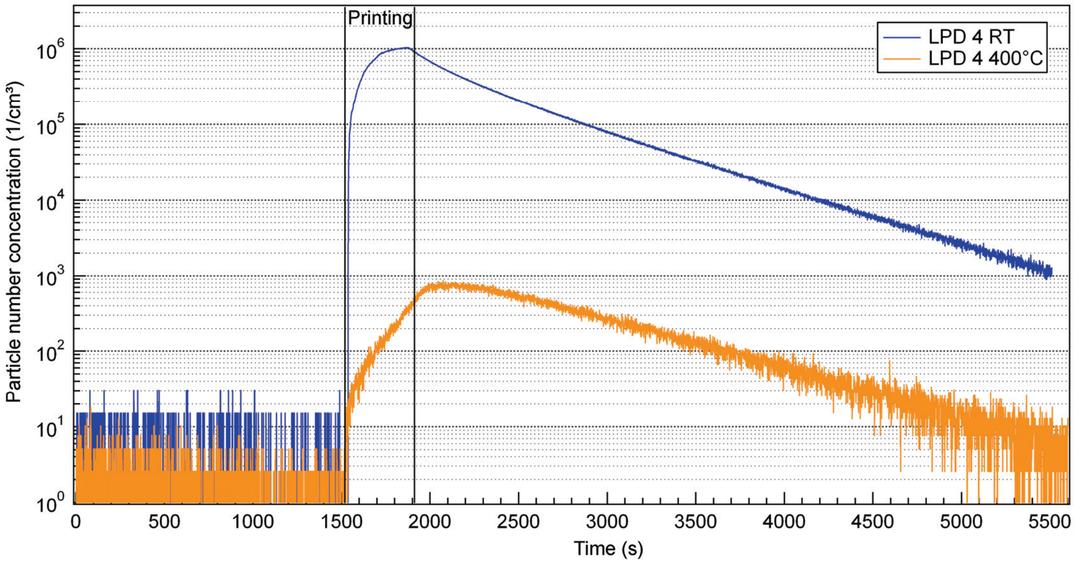

Figure 29: Particle number concentration vs. time curves for LPD 4 without (blue) and with thermoconditioning at 400 °C (orange)

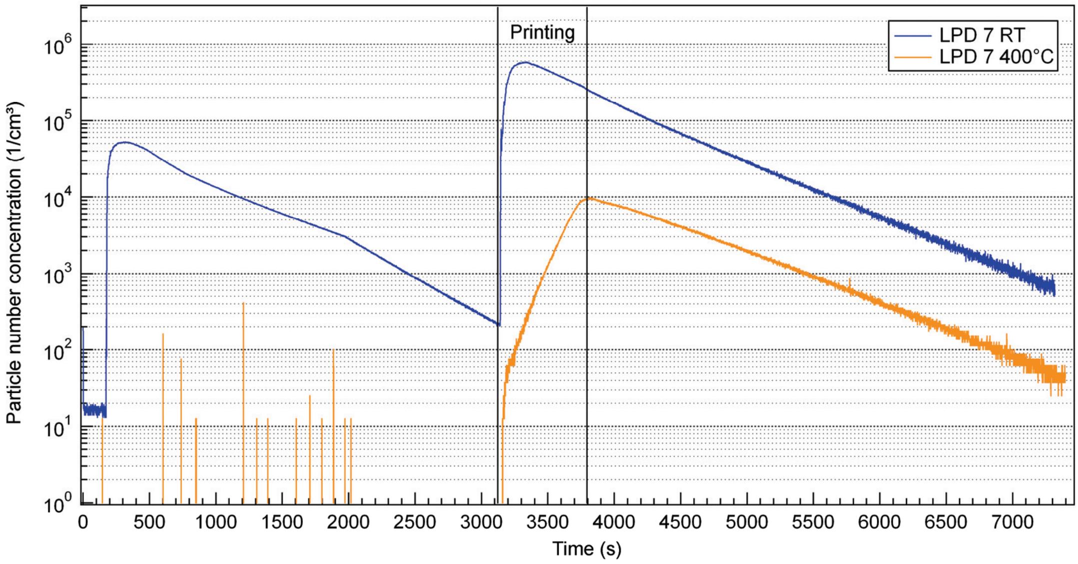

Figure 30: Particle number concentration vs. time curves for LPD 7 without (blue) and with thermoconditioning at 400 °C (orange)

Table 14: Calculated values for TP with and without thermoconditioning

	Calculated benchmark *TP*		**Proportion of solid particles (%)**
	Room temperature	**400 °C**	
LPD 4	6.0E11	1.2E9	0.2
LPD 7	7.4E11	1.4E10	1.9

The table shows the percentage of solid particles (%) after thermoconditioning at 400 °C in relation to the number of particles emitted at room temperature (*TP*).

The results are in good agreement with the findings of the XRF analysis. While the XRF results of LPD 4 show only small amounts of Ca-containing solid particles, the results of LPD 7 indicate a significant content of Ca, Si, Fe, Cr and Zn.

Trials to deposit the solid particles after evaporation of the main component of the aerosols by means of the cascade impactor and then analyse failed due to particle concentrations being too low.

4.1.4 Summary of the Qualitative Studies

The XRF analysis identified the elements silicon (Si), sulfur (S), chlorine (Cl), calcium (Ca), titanium (Ti), chromium (Cr), iron (Fe), bromine (Br) and traces of nickel (Ni) and zinc (Zn) as constituents of the aerosols of laser printing devices.

The study of paper, toner, and structural components using XRF resulted in the attribution of certain elements to potential particle sources: thus, Ca-containing aerosol components can be attributed primarily to paper dust, while Si, Cr, Fe, Ni and Zn aerosol components are assigned to toners. It is suspected that some of the Si aerosol constituents come from siloxanes. Evidence of substantial concentrations of bromine (Br) in the structural components of the printers suggests a connection between brominated flame retardants and Br in two of the ten aerosols tested.

Within the GC-MS analyses, mainly alkanes, alkenes, siloxanes, phthalates and esters were identified as aerosol components. A brominated compound was detected in the aerosol of one of the printers.

Studies of the materials involved in the printing process enable the SVOCs observed to be attributed to certain sources: while long-chain alkanes (C_{20} – C_{36}) were primarily found in the toner, long-chain esters were identified in the paper. In addition, alkenes with chain lengths of C_{18} – C_{22} were detected which sometimes also occur in the aerosols.

Plastic parts are suspected to be the source of phthalates, while siloxanes are attributed to their use as lubricants. However, it was not possible to unambiguously prove this attribution in any of the cases.

In the structural components, brominated compounds were found which are believed to be in connection with their use as brominated flame retardants and may be the cause of the compound detected in the aerosol. The available data do not allow for a conclusive assessment to be made.

Studies into the volatility of the deposited particles have led to the identification of non-volatile residues after heating the aerosol to 400 °C. It can be concluded in combination with the knowledge on the element composition of the particulate emissions that solid inorganic particles make up about 1 % of the total particle number.

4.2 Quantitative Studies

4.2.1 Modelling of Aerosol Measurement in an Emission Test Chamber

In the laser printing process, black and/or coloured toner powder with typical grain sizes above 1 µm is attracted by means of a static electrical charge from the toner cartridge to the paper. This creates the print image which is immediately fixed thermally to the paper in the so-called fuser unit at about 150-200 °C. This process includes the melting of the applied toner powder, a substantial thermal and mechanical effect on the paper and the heating of some components of the laser printer such as the fuser unit, transfer rollers, etc. During the printing process, volatile substances are vaporised and released as gases, some of these gases then create particles by cooling and re-condensation. Also chemical reactions may occur. The particles are transported as aerosols by the air flow within the laser printing device out of the housing and then into the environment. The particle generation is complex and depends strongly on individual designs of the LPDs. After long use also internal pollution of an LPD may contribute to its emission. Conditions within the LPD housings cannot be described and considered in all their details. It is to be expected that inside the housings the concentrations of particles and gases, the air temperature as well as the temperature of structural parts vary drastically in space and time. Directly at the origin particles may coagulate effectively until the aerosol is diluted by the air flow, at the latest when it leaves the housings. The time series shown below reveal that particle size distributions and particle number concentrations of aerosols emitted from LPD may change very quickly. For the quantitative analysis it is assumed that the aerosol generation entirely takes place within the LPD housings. Therefore temporally changing conditions within the housings are predominant for the observed temporal changes of particle distributions. Such conditions may be: Fluctuations of the fuser unit temperature by control cycles; increase of humidity, air temperature and concentration of VOCs with printing time; instable air flow and contamination of surfaces by recondensated substances. All these factors cannot be considered in any detail here and hence LPDs will be simply regarded as variable aerosol sources.

The aerosol emissions from LPD of the device pool were measured several times under comparable conditions in emission test chambers with 1 m³ and 5 m³ volume using aerosol measurement devices. Both accumulated particle number concentrations and size distributions of the number concentration of particles up to 20 µm in diameter were recorded as functions of time. In all measurements, only one type of pre-conditioned office paper and OEM toner cartridges were used exclusively.

An aerosol emitted from a source in an emission test chamber is subject to a number of influences on its way from its origin toward the instrument which may affect the particle size distribution, particle concentration and chemical composition:

- flow effects,
- chamber air exchange, wall deposition and coagulation,
- temperature and humidity changes,
- chemical reactions with other emitted substances.

These factors are discussed below with regard to their importance for particle emission measurement on an office device in an emission test chamber.

Flow effects occur particularly when an aerosol is exposed to high flow gradients or shear flow. The result may be a change in particle size distribution; smaller particles (< 1 µm) are less affected than big ones. Figure 31 shows the situation in a 1 m³ chamber with a maximum flow velocity of approximately 0.3 m/s. The aerosol source is placed in the centre of the chamber, the exchange air is supplied from the right and a fan distributes it in the direction indicated. Positions 1 and 2 mark the places where aerosol sampling from the chamber occurs. Flow conditions at the two positions differ to a large extent. Turbulence is likely to occur at the sampling points and around the test object.

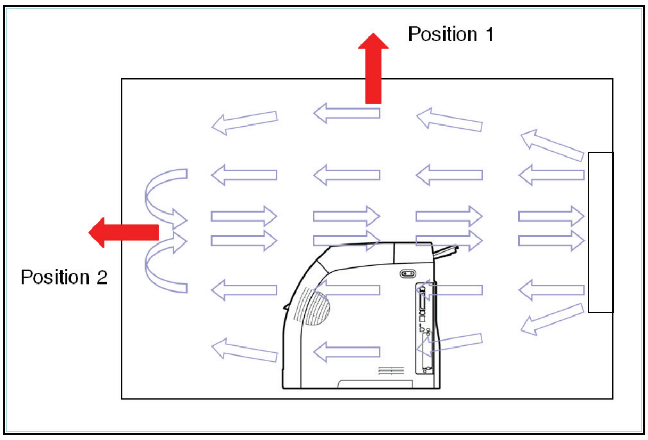

Figure 31: Aerosol sampling at two positions in a 1 m³ emission test chamber with horizontal air circulation and an LPD placed in the centre

During the operation of a LPD, the accumulated particle number concentration within the particle size range 300 nm - 20 µm was measured at Positions 1 and 2 as a function of time. The accumulated particle number concentration is the sum of the number concentrations over a defined particle size range. The curves are virtually identical. Lifetime effects have not been observed.

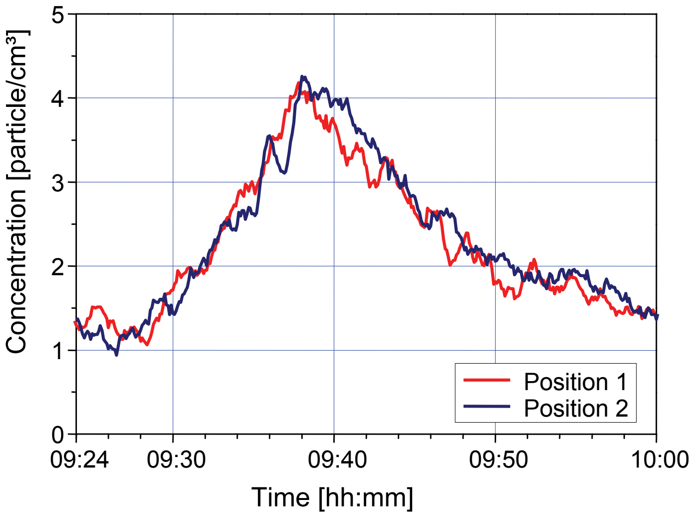

Figure 32: Comparison of the accumulated particle number concentration at Positions 1 and 2 in a 1 m³ emission test chamber.

Due to their much lower inertia particles smaller than 300 nm in diameter are not expected to be influenced by the measurement position. All in all, flow effects under the above conditions are negligible.

The aerosol dilution by air exchange (AE), deposition of particles on the chamber walls (D) and coagulation (C), i.e. the creation of fewer but larger particles from many smaller ones cause a steady reduction in particle number concentration. Coagulation is approximately proportional to the square of the number concentration and changes the particle concentration and particle size distribution with time, but not the particle mass concentration. Figure 33 shows the relationship between these factors.[53] There, the ratio of loss factors is plotted against the air exchange rate. Air exchange rates from

---

[53] Jamriska M. and Morawska L: Quantitative Assessment of the Effect of Surface Deposition and Coagulation on the Dynamics of Submicrometer Particles Indoors, Aerosol Science and Technology 37 (2003) p425–436

about 1.3 h^{-1} dominate particle losses in emission test chambers with the above-mentioned flow conditions for particles less than 1 µm in diameter. In these cases, an exponential decrease of the particle number concentration takes place after the end of emission. In areas of very high concentrations, thus possibly directly at the source of the particles in the office device casing, the conditions may be different. In particular, coagulation may remain dominant in the aerosol as long as the particles become rapidly diluted through discharge from the casing. Thus, the residence time of the aerosols in the device casing is an important factor in aerosol generation.

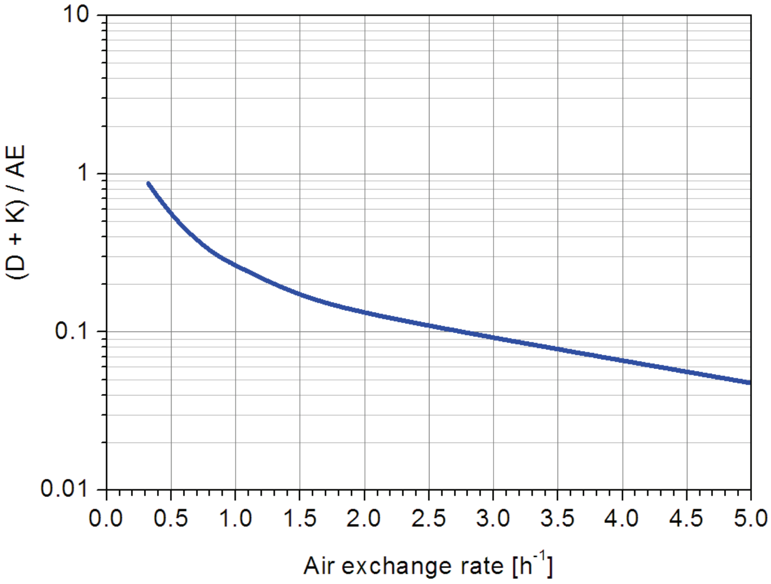

Figure 33: Ratio of particle loss due to coagulation (C), wall deposition (D) and air exchange (AE) at different air exchange rates

Depending on chamber volume and air exchange rate, the circulating air in the emission test chamber is only slightly warmed by printing. However, extreme temperature gradients may occur in the LPD casing and temperatures may possibly change rapidly over time. At the fuser unit of an LPD, temperature peaks of up to about 200 ºC occur. From about 20 cm distance and beyond from the test object, temperature variation of the chamber air is minimal and the temperature effect on the aerosol is therefore rather low. Humidity during a printing activity changes dramatically due to heat generation. When fixing the toner, some of the water contained in the paper evaporates. In extreme cases, condensing conditions may occur in small chambers and water is deposited on the chamber inner walls. This can affect the measurements of all emissions (VOCs, SVOCs, aerosols). Therefore in the test instructions UZ-122, Annex S-M, precautionary measures are described to limit the maximum moisture content at approximately 80 % RH. At larger chamber volumes and higher air humidity changes, the increase is much smaller. Through adequate comparisons of particle emission spectra of an LPD measured in different chamber volumes, the influence of humidity on the aerosol emitted can be qualitatively estimated.

Ozone is considered to be the prime partner for chemical reactions in the aerosols emitted. The concentration of both reactants determines the strength of this effect. Thus, the origin or source of both reactants is the zone having the highest probability of the occurrence of chemical reactions. As far as aerosol measurement is concerned, it can be assumed that chemical reactions in the aerosol after leaving the casing unit are generally rather unlikely.

BAM's earlier studies failed to find any significant relationship between either humidity increase or ozone concentration and particulate emission.[11]

As a result of the above factors, modelling of an aerosol measurement in an emission test chamber can assume simplified conditions with good approximation. The primary measurand is the accumulated particle number concentration $C_p(t)$ in a specified particle size range. Some instruments also offer the possibility of continuous recording of the particle size distribution. Absolute level and dynamics of $C_p(t)$ are essentially determined by the following factors:

- source strength of the LPD,
- chamber size,
- particle losses in the chamber, primarily through the air exchange rate, also by other factors.

The source strength of the LPD is influenced by its specific product features and the printing activity (length, number of pages and print mode). For different device-specific printing activities, a product comparison requires the standardisation of the length of the printing activity, the number of printed pages or other benchmarks. The size of the chamber decides which concentration range should be measured within the detection limits $C_p(t)$. In extreme cases, less sensitive instruments are not capable of recording low emissions in a large chamber. The red box marks the printing time from 10:13 to 10:23 hours in a chamber with AER = 4 h-1

Figure 34 shows an example of the $C_p(t)$ profile with an exponential decay after the end of particulate emissions. The printing phase is marked by a red box.

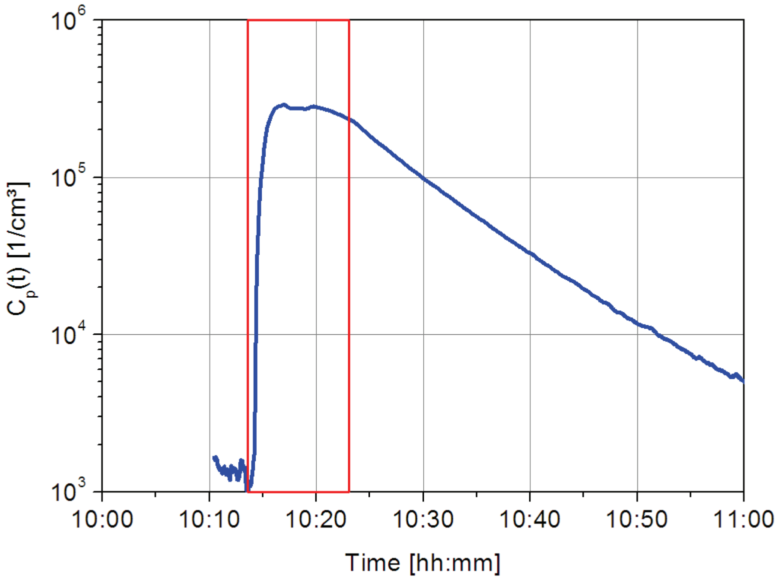

The red box marks the printing time from 10:13 to 10:23 hours in a chamber with AER = 4 h-1

Figure 34: Time profile of particle number concentration during operation of an LPD in a 1 m³ emission test chamber.

Particle losses in the chamber can be described by particle loss rate *β* by adjusting a chamber response function of the type

$$R(t) \propto e^{-\beta t} \tag{1}$$

to $C_p(t)$ after the end of the emissions. The source strength can be calculated as rate *PER(t)*, particles emitted per unit of time). $C_p(t)$ and *PER(t)* are linked via a convolution integral, which contains the response function *R(t)*:

$$C_p(t) = \int_{t=0}^{t=\tau} PER(t) \cdot R(t-\tau) d\tau \tag{2}$$

If the response function has the above-mentioned simple form, rate *PER(t)* can be

$$PER(t) = V_{ch} \cdot \left(\frac{dC_p(t)}{dt} - \beta \cdot C_p(t) \right) \tag{3}$$

determined analytically in [particles/unit time] by deconvoluting the convolution integral

The time derivative can be determined numerically. Equations (3) and (3a) are mathematically equivalent and contain only known quantities such as the chamber volume V_{ch} and $C_p(t)$.

$$PER(t) = V_{ch} \cdot \left(\frac{C_p(t) - C_p(t-\Delta t) \cdot \exp(-\beta\, \Delta t)}{\Delta t \cdot \exp(-\beta\, \Delta t)} \right) \tag{3a}$$

In formula 3a, *Δt* is the time difference between two successive data points. By integration of *PER(t)* and volume correction, one obtains the total number *TP* of the particles emitted during a printing activity. t_{start} marks the start of the printing phase.

$$TP = \int_{t_{start}}^{t_{stop}} PER(t)\, dt \tag{4}$$

Figure 35 shows the values *PER(t)* and *T* calculated by Equations (3) and (4) *P*. Time t_{stop} marks the decline of the emission rate to zero or below a selectable limit. The value of *TP* can be taken from the integral curve at the point t_{stop} or numerically calculated according to Equation (4).

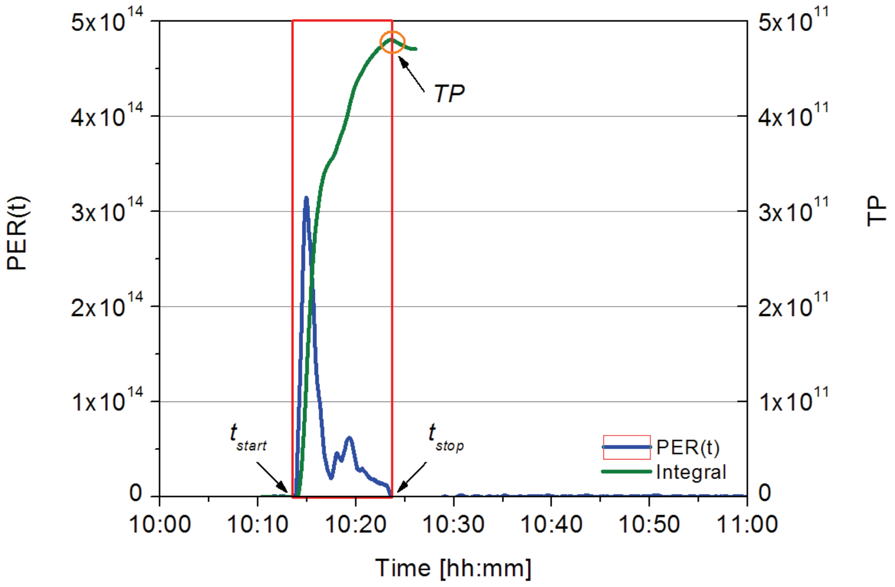

The value for *TP* is marked by an orange circle.

Figure 35: Time profile of the particle emission rate *PER (t)* and the integral according to Equation (4).

The end of particle emission, t_{stop} – as shown here – is not always identical to the end of the printing activity but must be determined from the curve of the particle emission rate *PER(t)* before the calculation of *TP*. The emission time is determined by the difference

$$t_{stop} - t_{start} \tag{5}$$

TP provides a benchmark for quantitative analysis of particulate emissions which will be used in the following sections.

TP may be related to the number of printed pages which defines the benchmark *TP/pp* [-] (pp stands for printed pages). Alternative definitions of benchmarks are possible. For instance the 10 minutes standard length of printing activity can be used as reference to specify an average emission rate PER_{10} [particle/10 minutes]:

$$PER_{10} = TP \cdot \frac{10}{t_{print} \ [min]} \tag{6}$$

In equation (6) t_{print} [min] stands for the actual duration of the printing activity.

4.2.2 Quantitative Comparison of Aerosol Emissions from LPD

In this section, only the accumulated particle number concentration $C_p(t)$ will be considered. Subsequent sections will analyse the observed particle size distributions. The aerosol emissions from the LPD of the device pool were measured several times and evaluated according to the scheme described in Section 4.2.1. The measurements were performed according to the following plan that was based on the measurement process of the existing test procedure RAL-UZ-122, Appendix 2:

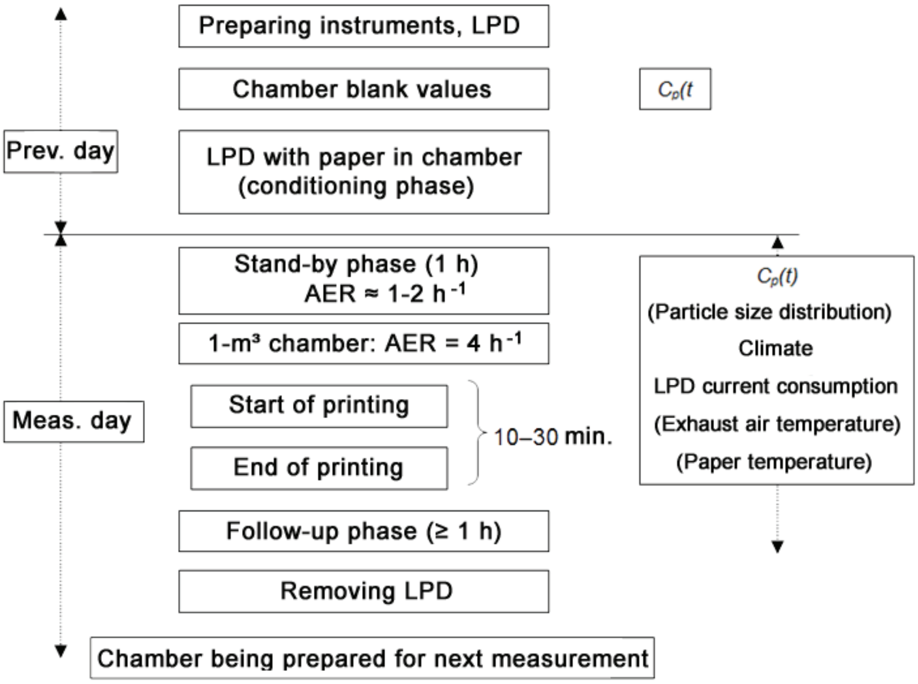

Figure 36: Schedule of particle emission measurements

Individual measurements were repeated on the same day with a rest period of at least one hour between measurements. On the day of measurement, climate parameters (temperature, humidity) and current consumption of LPD were continuously recorded. In addition, in some measurements the temperature of the printed paper was measured above the paper tray using an infrared sensor and the exhaust air temperature at the exhaust ports – if available. The aerosol measurements were made on stainless steel and conductive plastic hoses of 1.5 m length. Sharp kinks or bends in the pipes were avoided. The lines protruded to between 30 % to 50 % of the chamber height, and about 10 cm deep into the chambers. The following table shows the data from printing phases for the pool printers.

Table 15: Specifications of printing phases

LPD	**1**	**2**	**3**	**4**	**5**	**6**	**7**	**8**	**9**	**10**
Page number, colour mode	210	50	-	-	-	75	-	220	-	-
Length of colour mode [min]	10	10	-	-	-	10	-	10	-	-
Page number monochr.	210	160	250	250	160	75	333	220	230	210
Length of monochr. [min]	10	10	8.9	7.8	8.7	10	10	10	10	10

Figure 37 shows the results of the measurements converted to the benchmark PER_{10} and includes all measurements taken. The observed relatively narrow spread of those measurements considered valid, enable a very good distinction of particle emissions from office devices to be made. LPD 6 is conspicuous due to its extremely low particulate emissions. LPD 1 and 2 have significantly higher particulate emissions in colour mode, LPD 8 fails to show any difference between the modes. Red-marked data points represent results from repeated measurements on the same day. Such repeated measurements may be a cause for an increased scatter, as results from LPD 2 and 9 show. Results from 1 m³ and 5 m³ chambers are compared in Figure 38. There is no distinct trend with chamber volume; results from the larger chamber are for some LPD in the upper half of the region of scatter while the opposite is observable for other devices. Data from LPD 9 measured in the 5 m³ chamber - marked with a circle - appear isolated and lie far above the results in the 1 m³ chamber. There is no obvious cause for this behaviour.

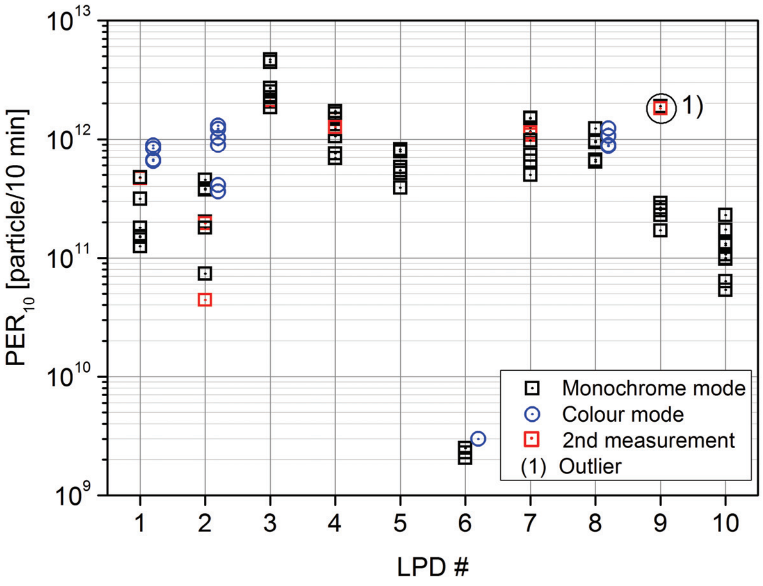

Figure 37: Quantification of particulate emissions, overview of results

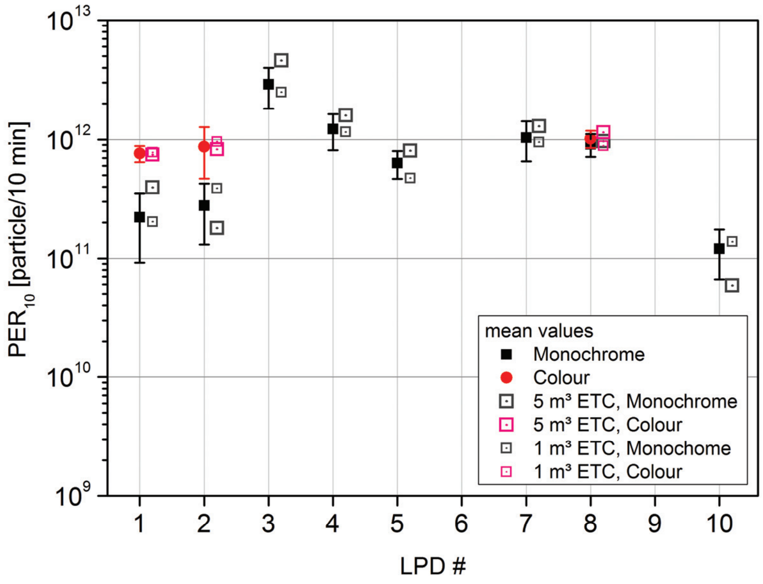

Figure 38: Quantification of particulate emissions, influence of chamber volume

The statistical data, including dispersion of valid values were evaluated numerically and are listed in Table 16.

Table 16: Overview of particle emission test results

LPD	**1**		**2**		**3**	**4**	**5**	**6**		**7**	**8**		**9**	**10**
PER_{10}	mono-chrome	colour	mono-chrome	colour	mono-chrome	mono-chrome	mono-chrome	mono-chrome	colour	mono-chrome	mono-chrome	colour	mono-chrome	mono-chrome
Arithm. average	2.2E11	7.6E11	2.8E11	8.7E11	**2.9E12**	1.2E12	6.4E11	**2.3E9**	3.0E9	1.0E12	9.1E11	1E12	5.2E11	1.2E11
Minimum	1.3E11	6.5E11	7.5E10	3.6E11	1.9E12	6.9E11	3.9E11	2.1E9	a	5E11	6.5E11	8.8E11	1.7E11	5.4E10
Maximum	4.8E11	8.9E11	4.5E11	1.3E12	4.7E12	1.7E12	8.2E11	2.5E9	a	1.5E12	1.3E12	1.2E12	1.9E12	2.3E11
Range	3.5E11	2.3E11	3.8E11	1.9E10	2.8E12	1.0E12	4.3E11	4E8	a	1.0E12	6E11	3.6E11	1.7E12	1.8E11
Std. dev.	1.3E11	1.2E11	1.4E11	4.0E11	1.1E12	4.1E11	1.7E11	2.2E8	a	3.8E11	2E11	1.7E11	6.8E11	5.4E10
Coeff. of var.	**0.58**	0.16	0.5	0.46	0.38	0.34	0.26	**0.1**	a	0.37	0.22	0.16	N/A	0.45

a: only one measurement, **bold**: maximum & minimum,
N/A: not calculated due to small number of measurements

The span of the coefficient of variation ranges from 10 % to 58 %. Comparative measurements in the 5 m³ emission test chamber allowed the estimation of the influence of the chamber volume. No clear trend has been observed since the readings for some LPD from the bigger chamber were at the top, others in the bottom range.

Since all tests were performed under reproducible, identical conditions, it can be assumed that the variations are under a product-specific influence. The observation that second measurements in particular on the same day and within a few hours of each other may have very different results supports this assumption and it must be taken into account when specifying the test conditions. As a conclusion of this finding, a second test on the same day should be omitted.

Some LPD already produced particle emissions in the standby phase when switching on the device. These so-called switch-on peaks were evaluated using the same procedure as described above. As figure 39 shows, the maximum of the switch-on peak may exceed the maximum of Cp(t) during the printing phase.

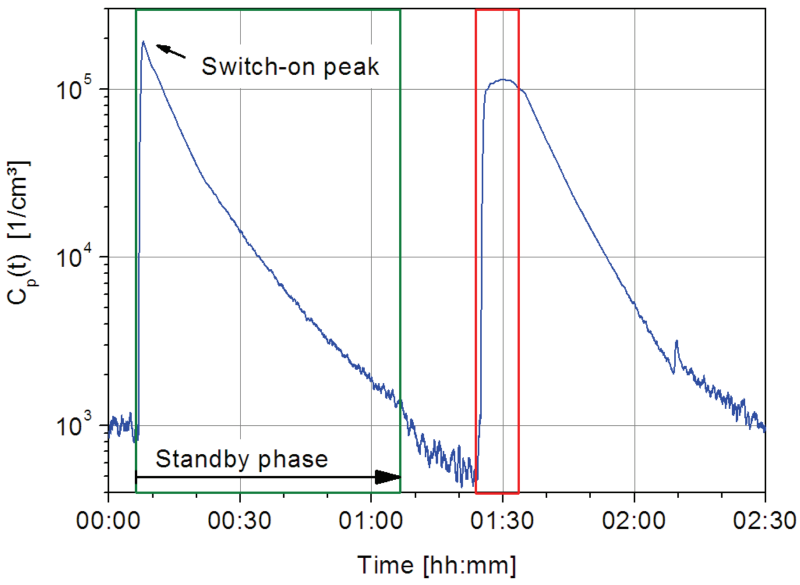

Figure 39: Example of a switch-on peak in the standby phase (red box marks the printing phase)

Table 17 contains the total number of particles calculated from the switch-on peak TP_{Peak} compared to the total number of particles from the printing phase TP_{Print}. The amount of emitted particles, TP_{Peak}, is significantly smaller than TP in all examples, or cannot be determined due to the lack of a switch-on peak.

Table 17: Particle emissions in switch-on peak

LPD	**1**		**2**	**3**	**4**	**5**	**6**	**7**	**8**		**9**	**10**
	mono-chrome	colour	mono-chrome	mono-chrome	mono-chrome	mono-chrome	mono-chrome	mono-chrome	mono-chrome	colour	mono-chrome	mono-chrome
$\mathbf{TP_{Peak}}$	1.7E11	2.3E11	N/A	5.0E11	N/A	N/A	N/A	5.0E9	1.2E11	1.5E11	1.4E10	N/A
$\mathbf{TP_{Print}}$	2.3E11	1.1E12	-	2.2E12	-	-	-	1.4E12	1.3E12	1.4E12	3.0E11	-
$\frac{\mathbf{TP_{Peak}}}{\mathbf{TP_{Print}}}$	0.74	0.21	-	0.23	-	-	-	0.004	0.09	0.10	0.05	-

N/A: no switch-on peak available

As shown in 4.2.1, other benchmarks are also possible. The following figure shows a comparison of *TP/pp* and PER_{10}, using data from BAM-Pool and Pool-2. Here, the results have been sorted according to PER_{10} magnitude.

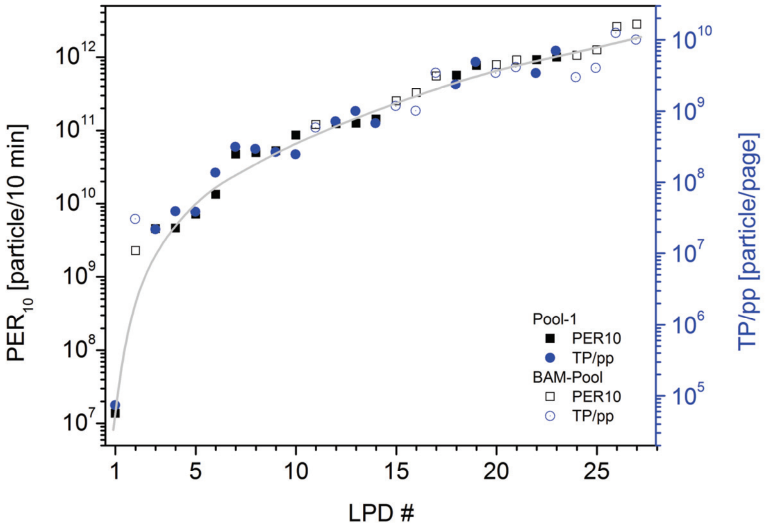

Figure 40: Particulate emissions, related to the number of printed pages (pp) or the duration of particle emission ($\Delta t = t_{stop} - t_{start}$).

There are no drastic changes in the ranking; *TP/pp* and *PER_{10}* are equally suitable as benchmarks. The statistical analysis of the ratio between *PER_{10}* and *TP/pp* is shown in the next figure, the conversion factor is 206.

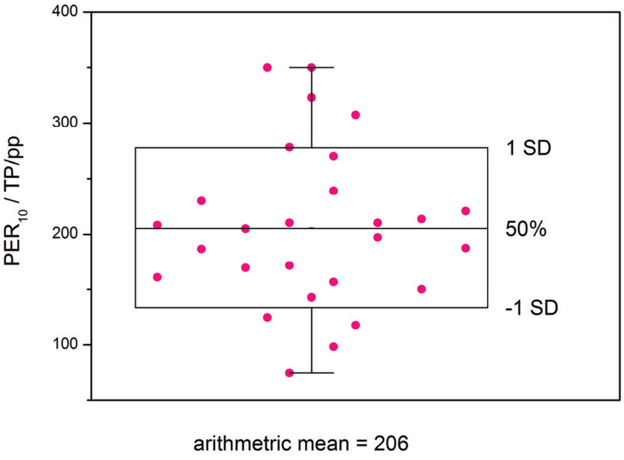

Abb. 41: Box-chart of the ratio PER_{10} / TP/pp

Tests were performed at different times during the project. Obviously, the total number of printed pages by a LPD at a certain time was variable under otherwise constant conditions. The following strong tendency outside the spread already discussed towards higher or lower values with increasing number of printed pages.

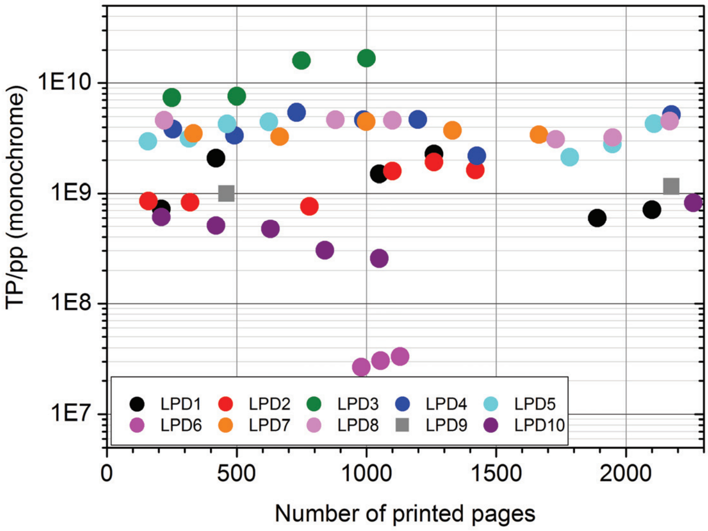

Figure 42: Particle emission as a function of the number of printed pages

Despite this positive finding, Annex S-M of the UZ-122 limits the maximum pre-loading of the LPD to be tested, since other emission tests within the award criteria are influenced by pre-loading.

4.2.3 mparison of particle size distributions

Particle size distributions were recorded by EEPS during standby, printing and follow-up phases. All spectra are enclosed in the Appendix. At this point, two extremely different spectra are compared to illustrate the range of observed spectrum shapes.

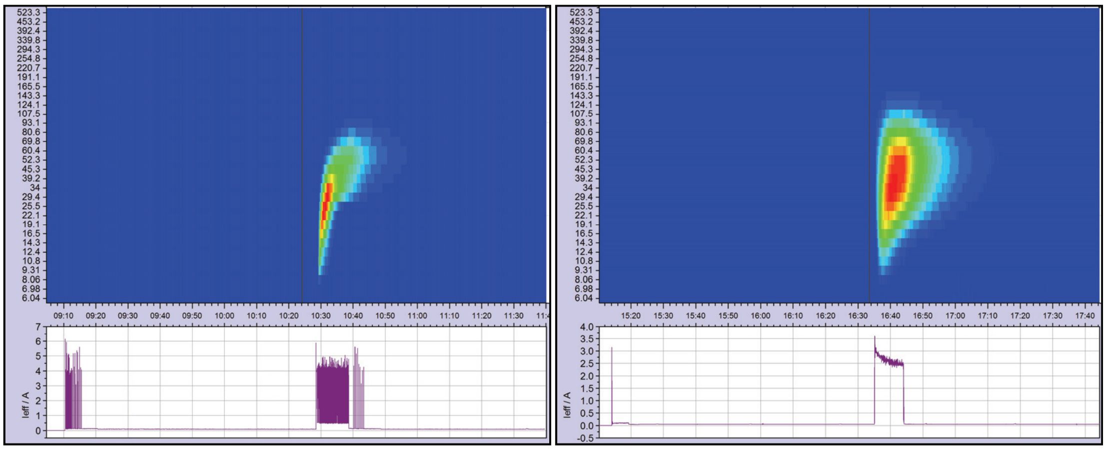

LPD 7, Spectrum type 1

LPD 10, Spectrum type 2

Vertical axes, top: Particle diameter [nm] in 32 logarithmically distributed particle size classes. Particle number concentration: linear colour codes, dark blue: lowest values, red: highest values. Horizontal axes: time [hh:mm]. Vertical axes, bottom: current consumption [Ampere].

Figure: 43: Particle size spectra of LPD7 and LPD10

Figure 43 bottom, shows the curves of current consumption for the devices. In these diagrams, both the time of switch-on and the printing phases can be recognised. Conspicuous is the different structure of current consumption which is due to different temperature regimes of the LPD fuser unit. The curves shown here are representative of the studied device pool, i.e. the LPD show either one or another type of control. The particle size distribution in LPD 7 rapidly changes its shape during the printing phase. Primarily, particles from 5-10 nm are produced; the particle size distribution then remains approximately constant at and after the end of the printing phase. This behaviour is classified as spectrum type 1. LPD 10 emits a wide-spread aerosol at the beginning, this spectrum type is referred to as spectrum type 2. In both spectra, the concentration decreases as a function of time due to the air exchange. The next figure shows the particle emission rates for LPD 10 and LPD 7.

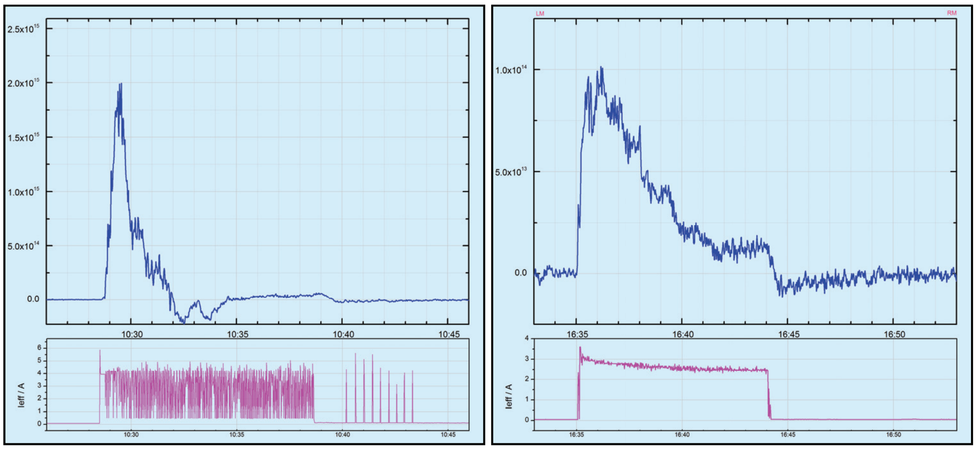

LPD 7, emission type A

LPD 10, emission type B

Vertical axes, top: particle emission rate [1/d], bottom: current consumption [Ampere].
Horizontal axes: time [hh:mm].

Figure 44: Particle emission rates *PER(t)* for LPD7 and LPD10

There are two extreme emission types to distinguish. While the emission rate of LPD 7 decreased to zero shortly after about half of the printing phase (emission type A), LPD 10 emitted over the entire printing phase at a variable rate (emission type B). The rate curves of the pool devices studied are between these extreme examples, which confirm earlier findings on other office devices for the LPD.[12] No correlation between emission types and the different curves of current consumption shown above has been found. Spectrum types 1 and 2 of the particle size distribution correlate with emission types A and B respectively.

In some measurements, the entire metrologically possible particle size range was measured from about 5 nm to 20 µm by combining EEPS and OPC. Examples of particle size distributions for LPD 3 are shown in the following figure.

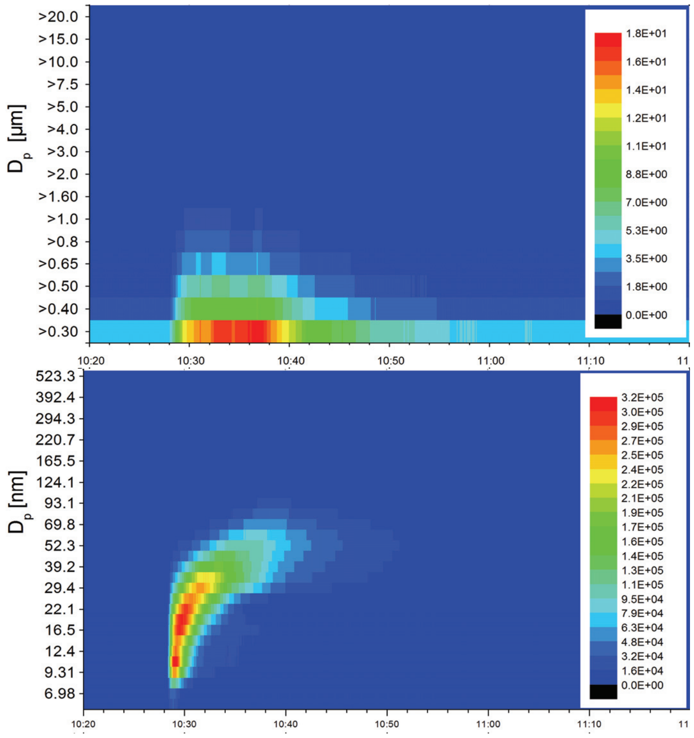

Vertical axes: particle size, horizontal axes: time [hh:mm],
colour codes: particle number concentration [cm^{-3}], top: OPC data, bottom: EEPS data

Figure 45: Particle size range from 5 nm to 20 µm for LPD 3 during and after the printing phase.

The OPC spectrum shows very small contributions in the size range from 300 nm to 1 µm. The maximum concentrations around < 20 particles/cm³ are near the lower detection limit of OPC in each size class. The maximum concentrations in the size range from 5.6 nm to about 100 nm, as measured by EEPS, are at least 4 orders of magnitude above. Measurements on all other LPD of the pool yielded comparable results: the contribution of particles > 300 nm to the total number of emitted particles can be neglected in the quantification. In the range of > 1 µm, no contributions to particle emission above the detection limit were observed. Toner powder particles with diameters > 1 µm were not detectable in aerosols typically emitted by LPD.

This finding is summed up once again in the following figure. The benchmark *TP/pp* was calculated both for the OPC range (300 nm - 20 µm) and the EEPS range (5.6 -

560 nm) for all LPD and then graphically compared. The proportion of the OPC fraction is at most 1/1000 of the EEPS fraction.

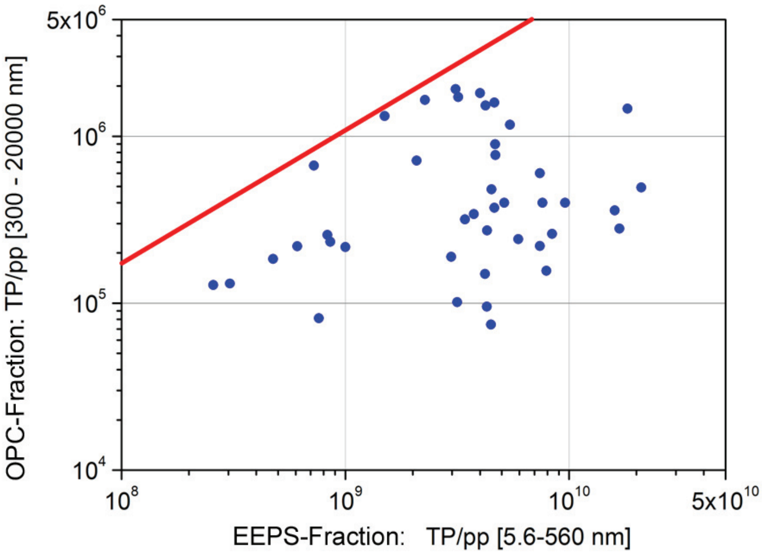

Figure 46: Comparison of the particle fraction determined by OPC with the fraction determined by EEPS using the benchmark *TP/pp*

4.2.4 Influences of methodological factors

Effect of chamber volume and air exchange on particle size distributions

The previously discussed and very different spectrum types 1 and 2 measured in emission test chambers of 1 and 5 m³ volume and air exchange rates of about 4 and 1 h^{-1} were compared and the particle size distributions failed to show any difference. Only the decay of the particle concentration in the 1 m³ chamber is faster due to a more intensive air exchange. The following figure shows the comparison; the periods of time are of equal length. As already observed for the measurand *TP,* no trend towards a systematic change in particle size spectra due to different chamber sizes was found.

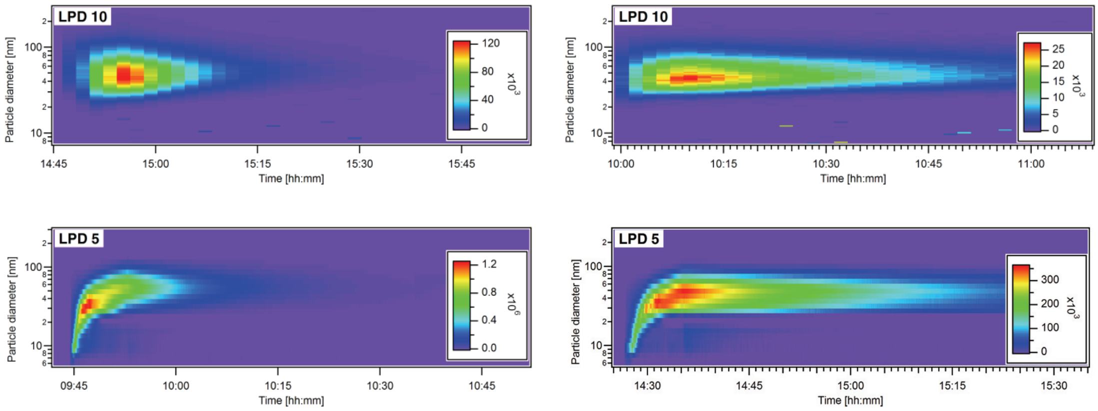

Colour code: particle number concentration [cm^{-3}]

Figure 47: Particle emission as a function of chamber size and air exchange (AE). Left: 1 m³ chamber with high AE, right: 5 m³ chamber with low AE.

Influence of aerosol measurement instruments

Figure 48 shows examples for LPD 1 and 2 to compare the measured data of two butanol CPCs (Grimm 5.414 and TSI 3775). To help distinguish, the data of the Grimm CPC were multiplied by a factor of 1.2. The curves correspond both quantitatively and in all details.

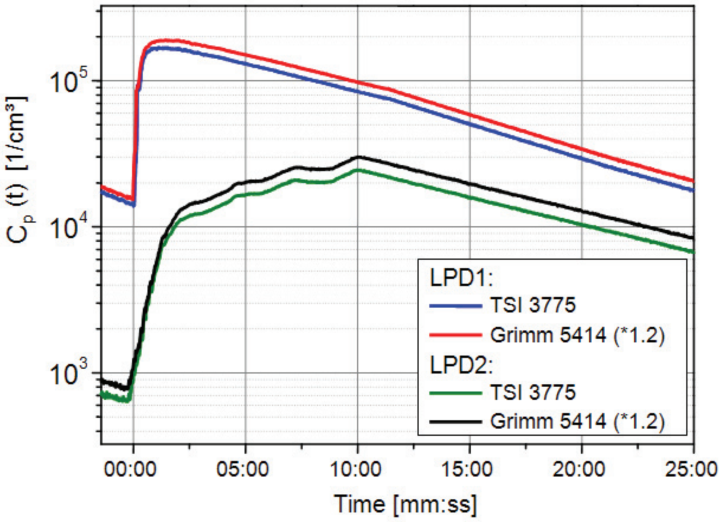

Figure 48: Comparability of two butanol CPCs

The comparison within a larger group of different aerosol measurement instruments is discussed based on the results of the interlaboratory comparison.

The following figure shows the measurement data of butanol CPCs Grimm 5414 and TSI 3775 with measured data of EEPS based on three independent measurements on LPD 4. The quantitative comparison is shown in Table 18.

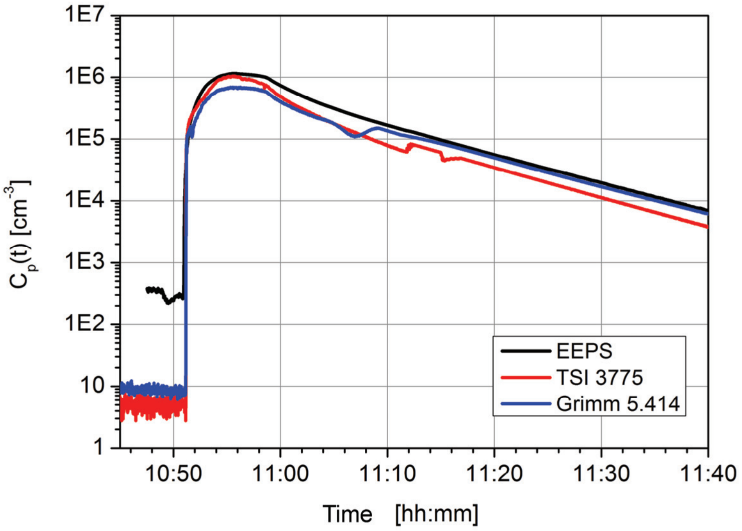

Figure 49: Comparison between butanol CPC and EEPS (emissions from LPD 4)

Table 18: Quantitative comparison between butanol CPC and EEPS

Emissions from LPD 4

	EEPS	**TSI 3775**	**Grimm 5.414**
TP/pp	5.6E9	4.0E9	3.3E9

This agreement can be considered very good in view of the discussed factors. The counting efficiency of CPCs for particles < 50 nm is influenced both by the working fluid and the physical and chemical properties of the particle surface.[54,55] For this reason, a sample comparison was conducted between a water CPC (TSI 3785) and EEPS. The

---

[54] Mordas G., Manninen H. E., Petäjä T., Aalto P. P., Hämeri K. and Kulmala M.: On Operation of the Ultra-Fine Water-Based CPC TSI 3786 and Comparison with Other TSI Models (TSI 3776, TSI 3772, TSI 3025, TSI 3010, TSI 3007). Aerosol Sci. Technol. 42 (200) p152-158

[55] Petäjä T., Mordas G., Manninen H., Aalto P. P., Hämeri K. and Kulmala M.: Detection efficiency of a water-based TSI Condensation Particle Counter 3785. Aerosol Science And Technology 40 (200) p1090-1097

EEPS is insensitive to the properties of the particle surfaces due to its operating principle.

Comparing the measured signals ($C_p(t)$) it can be seen that the water CPC shows a significant reduction in counting efficiency when the focus of emission is on particles with a diameter ≤ 50 nm

Figure 50, left). When particles > 50 nm contribute to the size distribution the deviations are significantly smaller (Figure 50 right). The reduced counting efficiency is due to the hydrophobic surface properties of the aerosols which mainly consist of waxes. A correction function would be difficult to determine because of the size effect. Water CPCs are therefore unsuitable for measuring particle emissions from office devices.

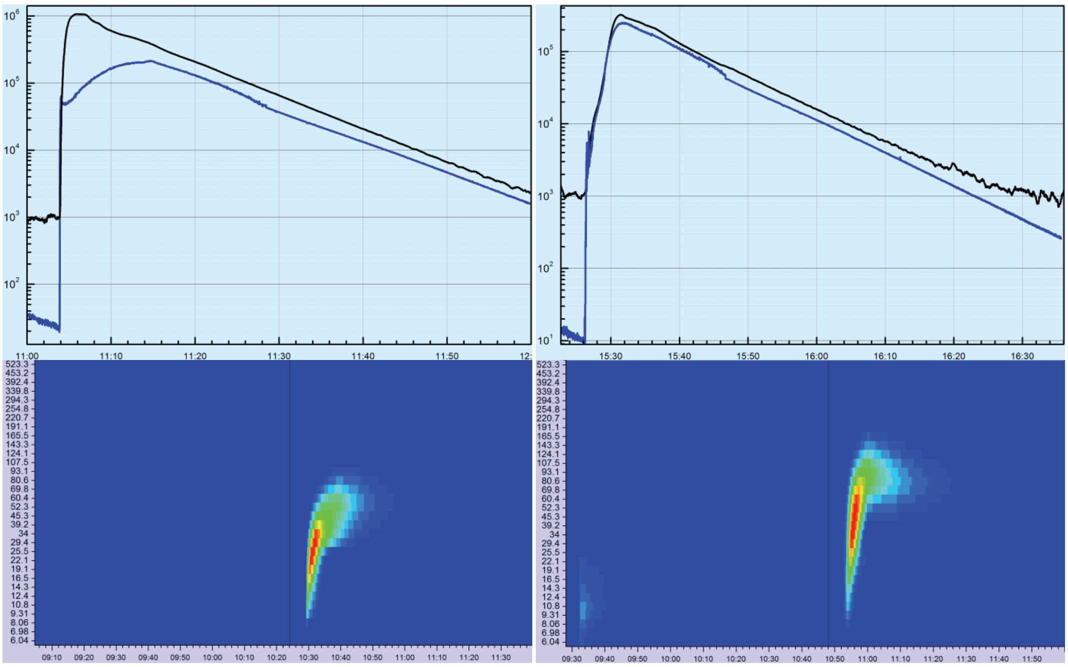

Top: $C_p(t)$ curves for EEPS (black) and W-CPC TSI 3785 (blue) in the printing and follow-up phases. Bottom: Particle size distributions in the stand-by, printing and follow-up phases. Vertical axes: particle size [nm], colour codes: particle number concentration. Horizontal axes: time [hh:mm].

Figure 50: Effect of counting efficiency of a water-based CPC, depending on the particle size, as shown by example spectra of LPD 7 (left) and 9 (right)

BAM's EEPS was compared with different CPCs in a Swiss Federal Office of Metrology (METAS) calibration workshop. A CAST (Combustion Aerosol Standard) generator produced soot particles of different diameters and number concentrations at a test site.

The data from this workshop were used to develop a correction function for EEPS. The following figure illustrates the effect of this correction compared with the CPC's measurement data. For 90 parallel measurements of EEPS and B-CPC covering about 4 orders of magnitude, the corrected EEPS data have shown a much better agreement.

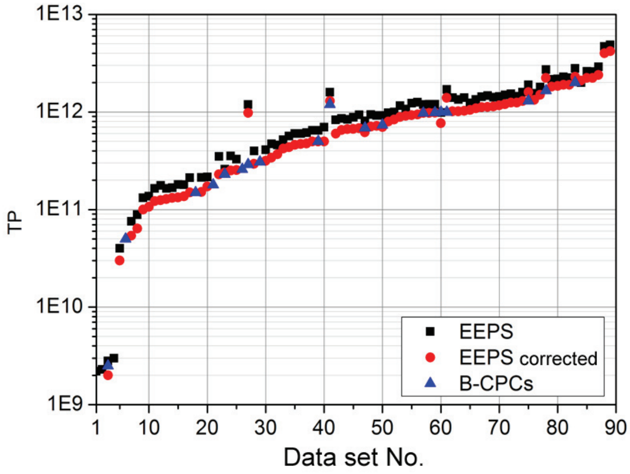

Figure 51: Benchmark *TP* calculated from uncorrected and calibration-corrected EEPS measurement data in comparison with B-CPC data

Influence of fitted auxiliary parameters and evaluation algorithms on quantitative results

The numerical model for quantitative results was introduced in Section 4.2.1. Particle loss factor β was used as an empirical quantity determined by a fit for each evaluation. The following figure shows the plot of values determined from the test data for BAM's 1 m³ and 5 m³ chambers.

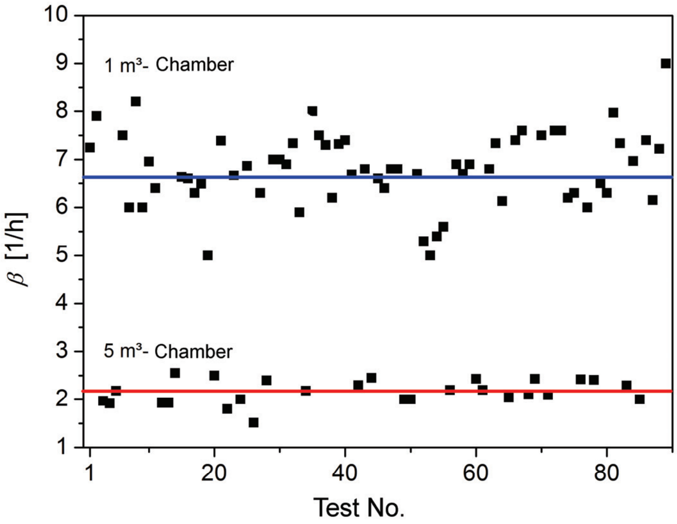

Figure 52: Particle loss factor β [1/h] for BAM's 1 m³ and 5 m³ emission test chambers

Although the values measured in the 1 m³ chamber scatter somewhat stronger than those in the 5 m³ chamber, these variations in β only slightly influence calculated results in comparison to other factors contributing to dispersion, i.e. less than 20 %.

The total number of emitted particles *TP* used in chapter 4.2.1 (see Equation 4) can also be calculated using the following method of approximation when the times t_{start} and t_{stop} were previously determined:

1. The difference ΔC_p [cm^{-3}] between the times t_{start} and t_{stop} is calculated from the data set of the smoothed particle number concentration $C_p(t)$:

$$\Delta C_p = C_p(t_{stop}) - C_p(t_{start}) \tag{7}$$

2. The arithmetic average C_{av} [cm^{-3}] between times t_{start} and t_{stop} is calculated from $C_p(t)$. Index n stands for the number of measurement values between times t_{start} and t_{stop}.

$$C_{av} = \frac{\sum_{i=1}^{n} C_{p,i}}{n} \tag{8}$$

3. *TP* is then given by:

$$TP = V_C \left(\frac{\Delta C_p}{t_{stop} - t_{start}} + \beta \cdot C_{av} \right) (t_{stop} - t_{start}) \tag{9}$$

ΔC_p: difference of $C_p(t)$ between t_{start} and t_{stop}, [cm^{-3}]
C_{av}: arithmetic average of $C_p(t)$ between t_{start} and t_{stop}, [cm^{-3}]
V_C: test chamber volume [cm³]
$ß$: particle loss rate [s^{-1}].

The advantage of this method is a somewhat simpler calculation; therefore it was applied to the test method in Annex S-M of UZ 122. A calculation of *TP* does not make sense for $\Delta C_p \leq 1000\ cm^{-3}$ because all relevant quantities cannot be determined with the required accuracy from the measured values. Annex S-M of UZ 122 suggests reporting the result of a measurement as "not quantifiable" for this case which is illustrated in the following figure.

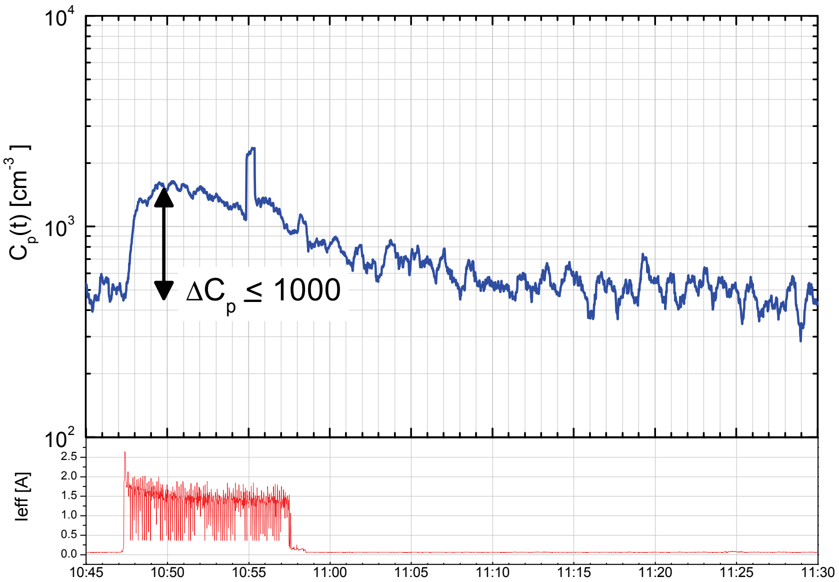

Vertical axes, top: particle emission rate [1/d], bottom: current consumption [Ampere].
Horizontal axes: time [hh:mm].

Figure 53: Particle number concentration during and after the printing phase for an LPD with very small particle emission

4.2.5 Summary of Quantitative Particle Emission Measurements

Quantitative measurements have shown that particulate emissions from LPD differ in their amount and size distribution of particles from each other. Contributions above 1 µm particle diameter to the number of emitted particles are at the detection limit of the counting measurement methods used and can be neglected compared to contributions from the size range up to about 300 nm. Award criteria for the test as per UZ 122 differentiated according to the particle size classes are not feasible because of differences in particle size distributions and the rapid changes in time observed. Therefore, the accumulated number concentration $C_p(t)$ over the relevant particle size is suggested as the primary measurand. As previously shown benchmarks such as *TP/pp* and PER_{10} can be calculated. Both benchmarks are suited for a comparison of particulate emissions from LPD and the determination of an award criterion. The testing and evaluation method presented here was tested in an interlaboratory comparison which will be discussed in the following chapter. Considerations about measurement errors and the way they can be taken into account in checking the award criteria include the results of this interlaboratory comparison and are therefore described in detail in Section 5.3.

5 Interlaboratory Comparison

The procedure currently developed by BAM and described in the draft of Annex S-M of UZ 122 Blue Angel awarding criteria as well as the Standard ECMA-328[56] (latter developed and adopted with a time flow) describe a particle number concentration measurement method. Measurements of fine and ultrafine particle emissions using counting methods to create and check assessment criteria or assign quality labels are currently a technically demanding task, since adequate national or international standards on the calibration of measurement instruments have only recently become available or are still being developed.[57,58] The European EURO 6 vehicle emission control[59] gives an important first example for count-based measurement of UFP emissions to regulate environmental pollution. The methodological part of EURO 6 which considers emissions > 23 nm particle diameter, was developed by the Particle Measurement Programme Working Group of UN/ECE[60]. An important aspect was to ensure the intra- and inter-laboratory comparability and quality of the measurements by interlaboratory comparisons. [61,62] Actually occurring measurement uncertainties and the problems of reproducibility (comparability and repeatability) could only be determined on an empirical basis.

---

[56] ECMA-328, Dezember 2010, 5th Edition, Determination of Chemical Emission Rates from Electronic Equipment, ECMA, Genf

[57] ISO 15900, 2009, Determination of particle size distribution - Differential electrical mobility analysis for aerosol particles

[58] ISO 27891 - Entwurf, Aerosol particle number concentration - Calibration of condensation particle number counters

[59] Verordnung (EG) Nr. 715/2007 vom 20. Juni 2007 über die Typgenehmigung von Kraftfahrzeugen hinsichtlich der Emissionen von leichten Personenkraftwagen und Nutzfahrzeugen (Euro 5 und Euro 6) und über den Zugang zu Reparatur- und Wartungsinformationen für Fahrzeuge

[60] Homepage der Arbeitsgruppe: http://live.unece.org/trans/main/wp29/wp29wgs/wp29grpe/pmp22.html

[61] Giechaskiel B. et.al.: Particle Measurement Programme (PMP) Light-Duty Inter-Laboratory Exercise: Repeatability and Reproducibility of the Particle Number Method, Aerosol Science and Technology 42, Iss. 7 (2008)

[62] Giechaskiel B. et.al.: Evaluation of the particle measurement programme (PMP) protocol to remove the vehicles' exhaust aerosol volatile phase, Science of the Total Environment Vol. 408, Iss. 21 (2010)

A reproducibility analysis based only on a single laboratory would have underestimated the differences. It is also known from a variety of test workshops and device comparisons of the past years[63] that significant deviations may occur even under well-controlled conditions and in narrowly specified aerosols.

Against this background of experience it was reasonable to carry out practical tests to ensure the quality of particle emission measurements from office devices within an interlaboratory comparison prior to the consultation about the new UZ-122 award principles and simultaneously with the discussions on the award criteria. A corresponding extension of the UFOPLAN research project was given unanimous approval by the project's expert group and the Federal Environment Agency. The data obtained in the interlaboratory comparison, along with other data of this current study, offer the possibility for estimating the measurement uncertainty of the test method.

5.1 Quantitative Studies in the Interlaboratory Comparison

Participants

For the interlaboratory comparison, 5 participants (one laboratory from the U.S. and Japan, 3 participants from Germany) were selected from among testing laboratories accredited under the currently valid UZ-122. The number of institutions interested in participating was higher than the maximum possible number of participants; manufacturer-independent institutions were given priority. The participants including BAM will be hereafter anonymously called Laboratory 1 to Laboratory 6; the numbering does not correspond to the chronological order of the measurements.

The participants' commitment, especially, in the elimination of unexpected problems and the rapid performing and evaluation of the tests and the provision of the measured data are sincerely acknowledged.

---

[63] Kalibrierworkshops METAS, Schweiz, http://www.metas.ch/metasweb/Fachbereiche/Partikel_und_-Aerosole

Measurement Devices and Equipment, Office Devices and Test Methods

The following particle measurement technology and test chambers were available at the laboratories:

Table 19: Equipment of the participants in the interlaboratory comparison

Labo-ratory	**Particle measurement technology**	**ETC**	
		Size [m³] / wall material	Nominal air exchange Prep / printing phase [h^{-1}]
1	B-CPC (TSI 3776) FMPS [1]	2 / stainless steel	1 / 4
2	B-CPC (Grimm 5.414) W-CPC (TSI 3785) EEPS [1] SMPS (TSI 3936)	1 / stainless steel 5 / stainless steel	1 / 4 1 / 1
3	FMPS [1]	1 / glass	1 / 3
4	B-CPC (Grimm 5.403)	1.25 / stainless steel	N/A
5	B-CPC (Grimm 5.414)	1 / stainless steel	5 / 4 - 5
6	B-CPC (TSI 3775) EEPS [1]	1 / stainless steel	1 / 4

[1] TM TSI Inc.

CPCs using butanol as a work fluid were used. LPD 8 and 10 were selected for the interlaboratory comparison from the office device pool established in the research project which will be referred to as D8 and D10. Selection criteria were:

1. significant difference in the amount of emitted particles per printed page,
2. different scattering of the emission data repeatedly measured in BAM,
3. the same printing speed and the almost equal number of pages in the printing phase,
4. the possibility to compare a colour and a monochrome printer, and
5. relatively low vulnerability to failure in comparison to other devices.

The following table summarises the most important data of these devices:

Table 20: Data from the office devices used in the interlaboratory comparison

Device	**D8**	**D10**
Function(s)	Printer	Printer, copier, scanner, fax
Type Volume [m³]	Desktop 0.138	Desktop 0.110
Printing speed [p /min] colour monochrome	21 21	N/A 21
Ventilation type	Blower	Blower

The term "blower" type ventilation is used for devices in which a fan expels air through at least one opening in the casing.

The devices were equipped with OEM toner cartridges and sent in their original packaging to the laboratories. As in the previous BAM tests, the paper type DeskTop X'tensa 80 g/m² was used exclusively (manufacturer: IGEPA, sales: Roy Schulz GmbH). All papers came from one delivery and were distributed to the participants from BAM's stock and shipped together with the devices. The intention was to use devices that had been pre-loaded before the interlaboratory comparison by more than 1000 pages printed in tests at BAM. Due to irreparable damage during transport, replacement units had to be procured while the interlaboratory comparison was running. Thus an additional aspect, i.e. the serial comparison of devices of the same type, emerged. This aspect has not yet been studied systematically because of the significant cost and time requirement.

In the following table the original pre-loaded office devices from the BAM pool are marked with #1, the devices procured later on are numbered consecutively. The table lists the serial devices used by the laboratories.

Table 21: Distribution of the series office devices among the participating laboratories

Laboratory	D8	D10
1	#1	#3
2	#1	#1
3	#1	#1
4	#1	#2
5	#2	#2
6	#2	#4
Control test	#1	#2

The participants of the interlaboratory comparison were required to perform at least one particle emission test in accordance with Section 8.6 of the Standard ECMA-328 on the office devices and evaluate the results according to the standard. Some laboratories have conducted multiple tests. The original measurement data were provided to BAM for a second evaluation. After the devices were returned to BAM, control measurements of particulate emissions were performed there. Because of damage suffered, it was not possible to perform control measurements on all series devices.

5.2 Results

The tests were successfully performed in accordance with ECMA-328 in all laboratories. Some shipments, as already mentioned, especially those transported by air cargo, exhibited damage and, in some cases, very significant contamination due to leaking toner powder. Despite precautionary measures such as previously removing and tightly packing all consumables and toner containers, it was not possible to completely avoid contamination. The affected devices were cleaned in the laboratory before the measurements. No external specialist service was commissioned. No correlation has been found between the contamination and the results of the particle emission measurements. In particular, no significant increase in pollution caused by particulate emissions has been observed.

Unless otherwise stated, the data in Table 22 are based on the evaluations of measurand TP (Total Number of Emitted Particles) as defined by ECMA-328. The number of pages printed and thus the printing phase length which was chosen by the laboratories differed slightly: 190-250 pages were printed in the measurement on D8, and 210-250 pages in the measurement on D10. Therefore, the ratio of *TP* to the page number in the printing phase *TP/pp* (Total Particles per printed pages) will be used as benchmark in Table 22 and below. In two cases, there were errors in the analysis: in one case, the evaluation method according to ECMA-328 was carried out incorrectly, and in the second case, the analysis was carried out correctly, but the protocol did contain a trivial calculation error in the result representation.

Table 22: Test results of the interlaboratory comparison

Laboratory	**D8 (f)** TP/pp	**D10 (b/w)** TP/pp	**Test flow**	**Result of calculation**
1	8.3E9 7.4E9	3.2E9 * 8.8E8	OK	OK
2	4.2E9 5.9E9 4.3E9 5.1E9	8.2E8 1.1E9 * 6.3E8 5.1E8 3.1E8 2.6E8 4.8E8 6.2E8	OK	OK
3	5.3E9	1.1E8	OK	OK
4	3.5E9 3.4E9 3.2E9	2.2E8 1.6E8 2.0E8 2.1E8 1.5E8	Problem in selection and reproducibility of the printing phase length	Error [1]
5	3.5E9 3.3E9	8.5E7 * 1.6E8	OK	Error [2]
6	6.4E9	3.7E8	OK	OK
Check measurement	5.5E9	4.7E8	OK	OK

[1] Error in the calculation, data analysis was performed only by BAM
[2] Error in the presentation of results, correction by BAM
* Not included in the analysis as outlier.

Figure 54 shows a comparison of all results by laboratories. The control values were measured after the devices were returned to BAM. Three values for D10 marked in red are considered device-specific outliers since they are far from the average of all laboratories and the corresponding values of the laboratories for D8 do not show abnormality. Based on the test results of the interlaboratory comparison, it has been found that particulate emissions from devices D8 and D10 show a significant difference. Contributions to the observed dispersion of the test results are discussed below.

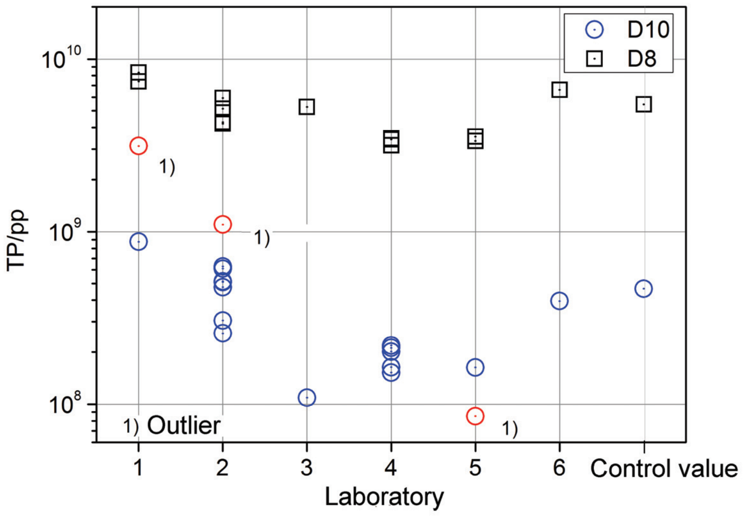

Figure 54: Comparison of individual results of the laboratories

In Figure 55, the results obtained by the laboratories are compared with the control evaluation of the same data by BAM for D8 and D10. The agreement is very good.

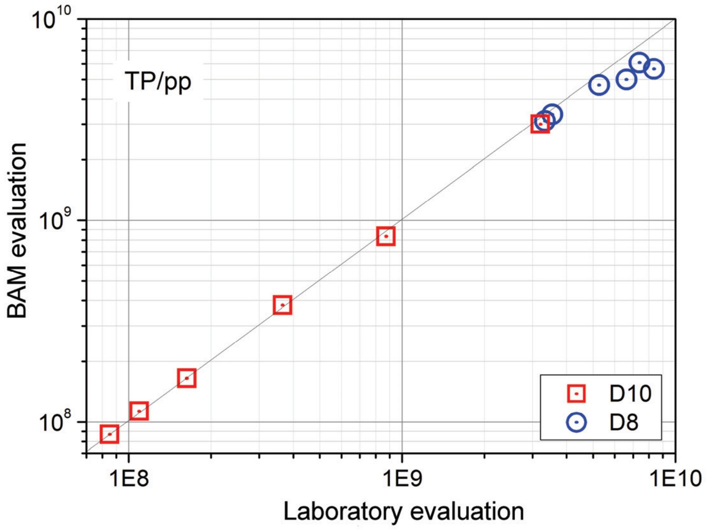

Figure 55: Comparison between laboratory and control evaluation

Figure 56 gives a comparison of the results sorted according to the aerosol measurement instruments used; outliers are not plotted. Simultaneous measurements using different aerosol instruments were not part of the interlaboratory comparison. The generally good agreement between the devices TSI 3775 (CPC) and EEPS is conspicuous. Condensation particle counters 2) and 3) have however, provided lower values at narrow dispersions.

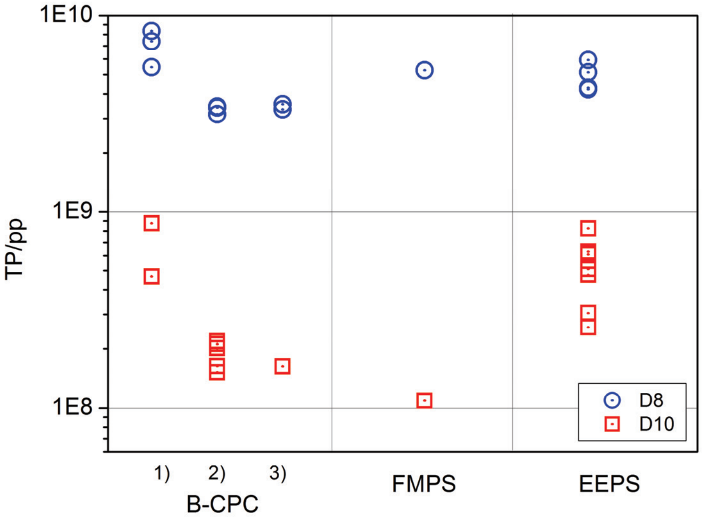

Figure 56: Comparison of the results of various aerosol measurement instruments: 1) TSI-CPC 3775; 2) Grimm-CPC 5.403; 3) Grimm-CPC 5.414

If the dispersion of data is analysed separately according to measurement instruments, it becomes clear that the individual reproducibility of the emissions for the two devices is very different. The series influence on the dispersion of the results is within the standard deviation of the individual single values of a device. The relationship is shown in Figure 57. For a better comparison, measurements of relatively well-matching instruments EEPS and TSI CPC 3775 were used only for D10. The scattering effect of different instruments in this presentation is therefore small. For D8, all available measured values have been taken into account.

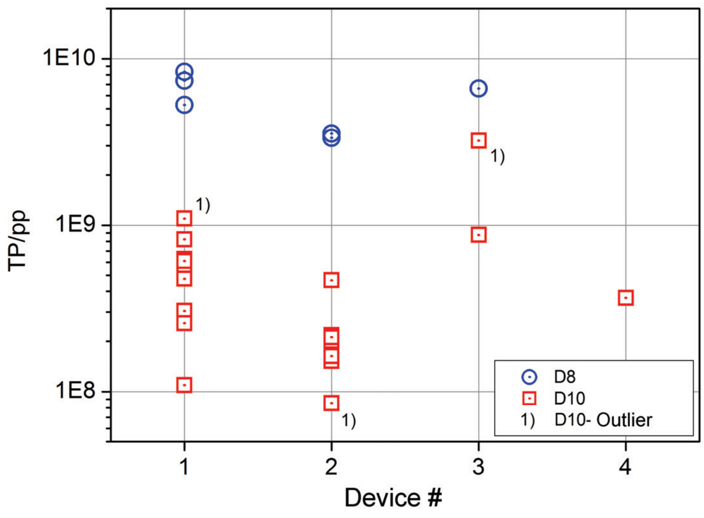

Figure 57: Comparison of results from series devices. Only readings of the measurement instruments EEPS and TSI 3775 are considered for D10; outliers are also presented.

Figure 58 shows the influence of chamber size on the results based on measured values from two laboratories. The measured values of the CPCs Grimm-5.403 and -5.414 were corrected by a constant factor to compare the dispersion over a broader data pool and indicated by filled symbols; outliers are not included.

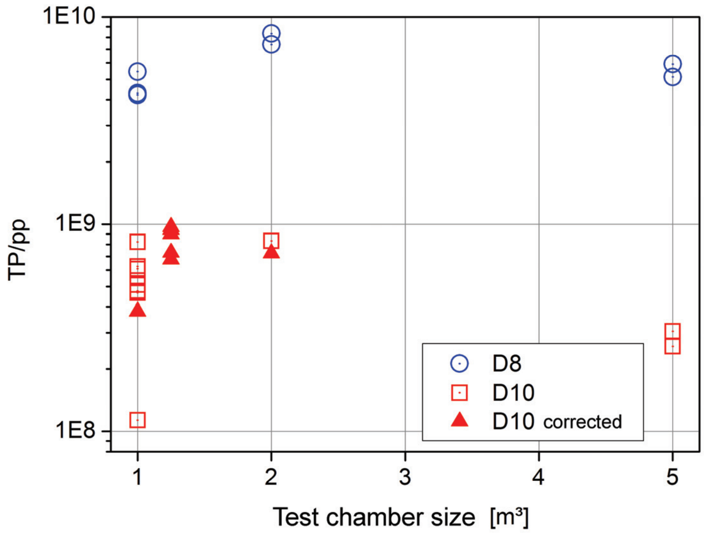

Figure 58: Comparing the results from test chambers of different sizes

There are no strong correlations and no trend between measured values and chamber sizes.

In summary, the following factors contribute differently to the dispersion of the measurement results:

1. stability of the evaluation algorithms of the test method,
2. reproducibility of particulate emissions
   (individual device-specific dispersion),
3. series influence of the dispersion of particulate emissions,
4. test-object-load-dependent influences on particle emissions,
5. differences among laboratories due to measurement technology.

Factor 1 can be neglected, the evaluation method is stable and the results are independent of the evaluator. Factor 2 is dominant: all D8 series devices have a relatively low dispersion, while a much greater dispersion can be observed in all D10 series devices. The serial effect is within the order of magnitude for the reproducibility of the emissions, there was only one obvious outlier in one of the D10 series devices in the interlaboratory comparison. Factors 2 and 3 cannot be separately evaluated on the basis of the available data pool. Factor 4 is not dominant: load-dependent effects, in particular, changes in the particulate emission behaviour with the total number of printed pages cannot be ruled out, a good agreement of the control measurements with previously measured values, however, indicates that this effect is not very strong. A systematic trend cannot be seen either. The test method UZ-122 Annex S-M also stipulates a limit on this factor by restricting the device pre-load. Factor 5, i.e. the measurement technology deviation among the laboratories, contributes clearly to the dispersion, especially in the case of D10. Here, the size of the test chamber and to a greater extent the deviations of the measurement instruments play an important role. This factor, however, is comparable with the reproducibility of the previously discussed issues for both office devices.

Conclusion

The observed variations between laboratory results are significantly influenced by the relatively poor reproducibility of particulate emissions and by the deviations in measurement technology. While reproducibility of the emissions is a direct, non-modifiable property of the test object, deviations in measurement technology – in particular instruments differences – can in principle be compensated for by correction factors. The extent of the interlaboratory comparison does not allow a detailed multifactorial analysis which would facilitate such a correction. A reduction of modifiable scattering factors is desirable but not essential for using the method in product testing.

The experiences of the interlaboratory comparison make possible a conservative estimation of measurement uncertainty. Thus the test method is applicable if no too severe demands on measurement uncertainty and quantitatively significant discernibleness are made. This must be considered in determining award values and award criteria.

The test reports have not reported any fundamental problems during the test. The errors in the result calculation gave rise to a correspondingly improved guidance in Annex S-M of UZ-122.

All in all, the interlaboratory comparison is considered as a proof that the Standard ECMA-328 is a useful basis for the test method UZ-122 Annex S-M.

5.3 Estimation of Uncertainty for a Single Measurement according to UZ-122, Annex S-M

The measurement of particle emission is a single measurement in each product test according to UZ-122, Annex S-M. Those factors contributing to the measurement uncertainty of this single measurement cannot be individually quantified due to methodological conditions. This excludes an individual evaluation of measurement uncertainty for each individual measurement. A type B evaluation of measurement uncertainty according to GUM (Guide to the expression of Uncertainty in Measurement)[64] is feasible under the condition that the dispersion of the measured values can realistically be estimated, for which the available data can be used. For two test objects, there are about 20 measurement results available obtained under comparable conditions from the interlaboratory comparison and BAM's measurements. Based on these data, two estimates of measurement uncertainty will be made in the following which can be used to estimate the maximum measurement uncertainty of a single measurement according to UZ-122 relying on a conservative interpretation.

---

[64] Guide to the expression of Uncertainty in Measurement GUM (JCGM 2008), see also the German draft standard DIN V ENV 13005 (current edition:1999-06)

5.3.1 Estimation of Uncertainty without Knowing the Distribution of Measured Values

To analyse the dispersion, the statistical parameters listed in Table 23 were calculated from the measurement data of Table 22. Those marked as outliers were not taken into account:

Table 23: Statistical parameters of the results of the interlaboratory comparison

Parameter		**D8** (color) TP/pp	**D10** (monochrome) TP/pp
Arithmetic average:	q	4.6E9	4.9E8
Maximum single value:	x_{max}	8.3E9	8.8E8
Minimum single value:	x_{min}	3.3E9	1.1E8
Range of all measured values:	Δ_X	5.0E9	7.7E8
Maximum range within a series:	Δ_S	5.2E9	3.0E8
Maximum range within a laboratory:	Δ_L	1.7E9	3.7E8

In a Type B evaluation of measurement uncertainty according to GUM, Section 4.3.7, a maximum interval is estimated by a width in which all values are practically with a probability of 1. An estimate of uncertainty is then performed by not assuming a continuous distribution of measured values (e.g., normal distribution or log-normal distribution). The measurement uncertainty is obtained from this interval as:

$$u = \frac{x_{max} - x_{min}}{\sqrt{12}} \tag{10}$$

The expected value of the measurand is then the midpoint of the interval:

$$m = \frac{x_{max} + x_{min}}{2} \tag{11}$$

Based on a comparison of 10 office devices, the assumption is justified that device D10 is a representative of the expected maximum dispersion of the measurement results. The maximum uncertainty interval of the measurement results for D10 can therefore be estimated as:

$$u_{max} = {}^{\Delta x_{D10}}\!\big/_{\sqrt{12}} \tag{12}$$

where the value Δ_{XD10} is taken from Table 23. The relative uncertainty for a single measurement of particulate emission according to UZ-122, Annex S-M, is obtained – estimated as maximum – as:

$$\delta = {}^{u_{max}}/_{m_{D10}} = 0{,}45 \tag{13}$$

For a single measured value x_i , thus the uncertainty u and confidence interval can be given as:

$$u = 0{,}45 \cdot x_i \tag{14}$$

and

$$[(x_i - u) \leq x_i \leq (x_i + u)] \tag{15}$$

As a result of the interlaboratory comparison, this maximum error analysis indicates that the particulate emissions of the two devices D8 and D10 were significantly different.

5.3.2 Estimation of Uncertainty Knowing the Distribution of Measured Values

The data in Table 22 were used for D10 as "worst case" for the dispersion analysis. Outliers were not considered. As the frequency analysis shows, the measured values rather tend to follow a lognormal distribution than a linear normal distribution. This is illustrated in the following figures:

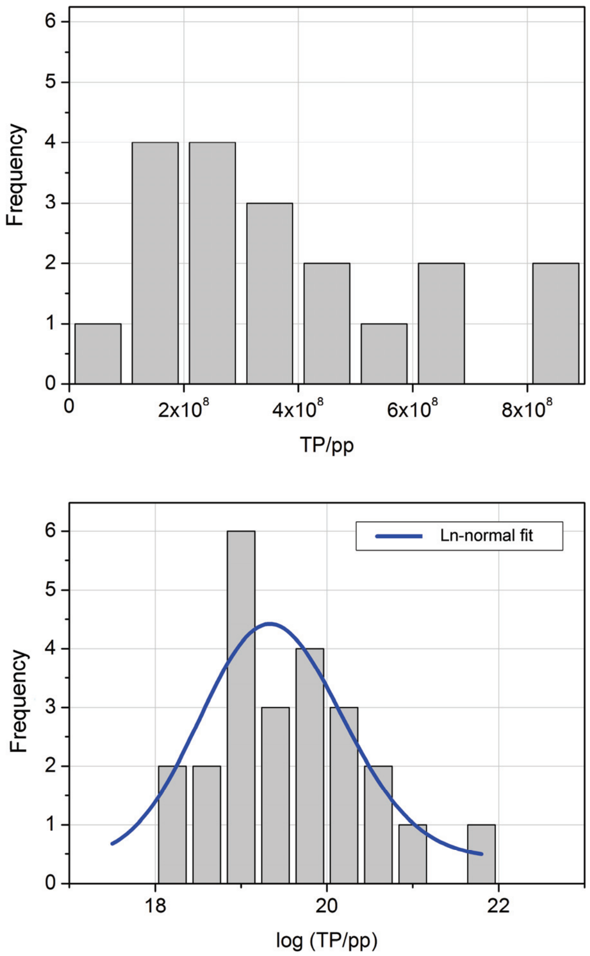

Top: frequency distribution of the benchmark TP/pp on a linear scale
Bottom: frequency distribution of the benchmark TP/pp on a logarithmic scale
Blue curve: fitted lognormal distribution (natural logarithm)

Figure 59: Frequency distribution of the benchmark TP/pp for D10

The parameters of the fitted ln-normal distribution for D10 are:

Median: $\mu = 19.45$

Std. deviation: $\sigma = 0.6924$

These parameters can be re-transformed to the linear scale by the following formulas: [65]

$$\sigma^* = e^{\sigma} \quad \text{and} \quad \mu^* = e^{\mu} \tag{16}$$

σ^* is called *multiplicative standard deviation*. The error intervals about μ* then become:

$$\left[{}^{\mu^*}/_{\sigma^*} \leq \mu^* \leq \mu^* \cdot \sigma^* \right] \tag{17}$$

for significance level 68.3 %, and:

$$\left[{}^{\mu^*}/_{(\sigma^*)^2} \leq \mu^* \leq \mu^* \cdot (\sigma^*)^2 \right] \tag{18}$$

for significance level 95.5 %.

The re-transformed values are:

Median of the benchmark TP/pp:	$\mu^* = 3E8$
Std. deviation:	$\sigma^* = 1.9$

For the significance level 95.5 %, the maximum estimate of the error interval of a single measurement x_i of particulate emission according to RAL-UZ-122, Annex S-M becomes:

$$[\, 0.3 \cdot x_i \leq x_i \leq x_i \cdot 3.6 \,] \tag{19}$$

---

[65] Limpert E., Stahel W. A., Abbt M.: Log-Normal Distributions across the Sciences: Keys and Clues, BioScience, Vol. 51, No. 5 (2001) p341-352

5.3.3 Uncertainty and Compliance of Test Values

So as to compare the measurands with award values, it must be proved that the measurand is within certain limits. When dealing with award values, either the uncertainty of the analytical result can be taken into account when assessing the comparison or an award value can be specified in view of the typical measurement uncertainty.[66] For practical reasons, the second strategy will be pursued in this study. The previously determined maximum uncertainty of the award value is taken as the tolerance range. In this procedure, it is not necessary to carry out an error calculation for each single product test. Figure 58 shows a simple approach to compare a measurement result with an award value.[67]

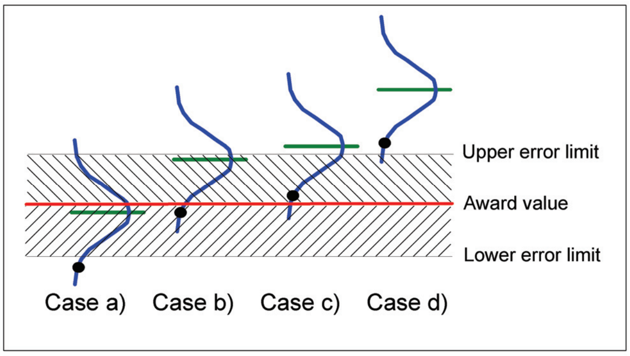

Figure 60: Measurement uncertainty and distribution of measured values – complying with or exceeding an award value

The award value is shown in Figure 60 as a red line along with its tolerance range. Possible measured values and their distributions are indicated by dots or by blue lines. The corresponding maximum expected values, i.e. the theoretically expected mean values of many individual measurements are marked in green. It is assumed in a conservative interpretation that the measuring points are in each case at the lower limit of the 95.5 % probability interval of the distributions. Cases a) and d) describe then a clear deceeding or exceeding of the award value, since the corresponding expected values are likely to be below or above the award value. In case b), the measured value

---

[66] EURACHEM/CITAC Guide (2004) "Quantifying Uncertainty in Analytical Measurement" Second Edition

[67] EURACHEM/CITAC (2007): Use of uncertainty information in compliance assessment. EURACHEM/CITAC Guide, First Edition

is less than or equal to the award value. The expected value is then – as indicated – still within the tolerance interval. In case c), this is no longer the case: the expected value is above the tolerance range with a probability of > 50 %.

Cases b) and c) can be regulated by convention. The following approach is suggested for the interpretation of measurement results for the award criteria RAL-UZ-122 (see source [67], Appendix A, Figure A1 for possible alternative arrangements): The measurement uncertainty is partly interpreted in favour of the test object. In cases c) and d), the award value has not been adhered to. In cases a) and b), an award value has been complied with. This regulation is independent of the absolute position of the upper limit of the tolerance range. However, the maximum accepted difference between expected value and award value is determined by the upper limit of the tolerance range. As discussed in 5.3.2, this is – estimated as a maximum at the significance level of 95.5 % – at 3.6 times the award value if a log-normal distribution is assumed for the measured values. If, however, the measured values are assumed to have a uniform distribution, the upper tolerance limit is at 1.45 times the award value. Arguments can be found for both interpretations.

To compare the award value with a measured value, it should be specified as a power of ten and rounded up to one decimal place (e.g. 1.5E8 instead of 0.15E9 or 15E7).

6 Supplementary Figures

6.1 Supplementary Figures to Chapter 4.1

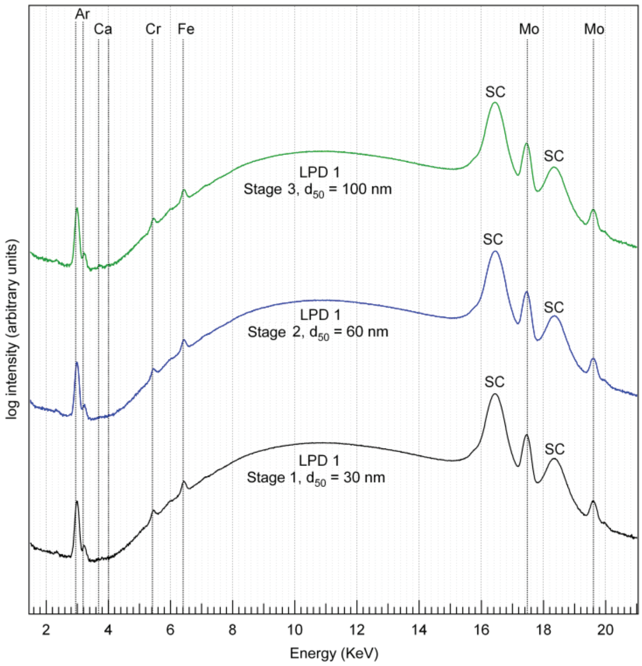

Figure 8-1: XRF spectra of the deposited particles of LPD 1 with an attribution of the detected elements.

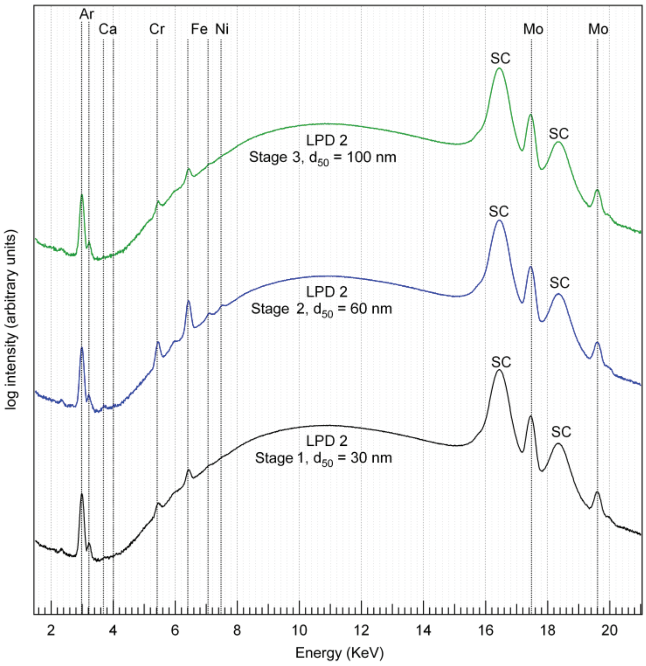

Figure 8-2: XRF spectra of the deposited particles of LPD 2 with an attribution of the detected elements.

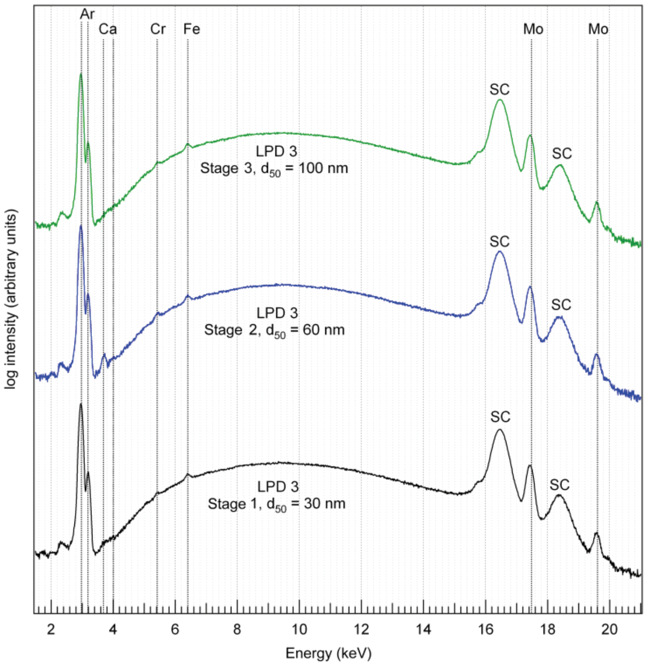

Figure 8-3: XRF spectra of the deposited particles of LPD 3 with an attribution of the detected elements.

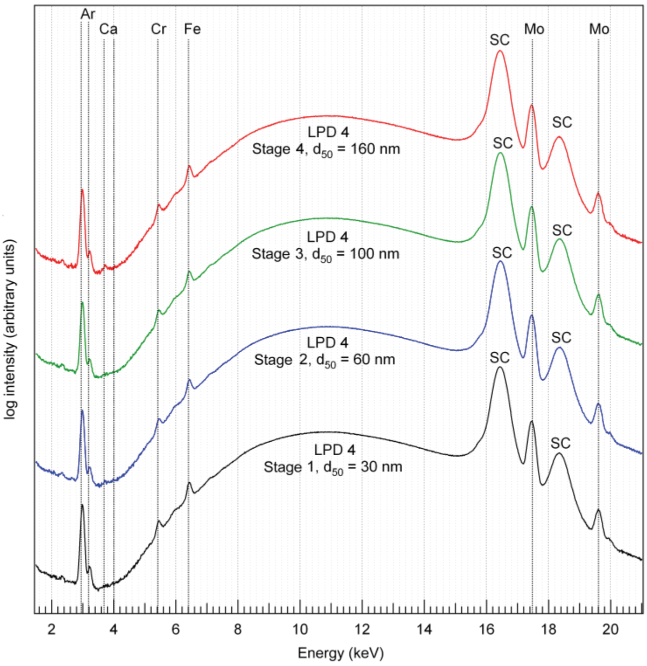

Figure 8-4: XRF spectra of the deposited particles of LPD 4 with an attribution of the detected elements.

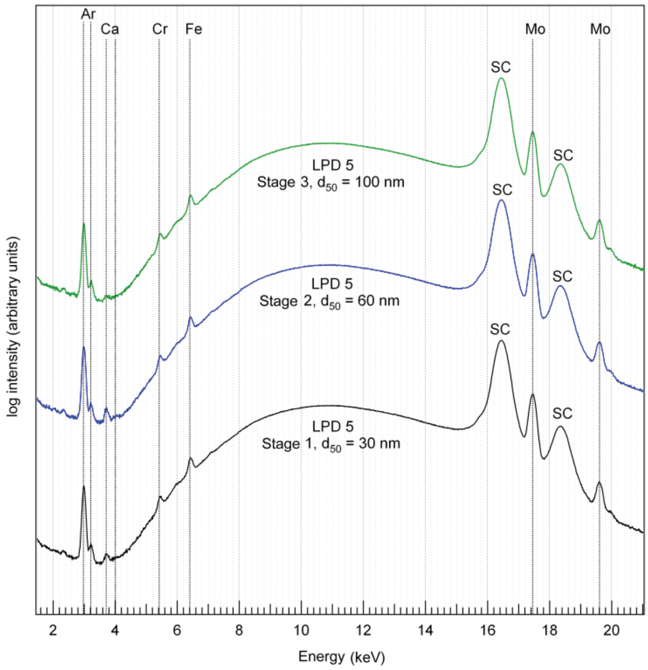

Figure 8-5: XRF spectra of the deposited particles of LPD 5 with an attribution of the detected elements.

Figure 8-6: not available

Figure 8-7: see Figure 8

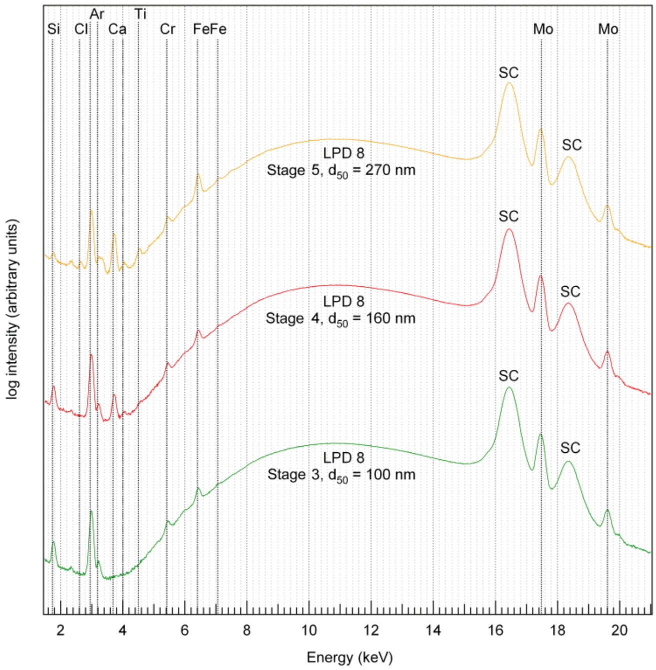

Figure 8-8: XRF spectra of the deposited particles of LPD 8 with an attribution of the detected elements

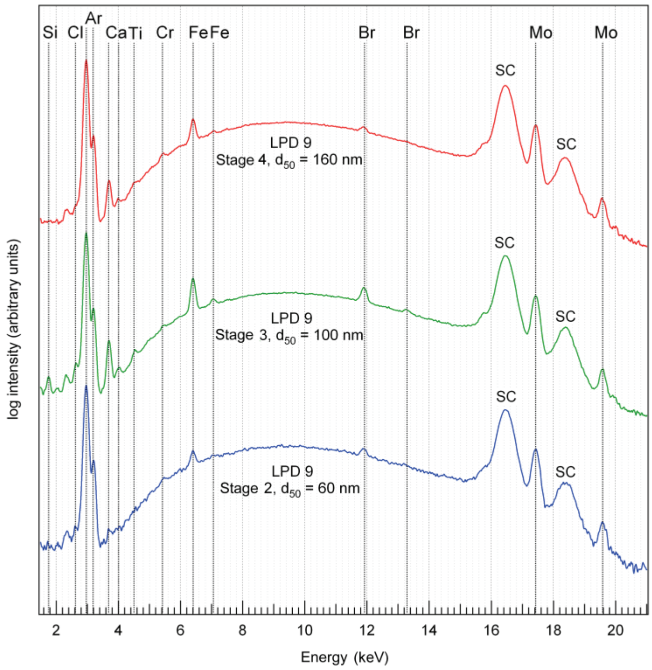

Figure 8-9: XRF spectra of the deposited particles of LPD 9 with an attribution of the detected elements

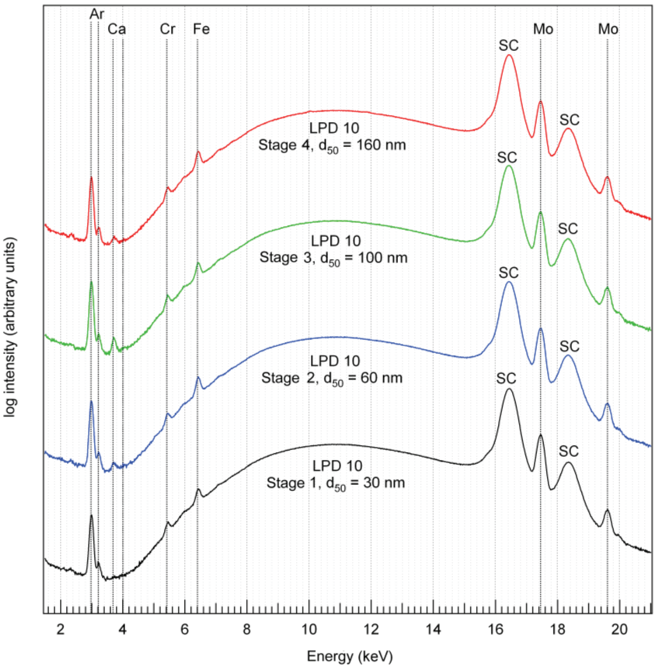

Figure 8-10: XRF spectra of the deposited particles of LPD 10 with an attribution of the detected elements

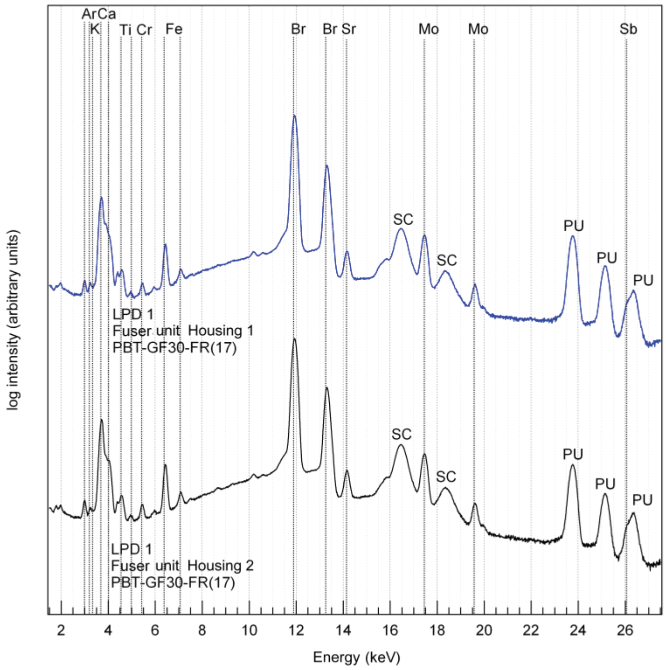

Figure 10-1: XRF spectra of the structural components of LPD 1

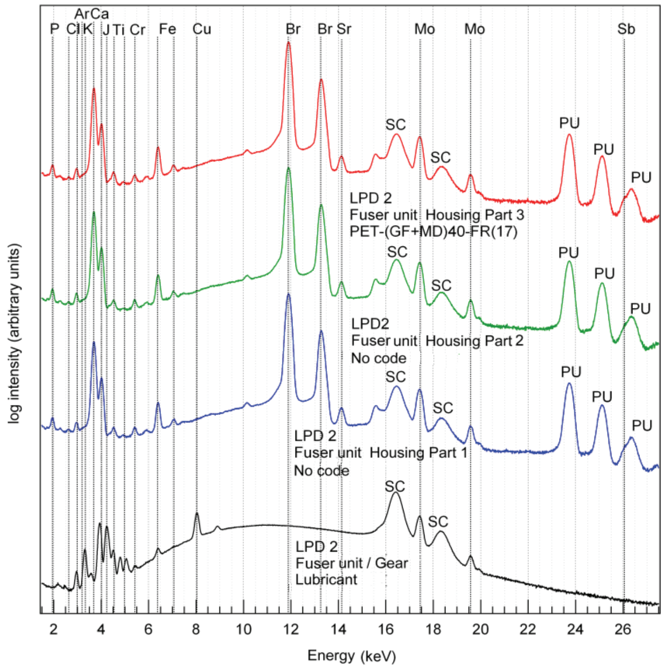

Figure 10-2: XRF spectra of the structural components of LPD 2

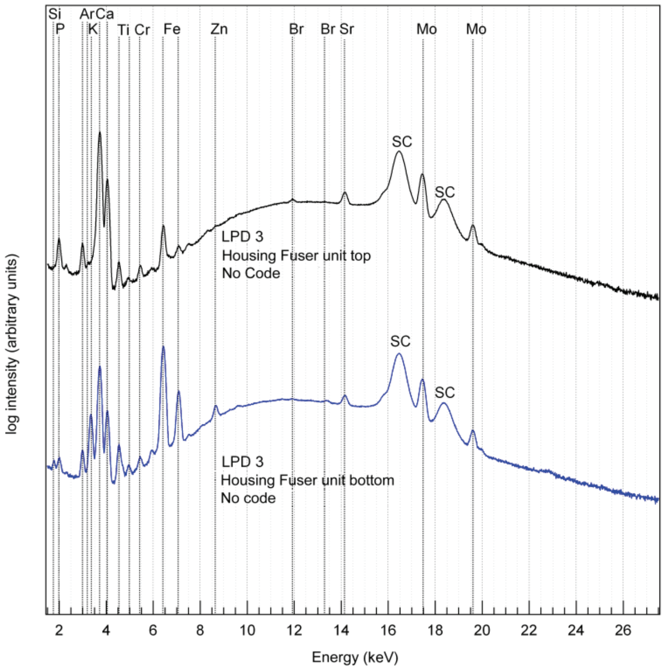

Figure 10-3: XRF spectra of the structural components of LPD 3

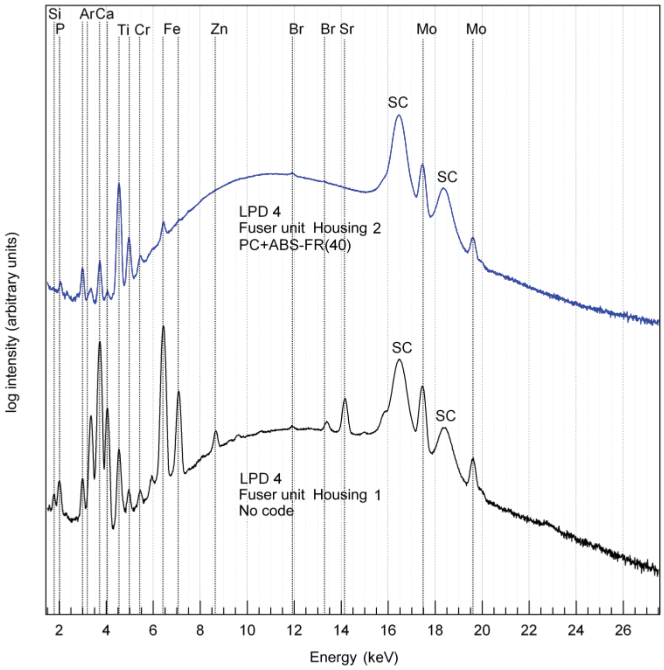

Figure 10-4: XRF spectra of the structural components of LPD 4

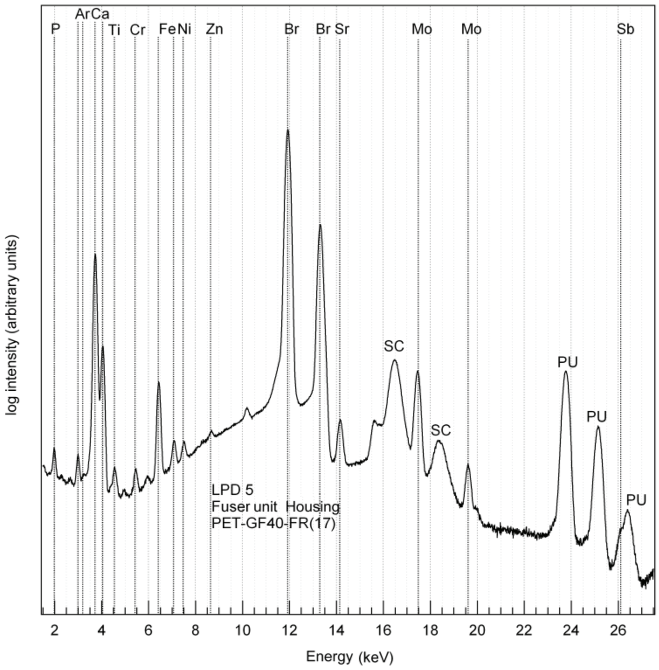

Figure 10-5: XRF spectra of the structural components of LPD 5

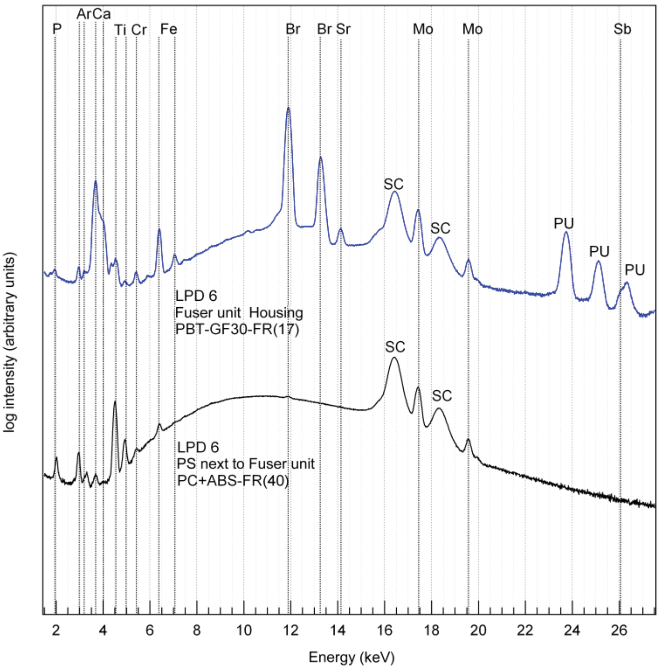

Figure 10-6: XRF spectra of the structural components of LPD 6

Figure 10-7: see Figure 10

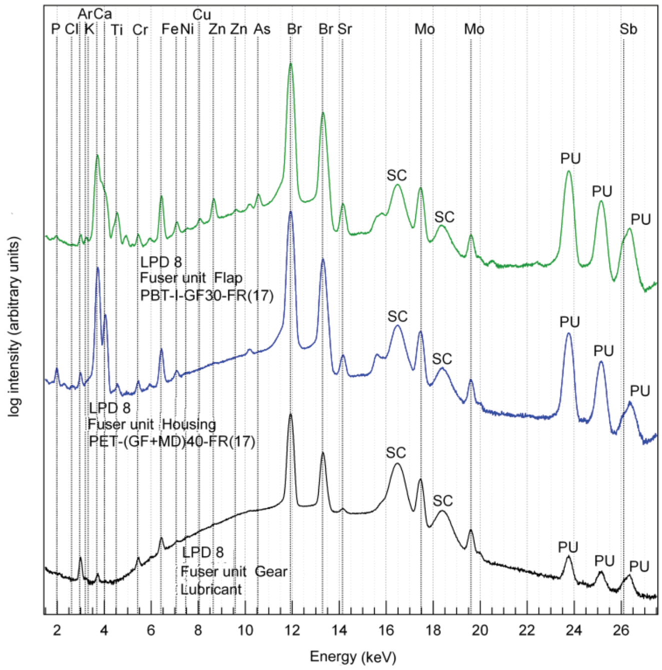

Figure 10-8: XRF spectra of the structural components of LPD 8

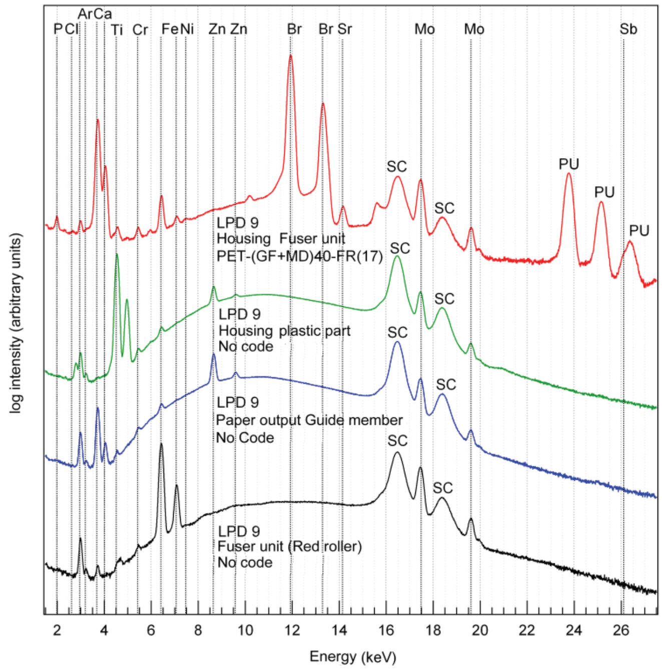

Figure 10-9: XRF spectra of the structural components of LPD 9

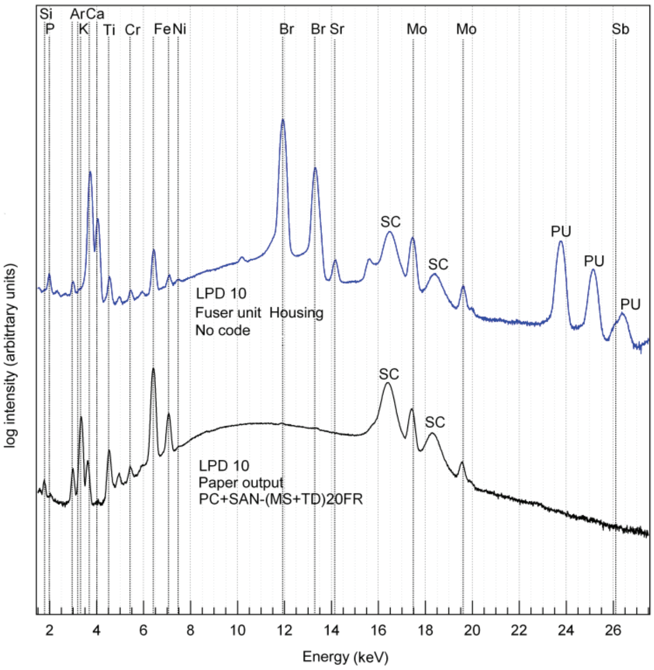

Figure 10-10: XRF spectra of the structural components of LPD 10

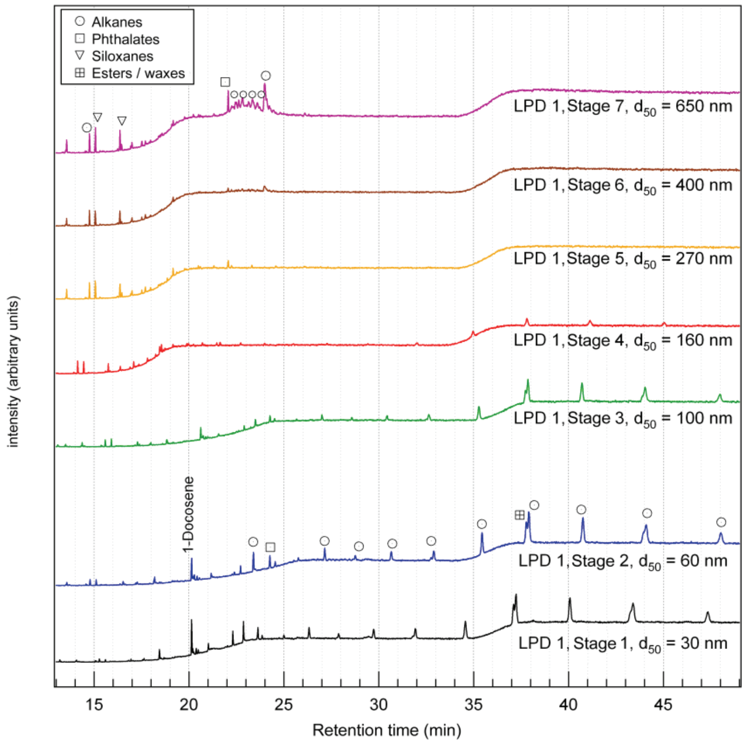

Figure 12-1: GC-MS results of the deposited aerosol of LPD 1

Figure 12-2: see Figure 12

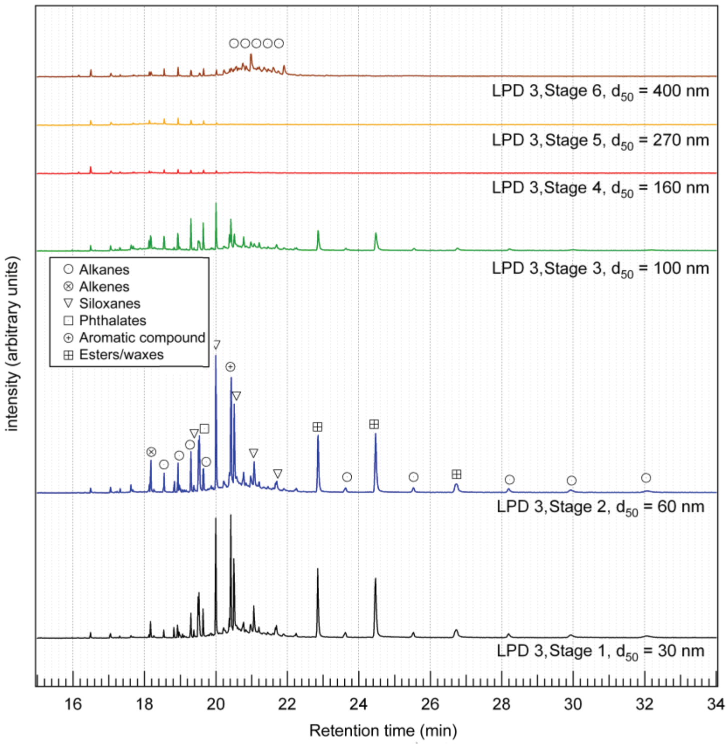

Figure 12-3: GC-MS results of the deposited aerosol of LPD 3

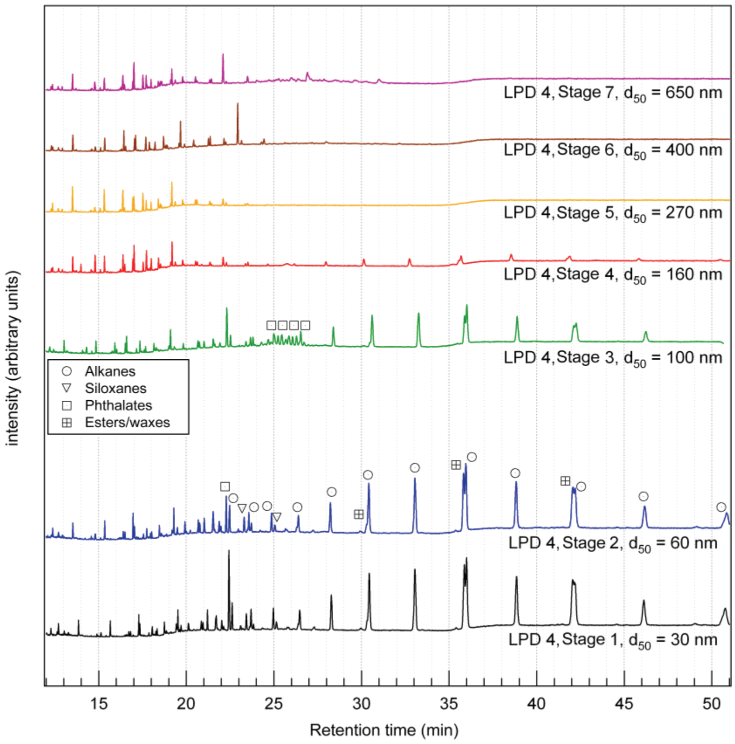

Figure 12-4: GC-MS results of the deposited aerosol of LPD 4

Figure 12-5: see Figure 14

Figure 12-6: Analysis has not been performed

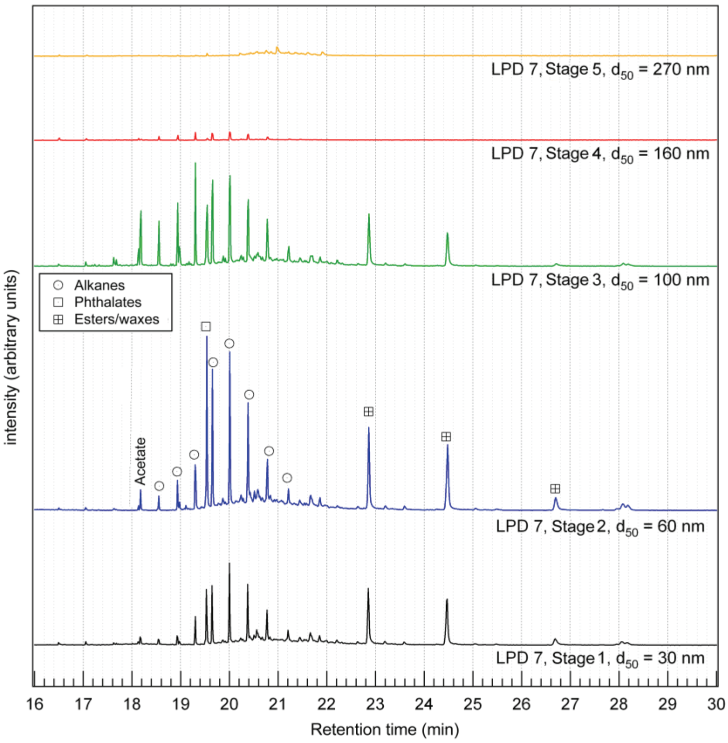

Figure 12-7: GC-MS results of the deposited aerosol of LPD 7

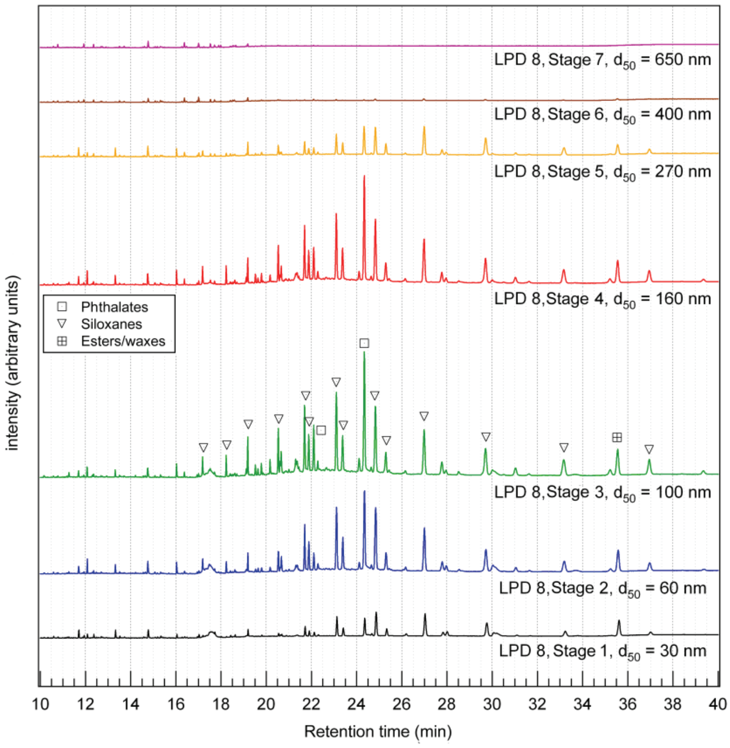

Figure 12-8: GC-MS results of the deposited aerosol of LPD 8

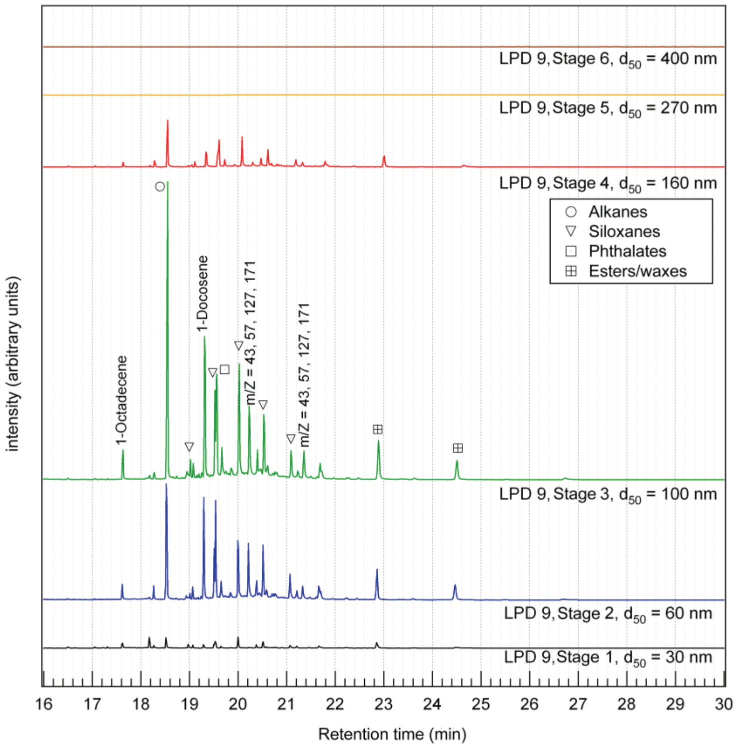

Figure 12-9: GC-MS results of the deposited aerosol of LPD 9

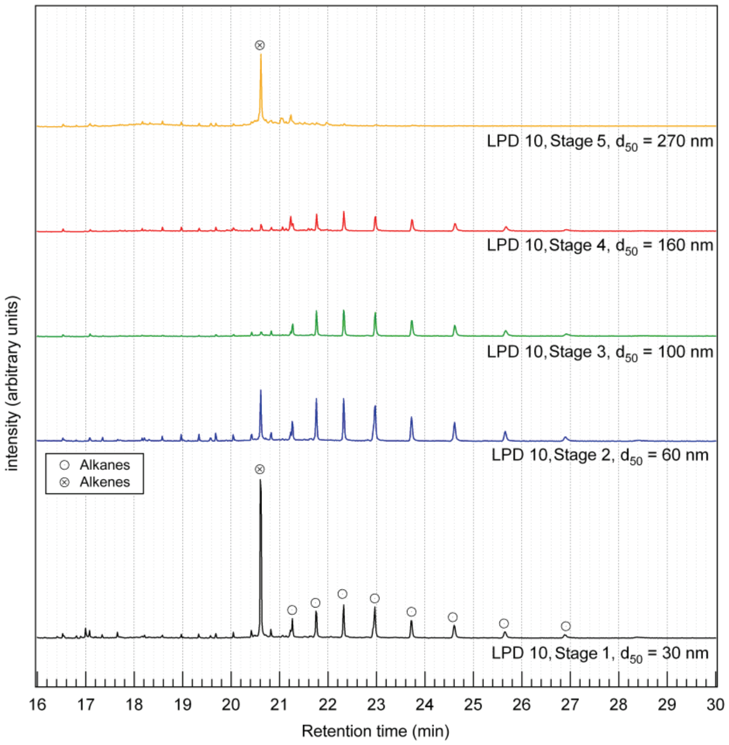

Figure 12-10: GC-MS results of the deposited aerosol of LPD 10

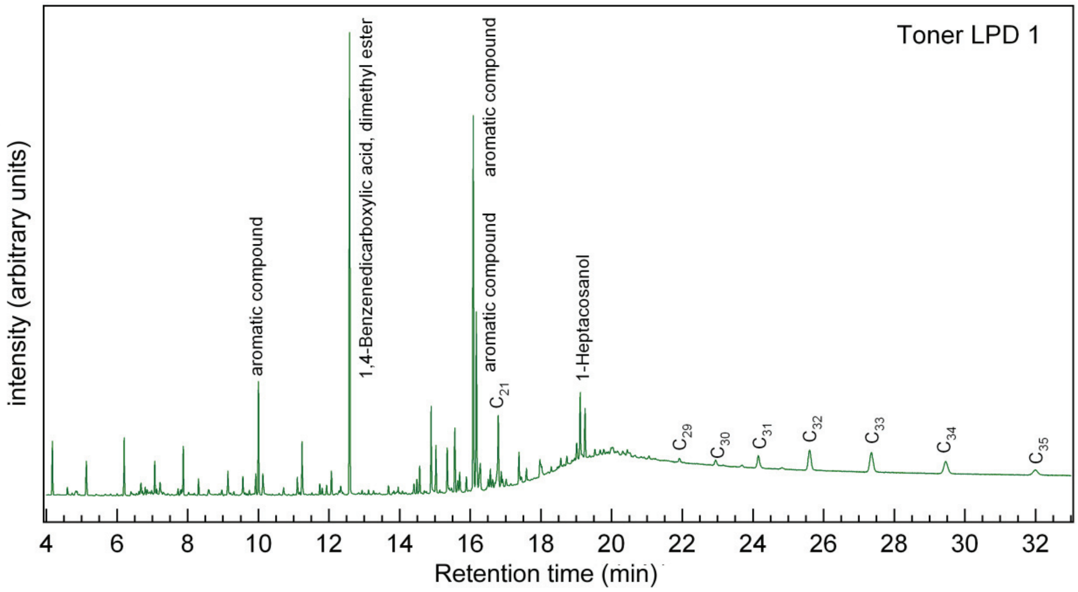

Figure 18-1: GC chromatogram of the toner (black) of LPD 1 with the identifiable substances attributed

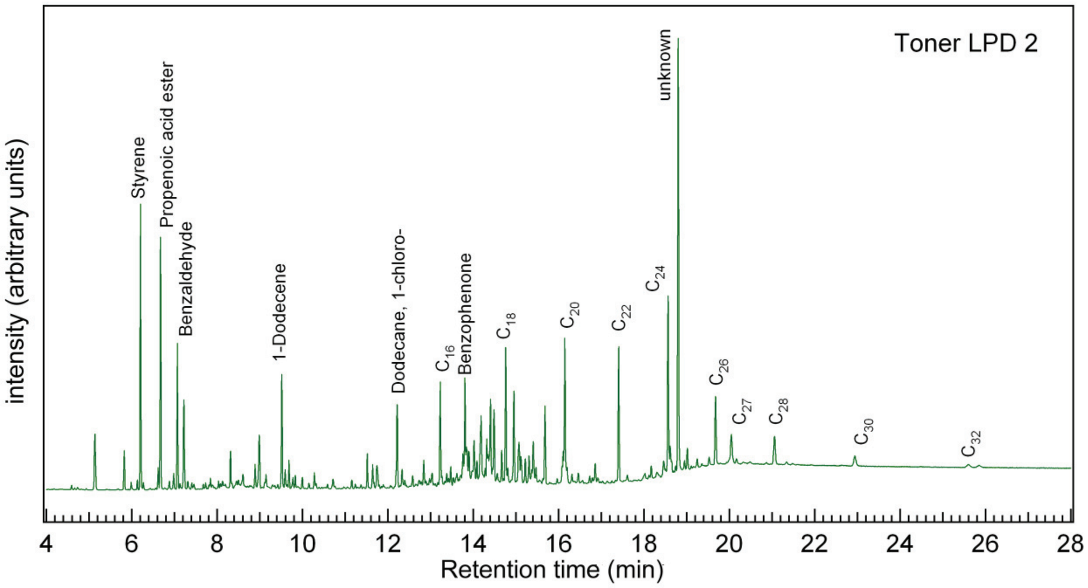

Figure 18-2: GC chromatogram of the toner (black) of LPD 2 with the identifiable substances attributed

Figure 18-3: see Figure 18

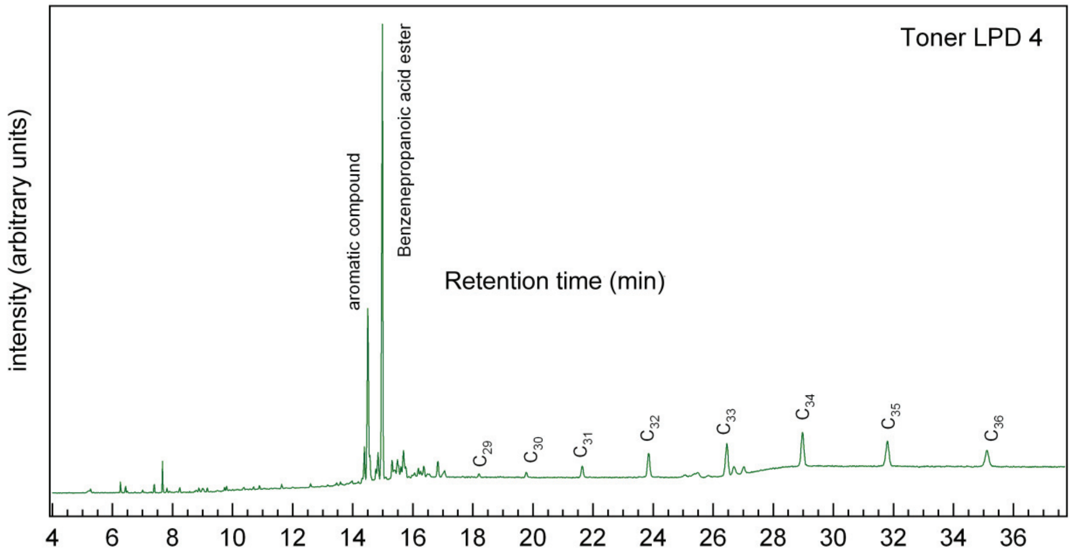

Figure 18-4: GC chromatogram of the toner (black) of LPD 4 with the identifiable substances attributed

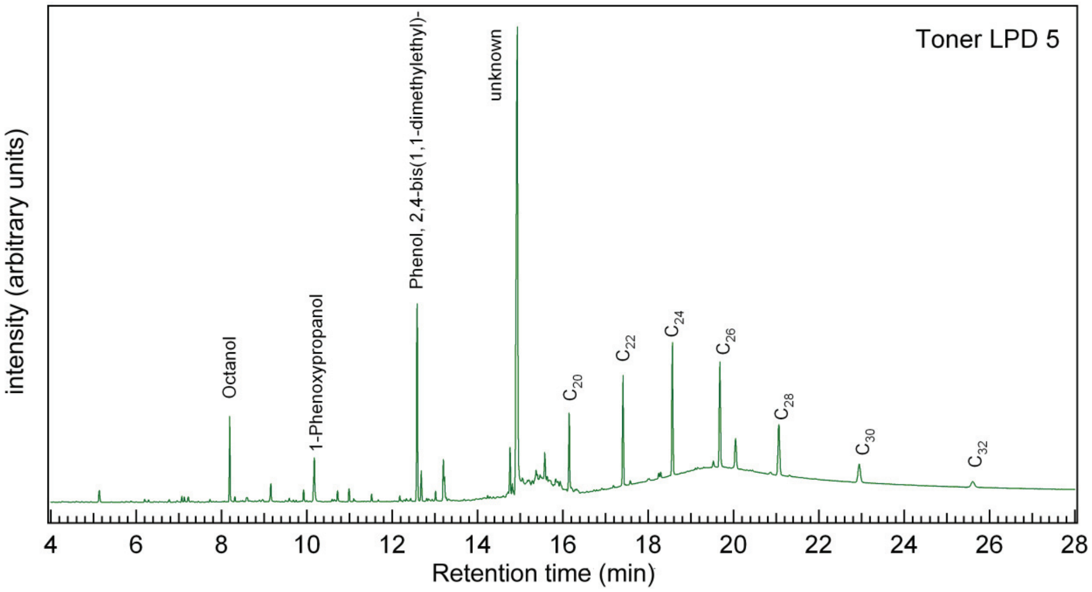

Figure 18-5: GC chromatogram of the toner (black) of LPD 5 with the identifiable substances attributed

Figure 18-6: see Figure 19

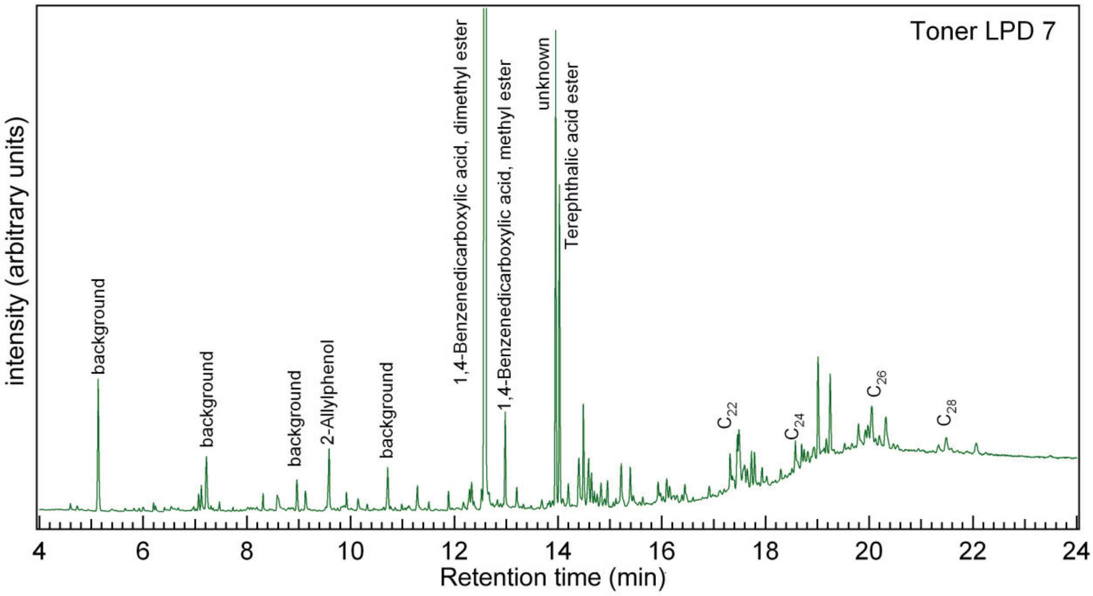

Figure 18-7: GC chromatogram of the toner (black) of LPD 7 with the identifiable substances attributed

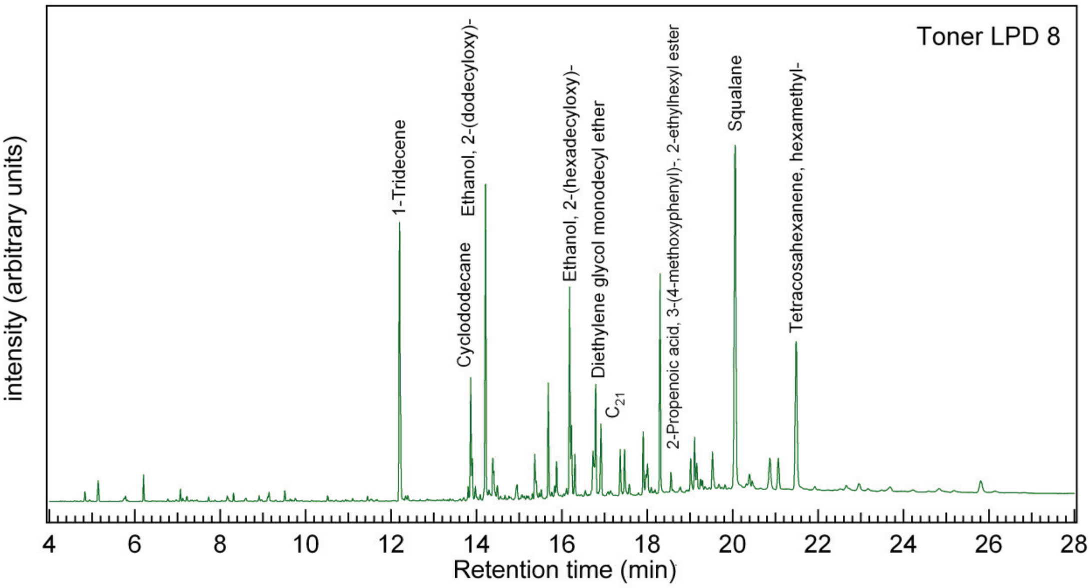

Figure 18-8: GC chromatogram of the toner (black) of LPD 8 with the identifiable substances attributed

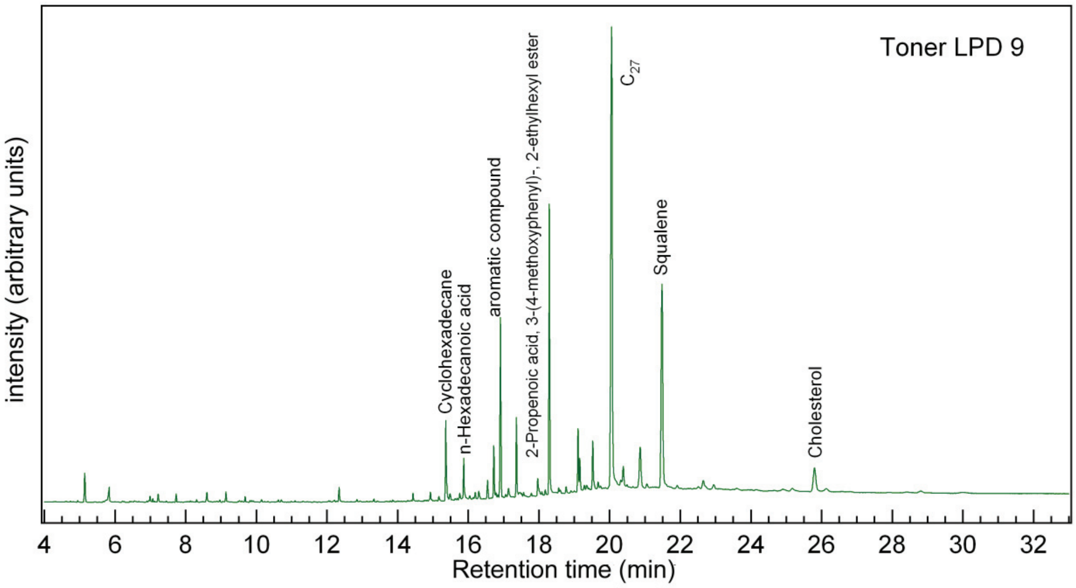

Figure 18-9: GC chromatogram of the toner (black) of LPD 9 with the identifiable substances attributed

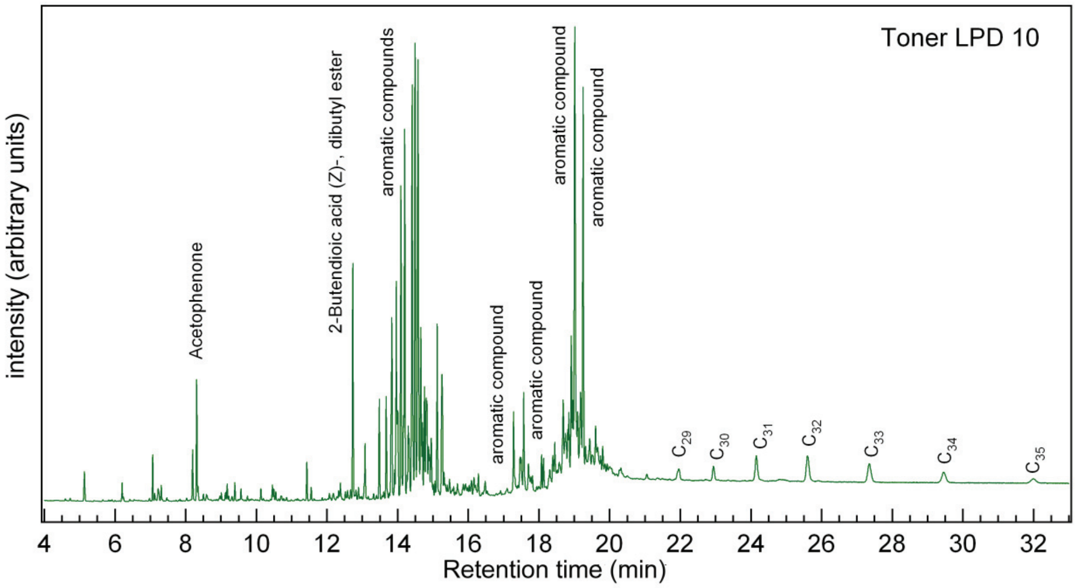

Figure 18-10: GC chromatogram of the toner (black) of LPD 10 with the identifiable substances attributed

6.2 Supplementary Tables to Chapter 4.1

Table 10.1: GC-MS results of the deposited aerosol of LPD 1.

The chemical composition is classified according to particle diameters of cascade impactor stages (d_{50}: cut point of the cascade impactor stages).

Aerosol LPD 1				**Toner LPD 1**	**Paper**
Stages 1 – 4 (d_{50} = 30 – 160 nm)		**Stage 7 (d_{50} = 650 nm)**			
RT (min)	**Compound**	**RT (min)**	**Compound**	**Compound**	**Compound**
20.1	1-Docosene	14.8	Alkane		1-Docosene
23.4	C_{26} alkane	15.1	Siloxane		
24.3	Phthalate	16.4	Siloxane		
27.2	C_{29} alkane	22.1	Phthalate	C_{29} alkane	
28.8	C_{30} alkane	22.4 – 24.0	C_{26} – C_{27}	C_{30} alkane	
30.7	C_{31} alkane			C_{31} alkane	
32.9	C_{32} alkane			C_{32} alkane	
35.5	C_{32} alkane				
37.8	Ester/wax				Ester/wax
37.9	C_{33} alkane			C_{33} alkane	
40.8	C_{34} alkane			C_{34} alkane	
44.1	C_{35} alkane			C_{35} alkane	
48.0	C_{36} alkane				

Table 10.2: see Table 10

Table 10.3: GC-MS results of the deposited aerosol of LPD 3.

The chemical composition is classified according to particle diameters of the cascade impactor stages (d_{50}: cut point of the cascade impactor stages).

Aerosol LPD 3				**Toner LPD 3**	**Paper**
Stages 1 – 3 (d50 = 30 – 100 nm)		**Stage 6 (d50 = 400 nm)**			
RT (min)	**Compound**	**RT (min)**	**Compound**	**Compound**	**Compound**
18.2	Alkene	20.2 – 22.0	Alkane		
18.6	C_{23} alkane			C_{23} alkane	
18.9	C_{24} alkane			C_{24} alkane	
19.3	C_{25} alkane			C_{25} alkane	
19.5	Cyclic siloxane				
19.6	Phthalate				
19.7	C_{26} alkane			C_{26} alkane	
20.0	Linear siloxane				
20.4	Aromatic compound				
20.5	Cyclic siloxane				
21.1	Cyclic siloxane				
21.7	Cyclic siloxane				
22.9	Ester/wax				Ester/wax
23.6	C_{30} alkane			C_{30} alkane	
24.5	Ester/wax				Ester/wax
25.5	C_{31} alkane			C_{31} alkane	
26.7	Ester/wax				Ester/wax
28.2	C_{32} alkane			C_{32} alkane	
29.9	C_{33} alkane			C_{33} alkane	
32.1	C_{34} alkane			C_{34} alkane	

Table 10.4: GC-MS results of the deposited aerosol of LPD 4.

The chemical composition is classified according to particle diameters of cascade impactor stages (d_{50}: cut point of the cascade impactor stages).

Aerosol LPD 4				**Toner LPD 4**	**Paper**
Stages 1 – 4 (d50 = 30 – 160 nm)		**Stage 4 (d50 = 160 nm)**			
RT (min)	**Compound**	**RT (min)**	**Compound**	**Compound**	**Compound**
22.3	Di-(2-ethylhexyl) phthalate	25.0 – 26.6	Phthalate		
22.5	C_{26} alkane				
23.3	Cyclic siloxane				
23.6	C_{27} alkane				
24.9	C_{28} alkane				
25.1	Cyclic siloxane				
26.4	C_{29} alkane			C_{29} alkane	
28.2	C_{30} alkane			C_{30} alkane	
30.3	Ester/wax				Ester/wax
30.4	C_{31} alkane			C_{31} alkane	
33.0	C_{32} alkane			C_{32} alkane	
35.8	Ester/wax				Ester/wax
36.0	C_{33} alkane			C_{33} alkane	
38.8	C_{34} alkane			C_{34} alkane	
42.1	Ester/wax				Ester/wax
42.2	C_{35} alkane			C_{35} alkane	
46.2	C_{36} alkane			C_{36} alkane	
50.9	C_{37} alkane				

Table 10.5: see Table 11

Table 10.6: Aerosol sample was not able to be analysed due to low particle concentrations

Table 10.7: GC-MS results of the deposited aerosol of LPD 7.

The chemical composition is classified according to particle diameters of cascade impactor stages (d_{50}: cut point of the cascade impactor stages).

Aerosol LPD 7 Stages 1 – 3 (d50 = 30 – 100 nm)		**Toner LPD 7**	**Paper**
RT (min)	**Compound**	**Compound**	**Compound**
18.2	Acetic acid ester		
18.6	C_{23} alkane		
18.9	C_{24} alkane	C_{24} alkane	
19.3	C_{25} alkane		
19.5	Phthalate		
19.7	C_{26} alkane	C_{26} alkane	
20.0	Alkane		
20.4	C_{27} alkane		
20.8	Alkane		
21.2	C_{28} alkane	C_{28} alkane	
22.9	Ester/wax		Ester/wax
24.5	Ester/wax		Ester/wax
26.7	Ester/wax		Ester/wax

Table 10.8: GC-MS results of the deposited aerosol of LPD 8.

The chemical composition is classified according to particle diameters of cascade impactor stages (d_{50}: cut point of the cascade impactor stages).

Aerosol LPD 8 Stages 1 – 4 (d50 = 30 – 160 nm)		**Toner LPD 8**	**Paper**
RT (min)	**Compound**	**Compound**	**Compound**
17.2	Cyclic siloxane		
18.2	Cyclic siloxane		
19.2	Cyclic siloxane		
20.5	Cyclic siloxane		
21.7	Cyclic siloxane		
21.9	Linear siloxane		
22.1	Phthalate		
23.1	Cyclic siloxane		
23.4	Linear siloxane		
24.3	Phthalate		
24.8	Cyclic siloxane		
25.3	Cyclic siloxane		
27.0	Cyclic siloxane		
29.7	Cyclic siloxane		
33.2	Cyclic siloxane		
35.6	Ester/wax		Ester/wax
37.0	Cyclic siloxane		

Table 10.9: GC-MS results of the deposited aerosol of LPD 9.

The chemical composition is classified according to particle diameters of cascade impactor stages (d_{50}: cut point of the cascade impactor stages).

Aerosol LPD 9 Stages 1 – 4 (d50 = 30 – 160 nm)		**Toner LPD 9**	**Paper**
RT (min)	**Compound**	**Compound**	**Compound**
17.6	1-Octadecene		1-Octadecene
18.6	Alkane		
19.0	Siloxane		
19.3	1-Docosene		1-Docosene
19.5	Cyclic siloxane		
19.6	Phthalate		
20.0	Siloxane		
20.2	Non-identifiable (m/Z = 43, 57, 127, 171)		
20.5	Siloxane		
21.1	Siloxane		
21.4	Non-identifiable (m/Z = 43, 57, 127, 171)		
22.9	Ester/wax		Ester/wax
24.5	Ester/wax		Ester/wax

6.3 Supplementary Figures to Chapter 4.2

Following figures: Colour Code top: Particle Number Concentration [1/cm³],
Vertical Axes, top: Particle diameters [nm], bottom: Electrical current uptake Ampere].
Horizontal Axis: Time [hh:mm]

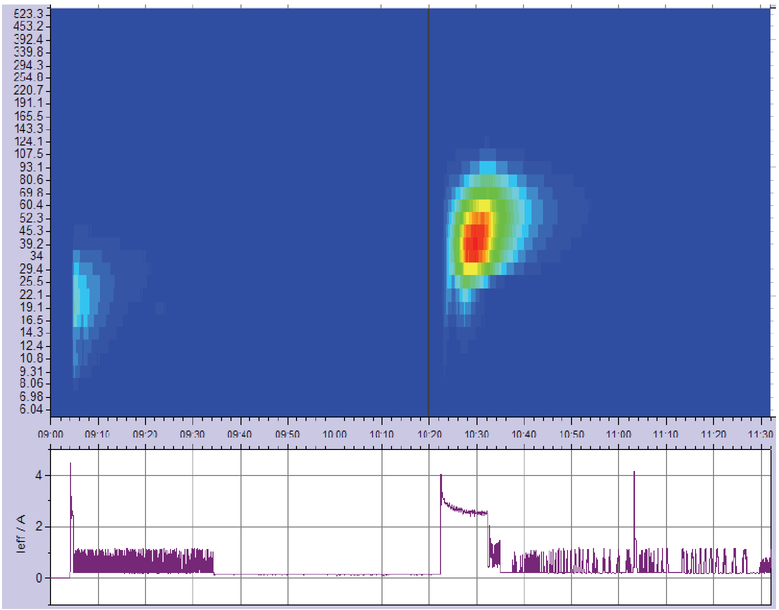

Figure 43-1: Particle size spectrum and current consumption of LPD1

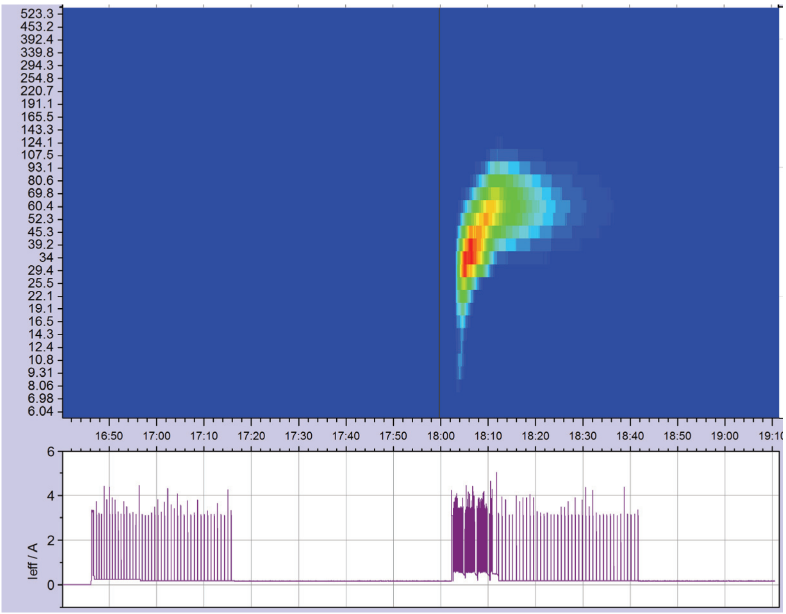

Figure 43-2: Particle size spectrum and current consumption of LPD2

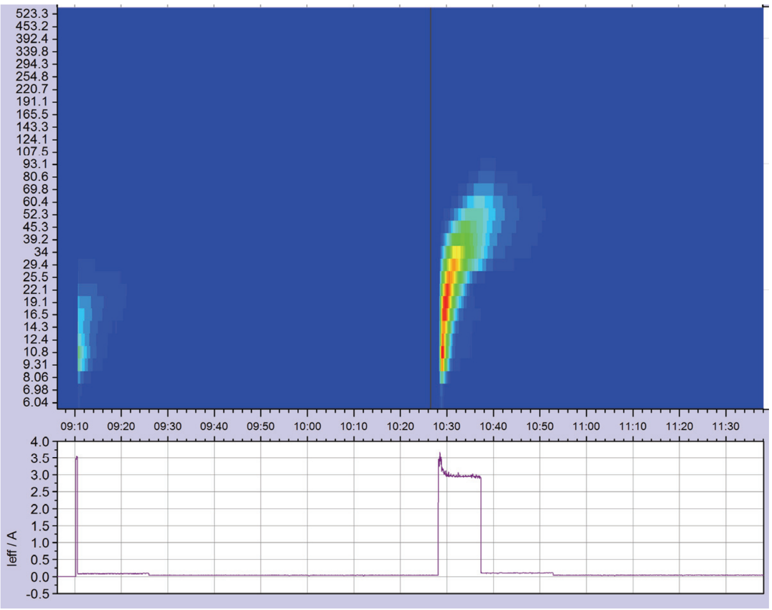

Figure 43-3: Particle size spectrum and current consumption of LPD3

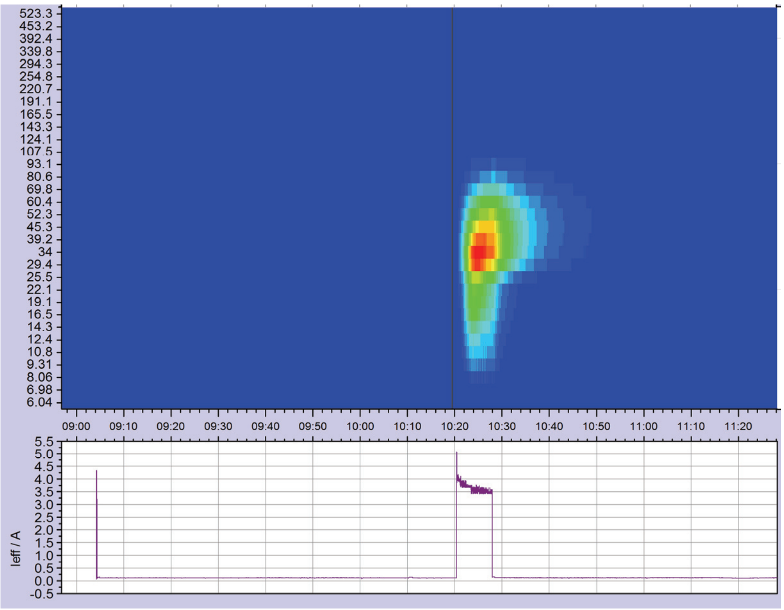

Figure 43-4: Particle size spectrum and current consumption of LPD4

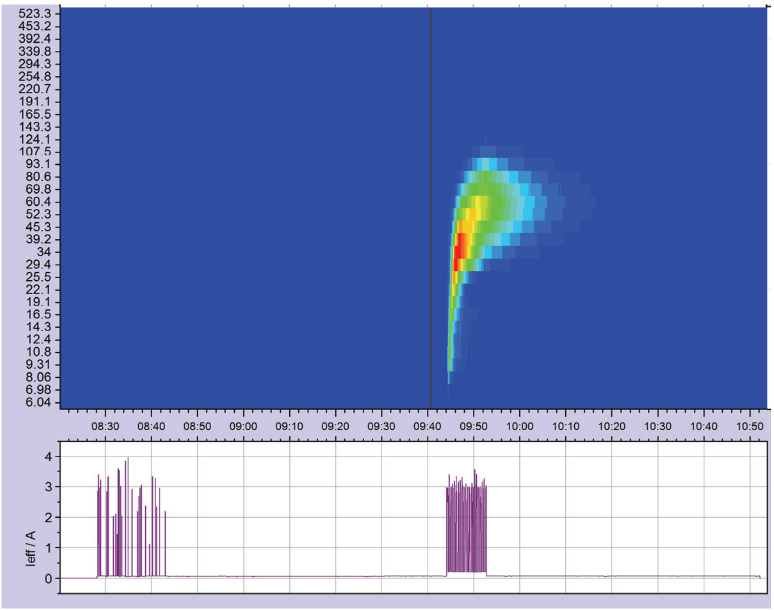

Figure 43-5: Particle size spectrum and current consumption of LPD5

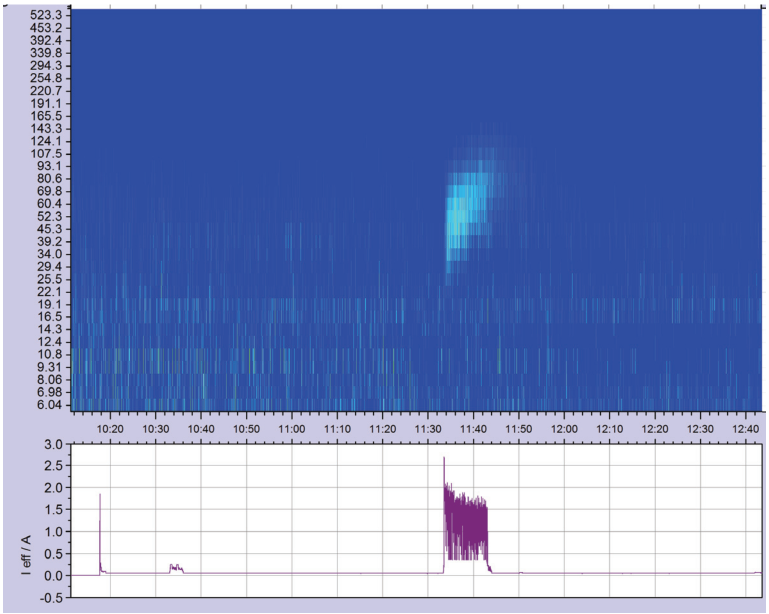

Figure 43-6: Particle size spectrum and current consumption of LPD6

Figure 43-7: see Figure 43

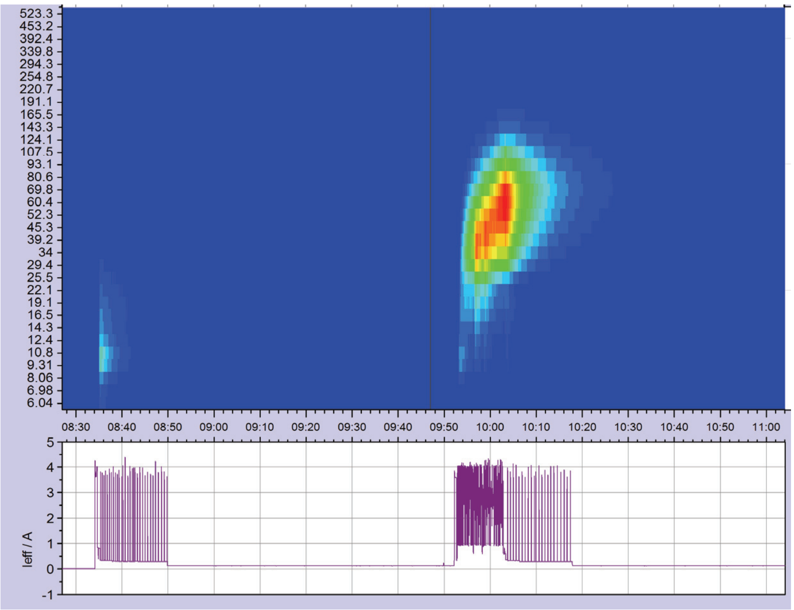

Figure 43-8: Particle size spectrum and current consumption of LPD8

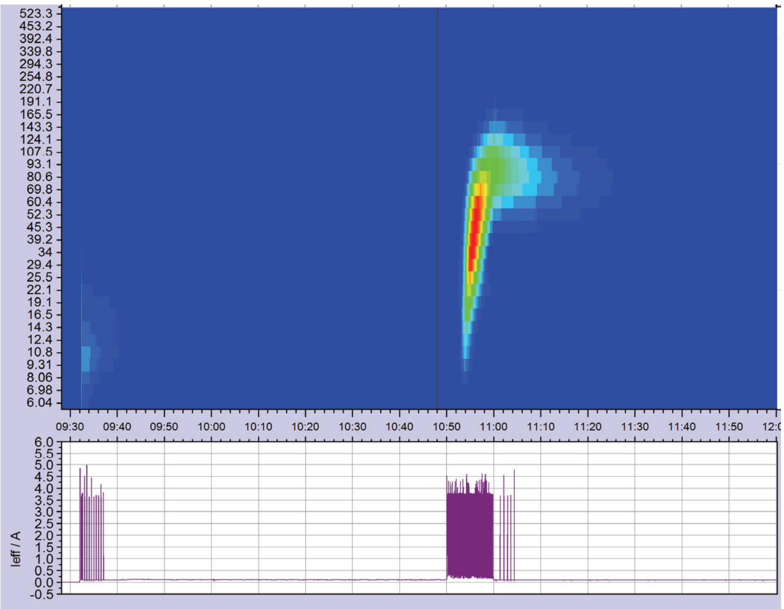

Figure 43-9: Particle size spectrum and current consumption of LPD9

Figure 43-10: see Figure 43

Following figures: Horizontal Axis: Time [hh:mm]:

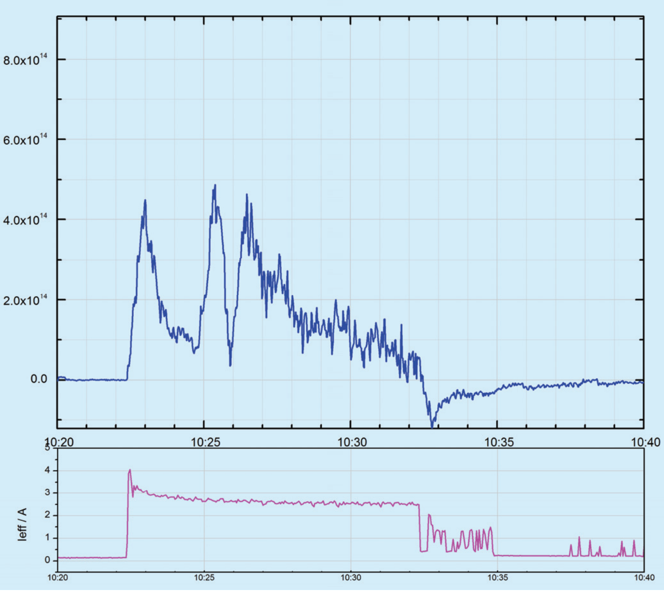

Figure 44-1: Particle emission rate *PER(t)* and current consumption for LPD1

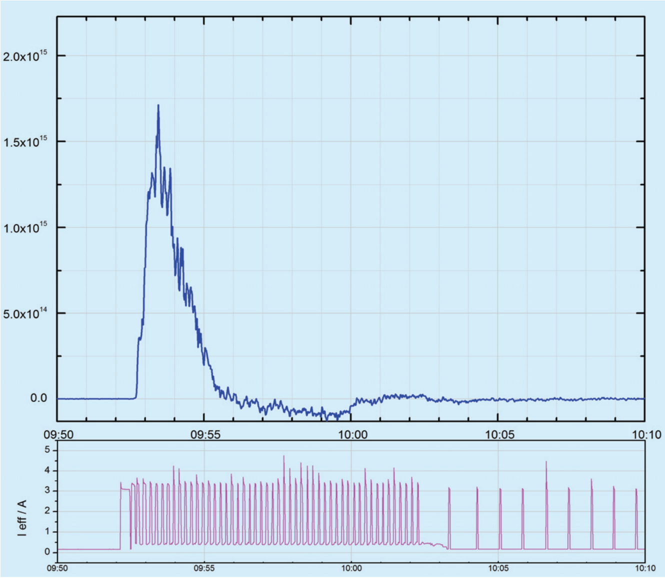

Figure 44-2: Particle emission rate *PER(t)* and current consumption for LPD2

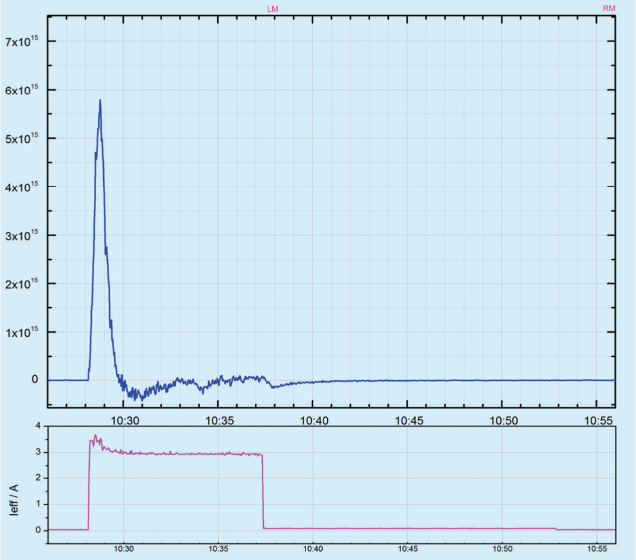

Figure 44-3: Particle emission rate *PER(t)* and current consumption for LPD3

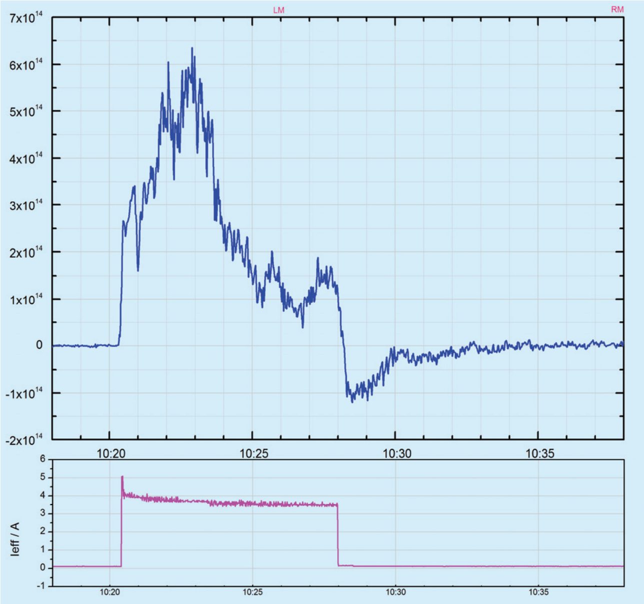

Figure 44-4: Particle emission rate *PER(t)* and current consumption for LPD4

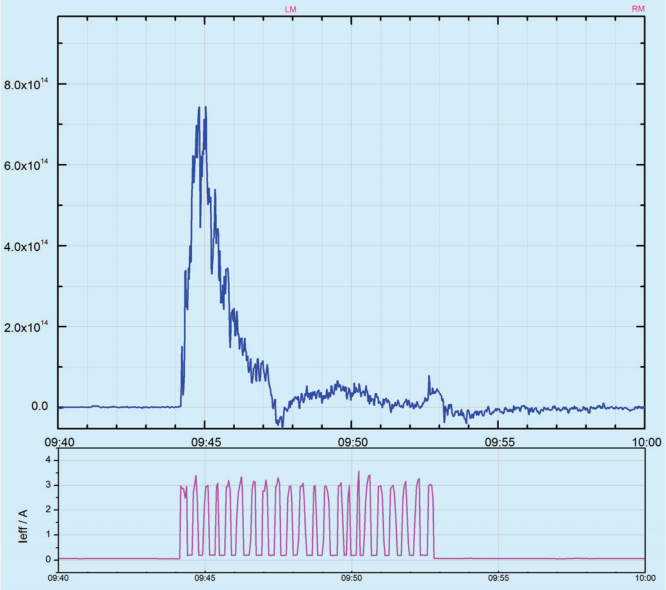

Figure 44-5: Particle emission rate *PER(t)* and current consumption for LPD5

Figure 44-6: not evaluated

Figure 44-7: see Figure 44

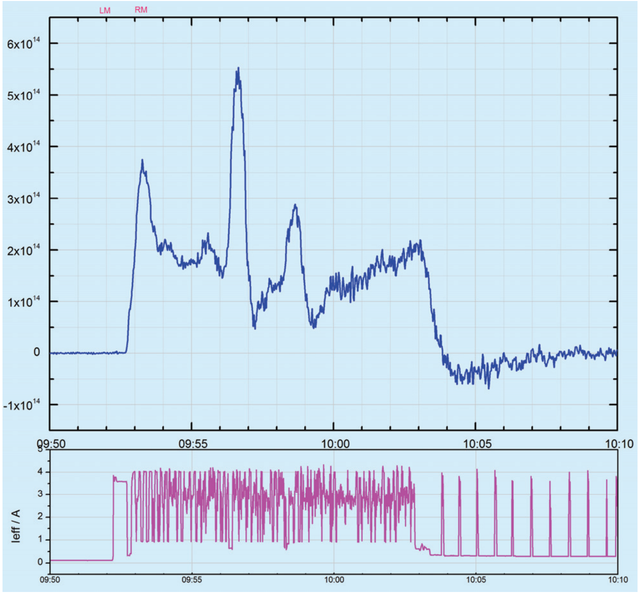

Figure 44-8: Particle emission rate *PER(t)* and current consumption for LPD8

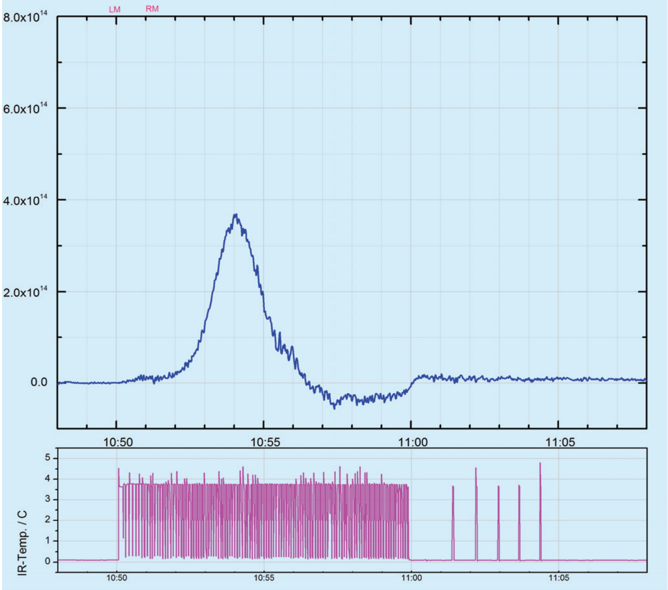

Figure 44-9: Particle emission rate *PER(t)* and current consumption for LPD9

Figure 44-10: see Figure 44

7 Summary

The continuous public debate on possible adverse health effects of fine (FP) and ultrafine particle (UFP) emissions from laser printing devices induced the German Federal Environment Agency (UBA) to initiate a research project aimed at developing a test method for particle counting under standard conditions in environmental test chambers. Chemical analysis of the aerosols was another project objective. As an outcome, the quantification of particle emissions was integrated into the test scheme Annex S-M (testing of chemical emissions) of the existing German standard RAL UZ-122 for awarding the German Blue Angel ecolabel to laser printing devices, as well as into the harmonised international test standards ECMA-328 and ISO/IEC 28360. The procedure for aerosol measurement was successfully tested in an international round robin. After approval of these modifications by RAL, the German RAL UZ-122 guideline considered quantitative criteria related to fine and ultrafine particle emissions as well as a respective test procedure for product testing and awarding the Blue Angel ecolabel. As a result of the secondary aim of the project, some particle sources within laser printing devices were identified by the coupling of analytical methods. The identified source contributions, the analysis of the chemical composition of the particles and their size distributions add to the knowledge on these emissions and may enhance the environmental risk assessment in comparison with other aerosol sources.

8 List of Literature

1. Afshari A., Matson U., Ekberg L. E.: Characterization of indoor sources of fine and ultrafine particles: A study conducted in a full-scale chamber, Indoor Air (2005) 15 p141–150

2. Rödelsperger K., Brückel B., Podhorsky S., Schneider J.: Abschlussbericht zum Projekt F 2075 „Charakterisierung ultrafeiner Teilchen für den Arbeitsschutz – Teil 2“ im Auftrag der Bundesanstalt für Arbeitsschutz und Arbeitsmedizin (2009).

3. Wichmann H. E., Heinrich J., Peters A.: Gesundheitliche Wirkungen von Feinstaub. In: Wichmann H. E., Schlipköter H. W., Fülgraff F. (Hrsg.) „Fortschritte in der Umweltmedizin“.Ecomed-Verl.-Ges. (2002)

4. Wichmann H. E.: Epidemiologie ultrafeiner Teilchen. BIA-Report. St. Augustin. HVBG (2003) p53-86

5. Abt E., Suh H., Allen G. und Koutrakis P.: Characterization of Indoor Particle Sources. Environ. Health Perspect. (2000) 108 (1) p35–44.

6. bald-Mulli A., Wichmann H.-E., Kreyling W. and A. Peters, A.: Journal of Aerosol Medicine (2002) 15(2) p189-201

7. Bundesgesundheitsblatt - Gesundheitsforsch - Gesundheitsschutz (2008) Springer Medizin Verlag

8. Politis M. et. al.: Global NEST Journal, (2008) Vol. 10, No 3, p439-452

9. Bake D., Moriske H.-J., Untersuchungen zur Freisetzung feiner und ultrafeiner Partikel beim Betrieb von Laserdruck-Geräten, Umweltbundesamt UBA, (2006) Februar

10. Seeger S., Wilke O., Bücker M., Jann O.: Time- and Size-Resolved Characterization of Particle Emissions from Office Machines. Proc. Int. Conf. Healthy Buildings (2006), Lisboa, Portugal, Vol. II p447-450.

11. Wilke O., Jann O., Brödner D., Schneider U., Krocker CH., Kalus S., Seeger S., Bücker M.: Prüfung von Emissionen aus Bürogeräten während der Druckphase zur Weiterentwicklung des Umweltzeichens Blauer Engel für Laserdrucker und Multifunktionsgeräte unter besonderer Berücksichtigung der Sicherung guter Innenraumluftqualität, Forschungsbericht: Umweltforschungsplan des Bundesministeriums für Umwelt, Naturschutz und Reaktorsicherheit - Förderkennzeichen (UFOPLAN) 204 95 373 / UBA-FB 001159 - Abschlussbericht 35 (2008) 8, p1-164; Hrsg.: Umweltbundesamt (UBA) ISSN 1862-4804

12. Schripp, Wensing, Uhde, Salthammer, He, Morawska: Evaluation of Ultrafine Particle Emissions from Laser Printers Using Emission Test Chambers Environ. Sci. Technol. 42, (2009) p4338–4343

13. Schripp, Mulakampilly, Delius, Uhde, Wensing, Salthammer, Kreuzig, Bahadir, Wang, Morawska: Comparison of ultrafine particle release from hardcopy devices in emission test. Gefahrstoffe - Reinhaltung der Luft 69(3) (2009) p71-76

14. Morawska, He, Johnson, Jayaratne, Salthammer, Wang, Uhde, Bostrom, Modini, Ayoko, Mcgarry, Wensing: An Investigation into the Characteristics and Formation Mechanisms of Particles Originating from the Operation of Laser Printers. Environ. Sci. Technol. 43 (2009) p1015–1022

15. Gallardo M., Romero P., Sanchez-Quevedo M. C., Lopez-Caballero J. J.: Siderosilicosis due to photocopier toner dust, The Lancet Vol. 334 (1994)

16. Smola, Georg & Hohensee, Gesundheitsgefahren durch Laserdrucker. Gefahrstoffe - Reinhaltung der Luft 62, (2002) p295-301

17. Siegmann, S., Jansing, P.-J.: Innenraumbelastung durch Laserdrucker und Fotokopiergeräte, Prakt. Arb. Med 2: 6-11 (2005)

18. Kagi N. et al.: Indoor air quality for chemical and ultrafine particle contaminants from printer Building and Environment 42 (2007) p1949–1954

19. Mersch-Sundermann et. al.: Evaluierung möglicher Beziehungen zwischen Emissionen aus Büromaschinen, insbesondere aus Fotokopierern und Laserdruckern, und Gesundheitsbeeinträchtigungen bzw. Gesundheitsschäden bei exponierten Büroangestellten, Abschlussbericht Projekt UFO-Plan FKZ 705 62 449, Bundesinstitut für Risikobewertung (BfR), Berlin, (2007)

20. Presseerklärung BfR 07/2008 vom 18.04.2008, BfR schließt gesundheitliche Beeinträchtigungen durch Emissionen aus Büromaschinen nicht aus, BfR 2008, http://www.bfr.bund.de/cd/11029, siehe auch: Gesundheitliche Bewertung Nr. 014/2008 des BfR vom 31. März 2008

21. Stelting H.-J.: Krank durch Toner – Erfahrungen mit einer Nanopathologie, Umweltmed Forsch Prax 11 (5) (2006) p329 – 337

22. Meyer U., Möhle K., Eyerer P., et al.: Entwicklung, Bau und Inbetriebnahme einer 1 m³-Bauteilmesskammer zur Bestimmung von Emissionen aus Endprodukten. Staub - Reinhaltung der Luft 54 (1994) p137 - 142.

23. Baron P., Willeke K.: Aerosol Measurement – Principles, Techniques and Applications, 2nd Edition Wiley Interscience, (2005)

24. schriftliche Mitteilung: Mechlinski A.; PiCA Prüfinstitut Chemische Analytik GmbH, Berlin (2011)

25. siehe z.B.: www.fujixerox.co.jp/eng/company/headline/2007/0201_ene_save.html

26. Final report on Task 1 “definition” for the EuP Preparatory Studies on Imaging Equipment (Lot 4), Chapter 6.2, Fraunhofer Institute for Reliability and Microintegration IZM, Berlin (2007)

27. He C., Morawska L., Wang H., Jayaratne R., McGarry P., Johnson G. R., Bostrom T., Gonthier J., Authemayou S. and Ayoko G.: Quantification of the relationship between fuser roller temperature and laser printer emissions. J. Aerosol. Sci. 41 (2010) p523 – 530

28. Wensing M., Schripp T., Uhde E., Salthammer T.: Ultra-fine particles release from hardcopy devices: Sources, real-room measurements and efficiency of filter accessories. Sci. Total Environ. (2008) p407, 418 – 427

29. Wensing M., Delius W., Fauck C., Omelan A., Petersen J., Schripp T., Uhde E., Salthammer T.: Measurement and characterization of UFP emissions from hardcopy devices in operation. BITKOM WKI UFP Project Final Report (2010)

30. http//:www.aerosil.com/product/aerosil/en/Pages/default.aspx

31. Rožić M., Rožmarić Mačefat M., Oreščanin V.: Elemental analysis of ashes of office papers by EDXRF spetrometry. Nucl. Instrum Meth. B 229 (2005) p117 – 122

32. Spence L. D., Baker A. T., Byrne J. P.: Characterization of document paper using elemental compositions determined by inductively coupled plasma mass spectrometry. J. Anal. Atom. Spectrom. 15 (2000) p 813 – 819

33. Manso M., Carvalho M. L.: Elemental identification of document paper by X-ray fluorescence spectrometry. J. Anal. Atom. Spectrom. 22 (2007) p164 – 170

34. Vergabegrundlage für Umweltzeichen, Bürogeräte mit Druckfunktion (Drucker, Kopierer, Multifunktionsgeräte) RAL-UZ 122, Ausgabe Juni (2006)

35. Pickering G.R., Olliff C.J., Rutt K.J.: The Mass Spectrometric Behaviour of Dimethylcyclosiloxanes, Org. Mass Spectrom. 10 (1975) p1035 – 1045

36. Wilke O., Seeger S., Bresch H., Brödner D., Juritsch E., Jann, O.: Sampling and characterisation of ultrafine particles released from laser printers. Proceedings of the 11th International Conference on Indoor Air and Climate. Copenhagen, (2008), ID 239

37. Wensing M., Delius W., Omelan A.; Uhde E., Salthammer T., He C., Wang, H., Mortawska L.: Ultrafine particles (UFP) from laser printers: chemical and physical charaterization. Proceedings of Healthy Buildings, Syracuse (2009), ID 171

38. Wypych G.: Handbook of Plasticizers, ChemTec Publishing (2004)

39. Wilke O., Jann O.: Bestimmung von Weichmacheremissionen aus unterschiedlichen Materialien in Messkammern, Tagungsband 4. Freiberger Polymertag, Forschungsinstitut für Leder- und Kunstledertechnologie, Freiberg, G/1-G/11; (1999)

40. Wilke O., Jann O., Brödner D.: VOC- und SVOC-Emissionen aus Fuhbodenaufbauten und den dafür verwendeten Materialien. Gefahrst Reinhalt Luft 63 (2003) p92 – 98

41. Wensing M., Uhde, E., Salthammer T.: Plastics additives in the indoor environment – flame retardants and plasticizers. Sci. Total Environ. 339 (2005) p19 – 40

42. Maddalena R. L., McKone, T. E., Destaillats H., Russell, M. Hodgson A. T., Perino C.: Quantifying pollutant emissions from office equipment. Final report, Lawrence Berkeley National Laboratory, Berkeley, CA, (2009)

43. Destaillats H., Maddalena R. L., Singer B. C., Hodgson A. T., McKone, T. E.: Indoor pollutants emitted by office equipment: A review of reported data and information needs. Atmos. Environ. 42 (2008) p1317 – 1388

44. Kemmlein S., Hahn O., Jann O.: Emissions of organophosphate and brominated flame retardants from selected consumer products and building materials. Atmos. Environ. 37 (2003) p5485 – 5493

45. NIST Standard Reference Database 1A, The NIST Mass Spectrometry Data Center, (2008)

46. Covaci A., Harrad S., Abdallah M. A.-E., Ali N., Law R. J., Herzke D., de Wit C. A.: Novel brominated flame retardants: A review of their analysis, environmental fate and behaviour. Environ. Int. 37 (2011) p532 – 556

47. Balabanovich A. I., Luda M. P., Camino G., Hornung A.: Thermal decomposition behavior of 1,2-bis-(2,4,6-tribromophenoxy)ethane. J. Anal. Appl. Pyrol. 67 (2003) p95 – 107

48. Balabanovich A. I., Luda M. P., Operti L.: GC/MS Identification of Pyrolysis Products from 1,2-bis-(2,4,6-tribromophenoxy)ethane. Journal of Fire Sciences 22 (2004) p269 – 292

49. Directive 2002/95/EC of the European Parliament and of the council of 27 January 2003 on the restriction of the use of certain hazardous substances in electrical and electronic equipment (2003)

50. European Court of Justice, Cases C-14/06 and C-295/06, Judgement of the Court, 1 April 2008, Directive 2002/95/EC and Commission Decision 2005/717/EC; 2008http:// curia.europa.eu. accessed July 2010

51. Ashton M., Kantai T., Kohler P.M., Roemer-Mahler A., Templeton J.: Summary of the Fourth Conference of the Parties to the Stockholm Convention on Persistent Organic Pollutants: 4–8 May (2009), http://chm.pops.int/Programmes/NewPOPs/The9newPOPs/tabid/672/language/en-US/Default.aspx.

52. Covaci A..; Harrad S., Abdallah M. A.-E., Ali N., Law R. J., Herzke D., de Wit C. A.: Novel brominated flame retardants: A review of their analysis, environmental fate and behaviour. Environ. Int. 37 (2011) p532 – 556

53. Jamriska M. and Morawska L: Quantitative Assessment of the Effect of Surface Deposition and Coagulation on the Dynamics of Submicrometer Particles Indoors, Aerosol Science and Technology 37 (2003) p425–436

54. Mordas G., Manninen H. E., Petäjä T., Aalto P. P., Hämeri K. and Kulmala M.: On Operation of the Ultra-Fine Water-Based CPC TSI 3786 and Comparison with Other TSI Models (TSI 3776, TSI 3772, TSI 3025, TSI 3010, TSI 3007). Aerosol Sci. Technol. 42 (200) p152-158

55. Petäjä T., Mordas G., Manninen H., Aalto P. P., Hämeri K. and Kulmala M.: Detection efficiency of a water-based TSI Condensation Particle Counter 3785. Aerosol Science And Technology 40 (200) p1090-1097

56. ECMA-328, Dezember 2010, 5th Edition, Determination of Chemical Emission Rates from Electronic Equipment, ECMA, Genf

57. ISO 15900, 2009, Determination of particle size distribution - Differential electrical mobility analysis for aerosol particles

58. ISO 27891 - Entwurf, Aerosol particle number concentration - Calibration of condensation particle number counters

59. Verordnung (EG) Nr. 715/2007 vom 20. Juni 2007 über die Typgenehmigung von Kraftfahrzeugen hinsichtlich der Emissionen von leichten Personenkraftwagen und Nutzfahrzeugen (Euro 5 und Euro 6) und über den Zugang zu Reparatur- und Wartungsinformationen für Fahrzeuge

60. Homepage der Arbeitsgruppe: http://live.unece.org/trans/main/wp29/wp29wgs/wp29grpe/pmp22.html

61. Giechaskiel B. et.al.: Particle Measurement Programme (PMP) Light-Duty Inter-Laboratory Exercise: Repeatability and Reproducibility of the Particle Number Method, Aerosol Science and Technology 42, Iss. 7 (2008)

62. Giechaskiel B. et.al.: Evaluation of the particle measurement programme (PMP) protocol to remove the vehicles' exhaust aerosol volatile phase, Science of the Total Environment Vol. 408, Iss. 21 (2010)

63. Kalibrierworkshops METAS, Schweiz, http://www.metas.ch/metasweb/Fachbereiche/Partikel_und_Aerosole

64. Guide to the expression of Uncertainty in Measurement GUM (JCGM 2008), siehe auch die deutsche Vornorm DIN V ENV 13005 (aktuelle Ausgabe:1999-06)

65. Limpert E., Stahel W. A., Abbt M.: Log-Normal Distributions across the Sciences: Keys and Clues, BioScience, Vol. 51, No. 5 (2001) p341-352

66. EURACHEM/CITAC (2004): Leitfaden Ermittlung der Messunsicherheit bei analytischen Messungen, Übersetzung der 2. Auflage des EURACHEM/CITAC-Guide "Quantifying Uncertainty in Analytical Measurement"

67. EURACHEM/CITAC (2007): Use of uncertainty information in compliance assessment. EURACHEM/CITAC Guide, First Edition

List of members of the project-related expert group

Frau Dr. Brigitte Lahm
Hewlett-Packard GmbH
HQ-TRE
Schickardstr. 32
71034 Böblingen

Frau Kerstin Thies
RICOH DEUTSCHLAND GmbH
Vahrenwalder Straße 315
30179 Hannover

Herr Hans van Heiningen
Océ-Technologies B. V.
P. O. Box 101
NL 5900 MA VENLO

Herr Dr. Michael Wensing
Fraunhofer Wilhelm-Klauditz-Institut (WKI)
Material Analysis and Indoor Chemistry
Bienroder Weg 54E
38108 Braunschweig

Herr Thomas von der Heyden
BGIA – Institut für Arbeitsschutz der
Deutschen Gesetzlichen Unfallversicherung
Alte Heerstraße 111
53757 Sankt Augustin

Herr Dr. Bernd Maciej
TÜV Rheinland LGA Products GmbH
TÜV Rheinland Group Tillystr. 2
90431 Nürnberg

Herr Martin Wesselmann (*)
Bau-Institut Hamburg-Harburg
Eißendorfer Str. 77
21073 Hamburg

Herr Manfred Santen
Greenpeace
Große Elbstrasse 39
22767 Hamburg

Frau Isabel Richter
Bitkom
Bundesverband Informationswirtschaft,
Telekommunikation und neue Medien e.V.
Albrechtstraße 10
10117 Berlin

Herr Dr. Jan Fiedler (*)
Umweltbundesamt
FG II 1.3
Corrensplatz 1
14195 Berlin

Herr Klaus Bandel
TÜV-Rheinland
Am Grauen Stein
51105 Köln
(*) not permanent

Herr Dr. Heinz-Jörn Moriske
Umweltbundesamt
FG II 1.3
Corrensplatz 1
14195 Berlin

Herr Dr. Jörn-Uwe Thurner
Umweltbundesamt
FG III 1.3
Umweltkennzeichnung, Umweltdeklaration,
Umweltfreundliche Beschaffung
Postfach 1406
D-06813 Dessau

Herr Dr. Olaf Wilke
BAM Bundesanstalt für Materialforschung
und –prüfung
FG 4.2
Unter den Eichen 87
12205 Berlin

Herr Dr. Stefan Seeger
BAM Bundesanstalt für Materialforschung
und –prüfung
FG 4.2
Unter den Eichen 87
12205 Berlin

Herr Dr. Mathias Barthel
BAM Bundesanstalt für Materialforschung
und –prüfung
FG 4.2
Unter den Eichen 87

Guests

Herr Dr. Oliver Jann
BAM Bundesanstalt für Materialforschung
und –prüfung
FG 4.2
Unter den Eichen 87
12205 Berlin

Frau Stefanie Protz
TÜV Rheinland LGA Products GmbH
TÜV Rheinland Group
Tillystraße 2
90431 Nürnberg

Herr Dr. Axel Hahn (*)
BfR Bundesinstitut für Risikobewertung
Thielallee 88-92
14195 Berlin

Herr Jens Küllmer
BMU
Robert-Schuman-Platz 3
D - 53175 Bonn

Meetings of the expert group

The expert group had three meetings at BAM, Berlin:
2009-02-27, 2010-02-17 and 2010-09-29

March 2012

Test Method

for the Determination of

Emissions from Hardcopy Devices

within the Award of the Blue Angel Ecolabel
for Office-Based Printing Devices according to
RAL-UZ-122 Annex S-M
Draft Version

Foreword

This test method has been adjusted for the implementation of the new requirements for the award criteria of the Blue Angel Ecolabel regarding the emission behaviour (VOC, ozone, gravimetrically measurable dust, fine and ultrafine particles) from hardcopy devices (printers, copiers and multifunction devices). It is based on the test method of June 2003 [1, 2], on the Standard ECMA-328 developed by ECMA International (European Association for Standardising Information and Communication System) (6th edition 2011, [3]) and the international standards ISO 16000-9 (draft) for emission test chambers [4] and DIN ISO 16000-6 for VOC analysis [5]. The ECMA 328 Standard will also be available as an ISO Standard (ISO/IEC 28360).

Consideration of these standards is an outright precondition for the application of the test method, provided they do not conflict with the test method.

The aim of the test method is the reliable determination of emission rates or emission amounts over a short continuous printing time, usually well below one hour, using a dynamic test chamber method at a specified air exchange rate.

Since the devices themselves may have a certain VOC emission which may decrease over time, the VOC emission rates must also be determined in the standby mode within the test procedure.

The emission rates determined must be regarded as system-specific emission rates, since printer, copier or multifunction devices only exhibit their specific emission behaviour in connection with the consumables used (e.g. toner, ink, paper).

The emission rates or emission amounts determined must not exceed the allowable limits specified in the award criteria of the ecolabel.

It is generally assumed that the devices do not print constantly as they are not designed for this, so it is appropriate to consider a utilisation factor <1. The indoor air concentrations calculated by modelling are in reality strongly influenced by adsorption effects on surfaces in the rooms, so that the actual concentrations in reality are lower than those calculated.

The revision of the test method was carried out within a project sponsored by the Federal Environment Agency (UBA) (project number 3708 95 301) at the BAM Federal Institute for Materials Research and Testing, with technical support from test institutes, manufacturers, UBA and associations. A detailed description can be found in the final report to be published by UBA (2011).

1 Definitions

Aerosol

System of solid or liquid particles suspended in gas.

Aerosol measurement device

For the purposes of this test method, a device for determining the time-dependent particle number concentration of an aerosol within a defined particle size range and with a certain time resolution.

Accumulated particle number concentration, $C_p(t)$ [cm^{-3}]

Time-dependent particle number concentration in a specified particle size range.

Load factor

Quotient of the volume of the test object and the volume of the empty emission test chamber

Standby phase

Experimental phase under normal climate conditions where the test object in the chamber is turned on and is waiting to start. The standby phase links directly to the conditioning phase without having to re-open the chamber. Explanation: At the beginning of the standby phase the test object is switched on. Thereafter the test object is operated with the default factory settings according to the specifications of the award criteria for RAL-UZ 122.

Blank value

Background concentration of the measuring system (emission test chamber, sampling tube and analyser) for individual substances and TVOC and FP/UFP

Printing phase

Examination of the test object during printing directly linked to the standby phase without opening the chamber. The printing phase begins when the first sheet starts printing and ends when the last sheet is printed.

Emission test chamber

Closed container with inlet and outlet and adjustable operating parameters (climate, air exchange rate) to determine the emissions (VOC, ozone, dust, fine and ultrafine particles) from test objects in an air flow (see also [4]).

Emission rate, SER_u [$\mu g h^{-1}$]

This quantity gives the mass of the analyte (VOC, ozone, dust), which is emitted from a test object per unit time.

Fine particles, FP

Particles having a particle diameter between 0.1 µm and 2.5 µm.

Averaged particle number concentration

Time dependent moving average of the measured particle number concentration formed over time intervals of 31 seconds.

Chamber loading

Placing a test object into the emission test chamber

Condensation Particle Counter, CPC

Instrument that measures the particle number concentration of an aerosol.

NOTE For the purpose of this standard a CPC is used as a standalone instrument which measures the total particle number concentration within a device dependent broad size range.

Conditioning phase

Experimental arrangement under normal climate conditions where the test object with pre-loaded paper is in the chamber for conditioning, the power switch is in the "on" position, but the power cord is not connected to the power supply. The reason for this is that, by inserting the plug into the socket, the device can be moved from this status into the standby phase without having to open the chamber.

Air exchange rate n [h^{-1}]

The ratio of the hourly net volume of air introduced into the emission test chamber to the free volume of the unloaded emission test chamber which is to be determined in identical units, expressed in air exchanges per hour.

Air flow rate [m^3h^{-1}]

Volumetric air flow rate supplied to the emission test chamber per unit time.

Air flow velocity v [ms^{-1}]

Air velocity over the surface of the test object (distance: ten millimetres).

Follow-up phase

Experimental arrangement in which the test object is still in the chamber with the same air exchange rate as in the printing phase, but printing has already been completed. The follow-up phase is directly linked to the printing phase without opening the chamber.

Normal climate

Standard climate conditions: 23°C ± 2 K, 50 ± 5 % relative humidity as per ISO 554 [6].

Ozone half-life

Time which elapses, starting from an initial ozone concentration, until the concentration has fallen to half its original value.

Particle

Small bodies suspended in air or gas having specified physical boundaries and consisting of liquid and/or solid substances

Particle emission rate, PER(t) [s^{-1}]

Time-dependant system-specific rate during the printing and follow-up phase

Particle size/particle diameter

Physical quantity to describe the physical dimension of a particle

Note: The term particle size is often used as a synonym for particle diameter. The term particle diameter is also used to classify particles in particle size classes.

Particle loss coefficient β [s^{-1}]

Coefficient for describing particle loss in the emission test chamber

Test object

Hardcopy device to be tested with consumables (toner or ink and paper)

Fast aerosol measuring instruments

Instruments with rapid time resolution and particle size classification.

Standard particle emission rate PER_{10} [particles / 10 min]

This quantity gives the number of emitted particles during a 10-minute printing phase. PER_{10} is calculated as the test result from the measured accumulated particle number concentration.

Dust

For the purposes of this investigation, the gravimetrically measurable particle fraction in an aerosol

Total Volatile Organic Compounds, TVOC

Total content of volatile organic compounds, i.e. the sum of the concentrations of identified and non-identified volatile organic compounds which elute from gas chromatographic separation on a nonpolar column between n-hexane and n-hexadecane, including these compounds

TP [-]

Number of emitted particles, TP is calculated as the test result from the measured accumulated particle number concentration based on the duration of particle emission.

Ultrafine particles, UFP

Particles having a particle diameter less than or equal to 0.1µm.

Volatile Organic Compounds, VOC

General: organic compounds that are emitted from the test object and are detected in the chamber air. For the purposes of this test method: identified and non-identified organic compounds which elute from gas chromatographic separation on a nonpolar column between n-hexane and n-hexadecane, including these compounds.

Very Volatile Organic Compounds, VVOC

For the purposes of this test method, identified and non-identified organic compounds which elute from gas chromatographic separation on a nonpolar column before n-hexane (e.g. ethanol, isopropanol, acetone, pentane).

2 Measuring instruments

- Emission test chamber in accordance with Section 4.1
- Instruments for climate measurement with recording capability in accordance with Section 4.4.1
- Colour mouse for determining the black value and the color values in accordance with Section 4.4.2
- Multimeter in accordance with Section 4.4.3
- Systems, adsorbents for air sampling in accordance with Sections 4.5 and 4.6
- Capillary gas chromatograph with thermodesorption unit coupled with a mass spectrometer with an evaluation unit (see example in Section 8.6)
- Ozone analyser in accordance with Section 4.7
- Dust measurement station in accordance with Section 4.8
- Aerosol instrument in accordance with Section 4.9

3 Test objects

3.1 Selection

The client is responsible for delivering the test object. In general, a production unit is delivered fresh from the current series or as a prototype. It is the manufacturer’s responsibility to ensure that the prototype does not differ from the subsequent series, and the maximum number of prints before the test as specified in 3.2 can be adhered to. The delivery contents, functionality and suitability of the test object to a test according to this test method will be checked by the test laboratory. The test object is then stored in its original packaging in a standard normal climate. The check should be made as soon as possible, but no later than ten working days after delivery.

3.2 Preparation of the test object

The control and monitoring of the test object and the printing process in the sealed test chamber is controlled from outside.

Power consumption in the standby phase and during printing, and print speeds (5 % area coverage, black and 20 % coverage, colour) are determined with the help of sample printouts of test pages with a time interval of at least one day before the test.

For this purpose a maximum of two 10-minute test cycles is permitted. The total number of prints (by the manufacturer, the testing laboratory or by others) prior to a test according to this test method is limited to a maximum of 1000 pages, an exceedance is only permitted to avoid possible technical problems. The preparation of the test object, including malfunctions that may occur and compliance with the criteria will be documented in the minutes.

The test object, filled with sufficient consumables, must be placed into the test chamber on the day before the test. It is important to ensure that the printed papers are arranged in an orderly way. Optionally, an additional collection container of inert material should be used.

In agreement with the manufacturer, a printing mode has to be selected for electro-photographic devices allowing a maximum printing time. The measured printing speeds as well as the capacity of paper trays and output trays must be taken into account. For inkjet printers, the default (normal printing) must be selected.

A device should be tested with a configuration that allows a 10-minute printing time. For devices which cannot achieve a printing time of 10 minutes due to design, the test will be carried out at the maximum possible printing time. When doing so, no less than 150 pages should be printed.

3.3 Consumables

<u>Toner and ink</u>

For each device, the toner or ink modules supplied by the manufacturer as original equipment or, similarly, the toner or ink in the device shall match the type as specified in the product documentation. The testing laboratory shall be informed of the exact name of the toner or ink modules so that a replacement can be acquired.

Toner or ink modules shall be stored according to the manufacturer’s instructions until the test. (After consultation with the manufacturer, they can also remain in the device.) The same conditions apply to storage as to the test object. Toner or ink should be provided in sufficient quantities.

Paper

Paper used for the investigations shall be in DIN A4 format with paper moisture content between 3.8 % and 5.6 %. The weight of the paper shall be within the range of 60 grams to 80 grams per square meter. The paper moisture content can be determined according to DIN EN 20287 (1994-06) [7].

Recommendation: By examining previous paper tests, (e.g. according to RAL-UZ 14) a contribution to VOC emissions by the paper can be estimated and possibly minimised by appropriate paper choice.

For reasons of test technology, the paper moisture content should not exceed 4 %. Higher paper moisture content can condense in the chamber during printing, thus necessitating the use of larger chambers or higher air exchange rates.

4 Measurement in the emission test chamber

4.1 General

Emission test chambers and their requirements are described in [1, 2, 3, 4]. Depending on the volume of the test object to be studied, a chamber with the appropriate volume shall be selected (see Equation 1). The volume of a test object is given by the smallest enclosing parallelepiped.

Test chambers shall have sufficient sealable bushings through the wall for passing power and control cables and allow aerosol measurements and the simultaneous sampling of VOC, dust, ozone and FP/UFP. The test chambers have to correspond to the requirements described in [4]. This means in particular:

- High-purity air supply (low VOC, ozone, dust, FP and UFP)
- High-purity water supply
- Chamber walls made of glass or stainless steel
- Extensive avoidance of sealing materials
- Effective air mixing

The following test conditions shall be observed in analogy to [4]:

Temperature	23 °C ± 2 K [1]
Relative humidity	50 % ± 5 % [1]

---

[1] Shortly after loading the chamber and during the printing phase, these air requirements generally will not be able to be maintained.

- Adjustable air exchange rate
  - Large chamber ($V > 5\ \text{m}^3$) $(1 \le n \le 2) \pm 5\ \%$
  - Small chamber ($V \le 5\ \text{m}^3$) $(1 \le n \le 5) \pm 5\ \%$
- Air flow rate $0.1 – 0.3\ \text{ms}^{-1}$

Both 1 m^3 chambers and chambers with volumes > 5 m^3 (e.g. 20 m^3) have been proved as suitable emission test chambers [2]. Chambers are to be regarded as suitable if, in addition to compliance with the above conditions, they have sufficiently low blank values for VOC, ozone and UFP/FP and dust and provide suitably long ozone half-lives.

Before the chambers are first used, and repeatedly thereafter, they shall be checked for compliance with the requirements.

The chamber blank values at an air exchange rate of $n = 1\ \text{h}^{-1}$ shall be less than the following values:

Individual substances	2	μgm^{-3}
TVOC	20	μgm^{-3}
Ozone	4	μgm^{-3}
Dust	10	μgm^{-3}
FP/UFP (accumulated particle number concentration)	2000	cm^{-3}

The lower detection limit of measuring instruments suitable for emission testing in accordance with Section 4.9 may be insufficient to check the chamber blank value for FP/UFP. Checking this chamber blank value requires appropriate instruments with a suitably low detection limit of particle number concentration. The ozone half-life of the chamber should be checked at an air exchange rate of $n = 1\ \text{h}^{-1}$. For this, a concentration of 0.1 to 0.2 ppm shall be ensured in the chamber. If the ozone half-life is at least ten minutes, then the test chamber is suitable for ozone determination. If the ozone half-life is less than ten minutes, the chamber shall be cleaned in an appropriate manner until the above target value is reached. At air exchange rates other than $n = 1\ \text{h}^{-1}$, different ozone half-lives also occur. The blank value for FP/UFP should be checked by a sufficiently sensitive instrument (usually a condensation particle counter, CPC).

The air exchange rates needed for the measurement shall be regularly checked and documented using an independent method, e.g. tracer gas method according to DIN EN 717-1 (2005) [8] in an unloaded state.

4.2 Test schedule (see also 8.1 Test schedule)

To determine the blank value and for the test in the standby phase, an air exchange rate of $n = 1\ \text{h}^{-1}$ should be adjusted in the chambers. The test object, filled with enough consumables, should be placed into the test chamber on the day before the test. The climate record begins with the start of the conditioning phase. The measurements of fine and ultrafine particles begin 5 to 10 minutes before the start of the standby phase. The VOC measurements begin 20 minutes before the end of the standby phase. The ozone concentration can be recorded.

In large chambers, the air exchange rate is adjusted to $n = 1 - 2\ h^{-1}$ at the end of the standby phase. In small chambers (up to 5 m³), an adjustment is made to a value of $n = 1 - 5\ h^{-1}$ (if necessary, dry air supply flow (< 10 % relative humidity)) to keep the relative humidity, which will increase as a result of water release from the paper during printing, below critical values (≤ 85 %).

There must be no condensation of water in the chamber as this would lead to an undue influence on the measurement results.

At the start of the printing phase, VOC, ozone and dust sampling should start. This continues to the end of the follow-up phase (VOCs only require one air exchange). The follow-up phase runs over a maximum period of four air exchanges (an hour at fourfold air exchange, and four hours at simple air exchange).

Testing in monochrome mode is carried out using the template in accordance with Section 8.3, for tests in the colour mode, the template in Section 8.4 is used.

The chamber size needed for the test object is selected based on the criterion for the load factor:

$$0.01 < \frac{V_{EUT}}{V_C} < 0.25 \qquad (1)$$

V_{EUT}: volume of the test object (EUT: equipment under test) [m³]

V_C: volume of the empty test chamber [m³]

If in doubt, the decision to use a smaller chamber shall be made, since the self-adjusting concentrations are greater and thus the uncertainty is reduced. During the test, only one test object may be in the chamber and neither the emission test chamber shall be opened, nor must people stay in it. When a fault (e.g. paper jam) occurs, the test shall be repeated. Such problems should be largely excluded through a careful preparation of the test.

4.3 Quality assurance measures

Quality assurance when applying the test procedure is a necessary prerequisite for obtaining reliable emission rates. The ECMA Standard 328 [3] and ISO/IEC 28360 give an overview of this.

The approved test institutes are required to regularly participate in comparative tests. The comparative tests are organised by BAM.

4.4 Climate, black and colour value determination, printer control

4.4.1 Climate

For the test cycle and evaluation of the measurement results, the climate data shall be recorded over the entire test procedure. For this purpose, a measuring system with an attached data logger is needed. After performing the calibration, as a minimum, the following measurement accuracies shall be ensured:

Temperature:	± 0.5 K
Relative humidity:	± 3.0 %

Section 8.5 shows an example of the climate profile during a test. For this example, the device Almemo 3290-8 from Ahlborn with a calibrated probe FH A 646-R and continuous data recording can be used.

4.4.2 Black and colour value determination

To prepare the emission tests for hardcopy devices, templates with 5 % coverage, black, and 20 % coverage (5 % per each colour [black, magenta, cyan, yellow]) shall be printed (see Section 8.3 [9] and 8.4).

The required printing templates are forwarded to recognised institutes by BAM.

The black value (L*) or the colour values (L*, a*, b*) are determined according to CIE [10] from a corresponding print-out for example using Colour Mouse CM2C (Savvy Systems Limited, USA).

The measured black value or colour values should be noted on the test report.

4.4.3 Control EUT

The printing process can be monitored and controlled according to the control capabilities specified by the manufacturer of the test object. In particular in standby and printing phases, the operating status of the printer should be continuously documented. This may for example be done by measuring the electrical current consumption of the test apparatus. For this, multimeters (e.g. multimeter M 3850 M, Metex Corporation, in the range of 20 A, with data logger for electronically gathering the measured values) are used.

Based on the current consumption as a function of time, the start and end of printing, as well as irregularities and disturbances in the operation can be seen. Section 8.5 shows an example of the current consumption demonstrating the operational conditions.

4.5 VOC

VOC sampling shall be carried out using Tenax TA followed by thermodesorption according to [5] and an analysis by GC/MSD. The test conditions shall be chosen so that individual substances with a concentration of ≥ 1.0 mg/m³ and that of benzene at a concentration of ≥ 0.25 mg/m³ can be detected.

Positive benzene findings in case of doubt shall be checked by a second independent sampling (e.g. using Carbotrap or activated carbon).

Sampling should be carried out at least at the following times:

a) blank value before chamber loading

b) twenty minutes before the one-hour standby phase (for twenty minutes at 100 to 200 ml/min) as a double determination

c) continuously from the beginning of the printing phase up to the time at which a simple air exchange is accomplished in the follow-up phase (at 100 to 200 ml/min) as a double determination

If possible, all substances should be identified and individually quantified by the relative response factors determined for the internal standard from the calibration. If substances are not identifiable or the relative response factors cannot be determined, the quantification is carried out assuming the response factor for toluene.

To specify the TVOC value, the sum of the concentrations of all identified and unidentified substances should be calculated whose retention times are between n-hexane and n-hexadecane and whose emission rates are above the following values.

For measurements in chambers ≤ 5 m³:

$SER_B \geq 0.005$ mg/h, $SER_{DN} \geq 0.05$ mg/h.

For measurements in chambers > 5 m³:

$SER_B \geq 0.02$ mg/h, $SER_{DN} \geq 0.2$ mg/h.

In addition, as described in [5], the TVOC value based on the response factor of toluene should be determined.

The concentrations to be used in the subsequent calculations should be determined by subtracting the corresponding blank values from the measured values.

Note: in particular the blind value of the Tenax pipe should be considered because it usually makes up a major part of the (total) blank value.

Calculating the emission rate during the standby phase

The emission rate during the standby phase can be approximately calculated by the following equation using the sample concentration in the last twenty minutes of the hour long phase:

$$SER_B = c_B \cdot n_B \cdot V_C \tag{2}$$

$$c_B = \frac{m_{VOC\,B}}{V_P} \tag{3}$$

c_B : VOC concentration [µgm^{-3}] during the standby phase
SER_B : VOC emission rate [µgh^{-1}] during the standby phase
$m_{VOC\,B}$: analysed VOC mass [µg] during the standby phase
n_B : air exchange [h^{-1}] during the standby phase
V_C : chamber volume [m³]
V_P : sample volume [m³] during the standby phase.

Calculating the emission rate during the printing phase

The emission rate during the printing phase is calculated by the following equation using the sample concentration from the start of the printing phase until the time when a simple air exchange has been accomplished in the follow-up phase:

$$SER_{DN} = \frac{\frac{m_{VOC\,DN}}{V_P} \cdot n_{DN}{}^{2} \cdot V_C \cdot t_G - SER_B \cdot n_{DN} \cdot t_G}{n_{DN} \cdot t_D - e^{-n_{DN} \cdot (t_G - t_D)} + e^{-n_{DN} \cdot t_G}} \tag{4}$$

SER_{DN} : VOC emission rate [µgh^{-1}] determined from the printing and follow-up phase
SER_B : VOC emission rate [µgh^{-1}] determined from the standby phase
$m_{VOC\,DN}$: analysed VOC mass [µg] during the printing and follow-up phase
n_{DN} : air exchange [h^{-1}] during the printing and follow-up phase
t_D : printing or copying time [h]
t_G : total sampling time [h]
V_C : chamber volume [m³]
V_P : sample volume [m³] during the printing and follow-up phase

The sampling and analysis methods described in Section 8.6 are suitable for a wide range of emittable compounds. A compilation of compounds which may occur in printer and copier emission tests can also be found in Section 8.6.

4.6 VVOC

VVOCs detected in the VOC sampling using Tenax should be quantified as VOCs and listed in the test report. The VVOCs should not be included in the TVOC value.

Any distortion of the test results by "breakthrough" shall be ensured against, especially in the presence of the volatile solvents of inkjet printer inks (according to information from the applicant or safety data sheet). For this, two Tenax pipes shall be arranged in series or the Carbotrap sampling carried out for benzene determination evaluated.

4.7 Ozone

The basis of this measurement method is preferably the flameless reaction of ozone with ethylene. The resultant chemiluminescence is measured photometrically. The ozone emission tests on printers and copiers should be carried out as follows:

a) Determination of the blank value
b) The ozone concentration can be recorded in the standby phase.
c) Ozone determination in printing / copying:

The ozone determination is performed from the beginning of the printing phase to the end of the follow-up phase. The concentration should be recorded at least every 30 seconds, preferably every 15 seconds. The ozone concentration should be recorded as a function of time in the appropriate concentration range.

The ozone production rate is determined from the increase in ozone concentration in the initial phase. Under these conditions, hardly any ozone loss by chemical reactions with air constituents and by discharge due to air exchange occurs. The emission during printing / copying under actual operating conditions also contributes to the increase in concentration.The relationship between mass and concentration is:

$$m = c \cdot V_c \tag{5}$$

m: ozone mass [mg]
c: ozone concentration [mg/m³]
V_c: test chamber volume [m³].

The emission rate is equal to the mass increase per unit time Δt:

$$\frac{\Delta m}{\Delta t} = \frac{\Delta c \cdot V_c}{\Delta t} \tag{6}$$

Δ*m:* generated ozone mass [mg]
Δ*c:* change of ozone concentration [mg/m³]
Δ*t:* time interval considered [min]

$$SER_u = \frac{\Delta c \cdot V_C \cdot p \cdot 60}{\Delta t \cdot T \cdot R} \tag{7}$$

SER_u: ozone emission rate [mg/h]
p: air pressure [Pa]
T: absolute temperature [K]
R: gas constant [PaK^{-1}], (for ozone: 339.8 [PaK^{-1}]).

To calculate the ozone emission rate, a time interval of two minutes should be used. The points used should be the measurement interval where the best-fit curve exhibits the greatest slope for the time interval ($c_2 - c_1$ = maximum).

Example of an ozone test instrument

Model 3010 ozone analyser (manufactured by UPM, Environmental Pollution Measurements). This device enables the continuous measurement of ozone concentration.

4.8 Dust

A gravimetric method is used to calculate the dust emission rate.

Sampling
Air sampling takes place from the beginning of the printing phase to the end of the follow-up phase. During this period, air is removed from the test chamber by a pump and drawn through a glass fibre filter. The volume of air drawn through the filter is measured (in m³). Differential weighing of the filter gives the absolute dust end weight in µg. From these two values, the dust concentration in the test chamber can be calculated (in µg m^{-3}), and from that, the specific emission rate (in µg h^{-1}).

Standard conditions of gravimetric dust measurement

Dust filter	Glass fibre filter with holder
Sampling location	Preferably centrally on the chamber wall
Sampling flow rate	Up to 80 % of the air flow rate in the chamber during the sampling phase
Sampling time:	Entire printing and follow-up time

Execution of the gravimetric dust measurement – climate correction

The glass fibre filters (test filters) used in gravimetric dust measurements shall be stored prior to measurement in an air conditioned room (weighing room) and conditioned to constant mass in the prevailing climate. Since even the smallest inevitable fluctuations in the relative humidity in the weighing room affect the weight of the glass fibre filter, at least one unloaded glass fibre filter (reference filter) is weighed at the same time as the test filter (tare) before dust sampling to minimise the influence of climate on the filter material by a climate correction.

Climate conditions in the weighing room

Temperature:	23°C ± 2 K
Relative humidity:	50 % ± 5 %

During dust sampling, air is drawn through the test filter. As the relative humidity of this air may differ from that in the weighing room, the test filter shall be conditioned again after dust sampling to a constant weight in the weighing room.

The reference filter is left in the weighing room constantly and re-weighed at the same time that the gross weight of the test filter (dust end weight) is determined. The mass difference determined between the first and second weighing of the reference filter is due to changing climate conditions and is subtracted from or added to the gross mass of the test filter.

Determining the absolute dust end weight of the test filter (climate correction)

$$m_{St} = (m_{MF\,brutto} - m_{MF\,tara}) + (m_{RF\,1} - m_{RF\,2}) \tag{8}$$

m_{St} : end weight of dust mass (climate corrected) [µg]
$m_{MF\,brutto}$: mass of the conditioned test filter after dust sampling [µg]
$m_{MF\,tara}$: mass of the conditioned test filter before dust sampling [µg]
$m_{RF\,1}$: mass of the conditioned reference filter simultaneously weighed with test filter before dust sampling [µg]

$m_{RF\,2}$: mass of the conditioned reference filter simultaneously weighed with test filter after dust sampling [μg]

Calculation of dust concentration and emission rate

$$SER_{u\,St} = \frac{m_{St} \cdot n \cdot V_C \cdot t_G}{V_P \cdot t_D} \tag{9}$$

$$c_{St} = \frac{m_{St}}{V_P} \tag{10}$$

c_{St} : dust concentration in the test chamber [μgm^{-3}]
$SER_{u\,St}$: dust emission rate [μgh^{-1}]
m_{St} : end weight of dust mass (climate corrected) [μg]
n: air exchange [h^{-1}]
t_D : pure printing or copying time [min]
t_G : total sampling time [min]
V_C : chamber volume [m^3]
V_P : volume of air drawn through the glass fibre filter [m^3]

Equipment example for a gravimetric dust measurement technique

Ultra-microbalance	Type UMX2/M	
Pump Müller	GSA 50	
Gas flow meter	Schlumberger	REMUS 4 G 1.6
Glass fibre filter	Schleicher & Schuell, diameter 50 mm	

4.9 Fine and ultrafine particles

The determination of the number of fine and ultrafine particles using an aerosol measuring instrument is performed in addition to the gravimetric determination of dust emission according to 4.8 and does not replace it

4.9.1 Requirements for an aerosol measuring instrument

The requirements defined here are intended as the minimum requirements. The aerosol measurement instrument shall be capable of recording the accumulated particle number concentration $C_p(t)$ within the size and concentration ranges defined below at the specified time resolution.

The preparedness of the aerosol measuring instrument shall be first confirmed in accordance with the requirements and criteria in Section 8.9.

Particle size range

The number of particles emitted shall be determined within the size range 7-300 nm which is considered the most relevant for electrophotographic devices. The detection efficiency for particles at the lower interval size limit as specified by the instrument manufacturer shall be at least 50 %.

Particle number concentration range

CPCs

The lower particle number concentration detection limit should be 1 cm^{-3} within the previously specified particle size range.

The upper particle number concentration detection limit should be at least 10^7 cm^{-3} in the previously specified particle size range. It may be necessary to use a calibrated aerosol dilution stage with a specified dilution factor.

Fast aerosol measuring instruments

The lower detection limit for particle number concentration should be a maximum of 5000 cm^{-3} in the size channel which is closest to the lower particle size detection limit of 7 nm.

The corresponding upper detection limit should be at least 10^6 cm^{-3} in the size channel which is closest to the upper particle size detection limit of 300 nm.

The above values are based on particle number concentrations normalised to the width of each particle size class ($dN/dlogD_P$) and a time resolution of 1 s.

Time resolution

The particle number concentration should be recorded at a frequency of at least 0.5 hertz.

Connection between the aerosol measuring instrument and emission test chamber

The hose connection between the sampling port of the emission test chamber and the aerosol measuring instrument should be made of an electrically conductive material (e.g. conductive silicone tube, stainless steel) and should not exceed a length of 3 m. Kinks and cross-section changes as well as sharp bends in the connection should be avoided. Ideally, the connection is rectilinear. The connecting hose should protrude at least 10 cm deep into the emission test chamber.

Quality assurance

The aerosol measuring instruments used shall have the following characteristics:

- device-side controlled flow rates
- automatic display of malfunctions during measurement
- export of measurement data for evaluation
- display of the individual device settings to be selected by the user
- ability to adjust or synchronise time and date
- measurement of electrometer noise level for fast aerosol measuring instruments
- a detailed description of cleaning and maintenance procedures shall be available

4.9.2 Performing the measurement

The concentration of fine and ultrafine particles should be recorded during standby, printing and follow-up phases in a storable data set.

When using CPCs the curve of the particle number concentration during and after the printing phase should be free of irregularities such as sudden step-like changes in $C_P(t)$. Any possible steps should not exceed a maximum acceptable level of 15,000 cm^{-3}. To avoid such interference, a calibrated aerosol dilution stage with a specified dilution factor (e.g. 1/1000) is recommended.

Note on step-like changes in the particle number concentration in CPCs: At low concentrations, the CPC operates in single count mode. With increasing particle number concentration, the measured signal is corrected. At high concentrations, the CPC will automatically switch to photometric mode. The concentration range in which the change occurs is typically between 10,000 and 50,000 cm^{-3}*. Depending on the correction algorithm used, the described irregularities may occur in this range.*[2]

When using fast aerosol measuring instruments, due to sudden fluctuations in the electrometer currents, very short peak-like irregularities may occur, which however, generally have only a negligible influence on the test result.

---

[2] Richard J.J. Gilham and Paul G. Quincey: Measurement and mitigation of response discontinuities of a widely used condensation particle counter, Journal of Aerosol Science, Volume 40, Issue 7, July 2009, pages 633-637.

Before further evaluation, the measured values should be checked using appropriate software (e.g. the instrument's software) with regard to malfunctions and irregularities which may occur.

The data set can be exported in an appropriate file format for further analysis.

4.9.3 Calculation of the test results

The number of emitted particles TP and the standard particle emission rate PER_{10} are calculated as the results of the test. For this purpose, auxiliary variables will be determined as described below. The basis of the calculation is the data set from the measured accumulated particle number concentration $C_P(t)$.

When a dilution step is used, $C_P(t)$ shall be corrected accordingly by the dilution factor. The corrected data set and/or file with the corrected values should be clearly labelled. The corrected data set in this case is the basis for the subsequent calculation.

$C_P(t)$ is shown in a graph as a function of time, which can optionally be attached to the protocol.

The evaluation requires the data set of the particle number concentration $C_P(t)$ to be smoothed. For this purpose, the method of moving average[3] over a time interval of 31 s is used. The smoothed data set and/or the file containing the smoothed values should be clearly labelled. In the evaluation steps described below, only the data set of the smoothed particle number concentration will be used.

Note:

Commonly used evaluation programs (e.g. EXCEL, ORIGIN, IGOR and others) provide functions for calculating the moving average.

Note on $C_p(t)$ as a function of time:

$C_p(t)$ may continuously decrease after the end of the printing phase. This behaviour characterises the end of the particulate emissions with the completion of the printing phase. Alternatively, $C_p(t)$ may continue to increase or remain constant for a short while after the end of the printing phase before the

---

[3] see z.B. *http://www.statistics4u.info/fundstat_germ/cc_moving_average.html*, H. Lohninger "Grundlagen der Statistik", electronic book

onset of a decrease. This behaviour characterises particulate emissions which continue for a while after the end of the printing phase. The evaluation steps described below are equally applicable to both versions.

Evaluation steps

1. The smoothed curve of the accumulated particle number concentration is plotted as a function of time, about 5 minutes before the printing phase, during the printing phase and at least for 30 minutes thereafter. The diagram is part of the protocol. Figure 4.9.1 shows an example which illustrates various markings used in the subsequent steps, as well as the measured course of the particle number concentration of $C_P(t)$.

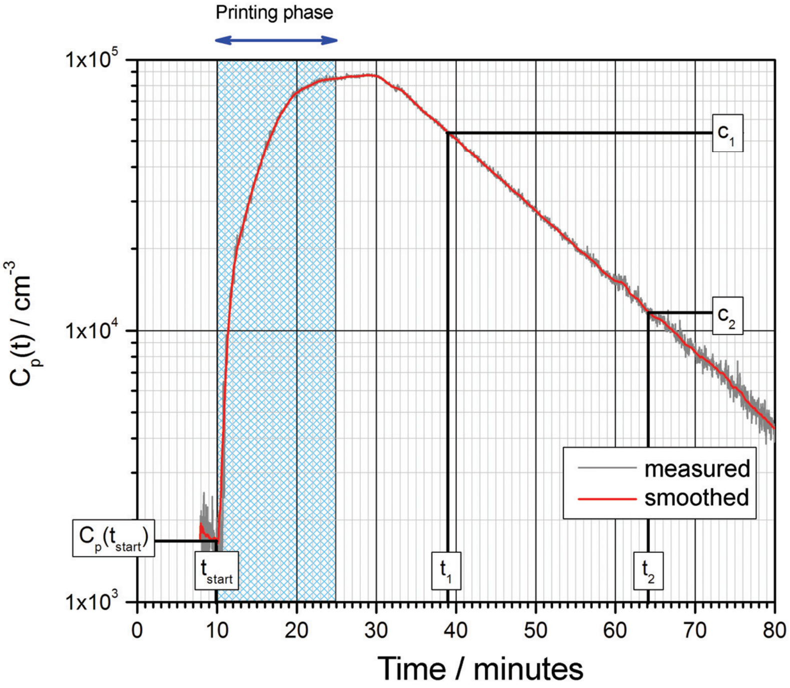

Figure 4.9.1: Particle number concentration as a function of time (example)

2. As indicated in Figure 4.9.1, the value pairs c_1, t_1 and c_2, t_2 should be read from the smoothed time-dependent curve of particle number concentration as accurately as possible or determined by means of a cursor. On a logarithmic scale, t_1 should be chosen within the linear descending range at least 5 minutes after the end of the printing phase and t_2 at least 25 minutes after t_1.

3. Calculation of particle loss coefficient β [s^{-1}]:

$$\beta = \frac{ln\left(\frac{c_1}{c_2}\right)}{t_2 - t_1} \qquad (11)$$

Note: Time difference $t_2 - t_1$ shall be calculated in the unit [s].

4. The values t_{start} and $C_p(t_{start})$ should be read from the smoothed time-dependent curve of particle number concentration (cf. Figure 4.9.1) as accurately as possible or determined by means of a cursor.

5. The time difference Δt between two successive data points of the particle number concentration $C_p(t)$ will be determined.

Note: Δt shall have the unit [s].

6. *PER(t)* [s^{-1}] will be calculated using Δt, β and the data set of the smoothed particle number concentration.

$$PER\ (t) = V_C \left(\frac{C_p(t) - C_p(t - \Delta t) exp\left(-\beta \cdot \Delta t\right)}{\Delta t\ exp\left(-\beta \cdot \Delta t\right)} \right) \qquad (12)$$

$C_p(t)$: smoothed curve of particle number concentration [cm^{-3}]
V_C: test chamber volume [cm^3]
Δt : time difference between two successive data points [s]
β : particle loss coefficient [s^{-1}]

Note: $C_p(t)$ is usually in the unit [cm^{-3}]. The chamber volume V_C shall be accordingly converted into the unit [cm^3]. Δt shall be substituted in the unit [s].

7. *PER(t)* and the smoothed $C_p(t)$ curve will be plotted according to the example in Figure 4.9.2. The diagram is part of the protocol.

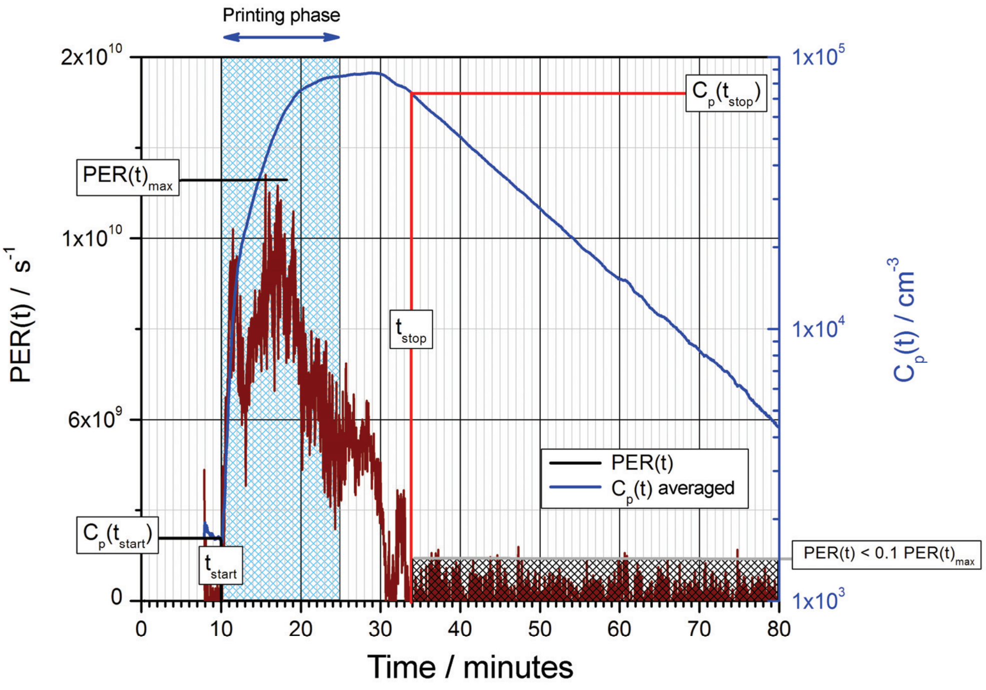

Figure 4.9.2: Plotting *PER(t)* and $C_p(t)$ (example).

8. The values t_{stop} and $C_p(t_{stop})$ shall be read from the diagram according to Figure 4.9.2 as accurately as possible or determined by means of a cursor. t_{stop} marks the point on the time axis from which *PER(t)* remains steady, i.e. at least over the next 10 minutes, below 10 % of the maximum of *PER(t)*.

Note: In some cases, the calculated emission rate PER(t) may assume negative values due to influences which cannot be considered in the calculations. Before and after the printing phase, the absolute values of the deviations of PER(t) should not exceed 5 % of the maximum value of PER(t) below the zero line.

9. The difference ΔC_p [cm^{-3}] between the times t_{start} and t_{stop} will be calculated from the data set of the smoothed particle number concentration:

$$\Delta C_p = C_p\left(t_{stop}\right) - C_p\left(t_{start}\right) \tag{13}$$

TP cannot be calculated for $\Delta C_p \leq 1000$ cm^{-3}. In this case, the measured value TP is called “non-quantifiable“ in the test report. The following calculation steps are then not needed.

10. The arithmetic average C_{av} [cm^{-3}] between the times t_{start} and t_{stop} will be calculated from the data set of the smoothed particle number concentration. The index *n* stands for the number of measured values between time points t_{start} and t_{stop}.

$$C_{av} = \frac{\sum_{i=1}^{n} C_{p,i}}{n} \tag{14}$$

11. TP will be calculated as follows:

$$TP = V_C \left(\frac{\Delta C_p}{t_{stop} - t_{start}} + \beta \cdot C_{av} \right) \left(t_{stop} - t_{start} \right) \tag{15}$$

ΔC_p : difference of $C_p(t)$ between t_{start} and t_{stop}, [cm^{-3}]
C_{av} : arithmetic average of $C_p(t)$ between t_{start} and t_{stop}, [cm^{-3}]
V_C: test chamber volume [cm^3]
β : particle loss coefficient [s^{-1}]
$t_{stop} - t_{start}$: emission time [s]

Note: ΔC_p and C_{av} have the unit [cm^{-3}]. β is defined in the unit [s^{-1}]. For the correct application of the formula, the chamber volume V_C shall be substituted in the unit [cm^3] and the emission time $t_{stop} - t_{start}$ in the unit [s].

12. The standard particle emission rate PER_{10} for a printing phase of 10 minutes (i.e. 600 seconds) is calculated from TP using the following formula:

$$PER_{10} = TP \cdot \frac{600}{t_{Druck}} \tag{16}$$

The length of the printing phase t_{print} shall be substituted in the unit [s].

5 Evaluation and test report

The full test and the complete evaluation for the test object shall be recorded in the test report. In particular, the following data should be included:

Data on the test laboratory:

- Name and full address
- Name of the responsible person

Data on the test object:

- precise product specification, indicate if desk-top or stand-alone device, device number, print or copy speed specified by manufacturer
- production date
- date of receipt
- type of packaging
- storage time before the test
- study date / period
- identification of consumables used (e.g. batch numbers, type specification, identification numbers)
- volume or external dimensions of the test object

Data on the test:

- study date / period
- black or colour values of prints
- experimental conditions (type and size of the chamber, temperature, relative humidity, air exchange and air flow rate)
- compliance with the condition of the load factor (see Formula 1)
- description of the aerosol measurement instrument used:
- manufacturer, type and serial number
- name and version of the software
- date of last calibration or maintenance
- currently used equipment settings
    - type and dilution factor if an aerosol dilution stage was used
    - result of measures to ensure the readiness of the aerosol measuring instrument according to Section 8.9
- start, end and duration of preparation, printing and follow-up phases
- printing speed during the test
- printing mode during the test (black/white, colour, one-sided or double-sided printing)
- the number of printed pages

- timing and duration of air sampling, volume and volumetric flow rate of air sampling for VOCs, ozone and dust
- VOC, ozone and dust sample identifications
- identification and location of the files with continuously recorded readings (climate, ozone, uncorrected and, if necessary, corrected particle number concentration)

Data on evaluation:

- Name, CAS-No. and concentration of identified VOCs, and concentration of non-identified VOCs in the standby phase and printing phase and calculated emission rates; benzene and styrene to be listed separately in any case
- details of the TVOC value as the sum of the quantified and non-identified compounds (relevant value for award basis), and, in addition, by calculation using the response factor for toluene
- specification of VVOCs if any
- ozone half-life of the empty chamber and from the follow-up phase
- ozone concentration and ozone emission rate calculated during printing
- gravimetrically determined dust mass and dust emission rate determined from it
- specification of detection and determination limits for VOCs, ozone and dust emission rates
- diagram according to Section 4.9.3, evaluation step 1
- diagram according to Section 4.9.3, evaluation step 7
- table of values for auxiliary variables determined in accordance with Section 4.9.3: t_1, t_2, c_1, c_2, β, t_{start}, $C_p(t_{start})$, t_{stop} and $C_p(t_{stop})$, ΔC_p and C_{av}
- test results TP and PER_{10}
- a report of any malfunctions and deviations from test algorithms
- summary of the results by the test institute in view of the ecolabel criteria (if necessary, an indication that the emission characteristics determined only apply in conjunction with the tested type of toner and paper)
- signature under the summary which shall again include the exact device identification

6 Testing institutes

The emission test may only be performed by suitable institutions.Testing laboratories are suitable if they have the necessary apparatus, equipment and a quality management system (or are accredited for the area of such tests) and have proved their competence to carry out the tests described in this Annex by a successful participation in relevant interlaboratory comparisons or comparative tests. The same applies to the manufacturer's testing laboratories.

Evidence of compliance with these requirements may be provided to BAM Federal Institute for Materials Research and Testing, Division "Environmental Material and Product Properties / Emissions from Materials". BAM will notify the institute concerned in writing whether it is considered suitable to perform emission tests.

7 Literature

1 Prüfverfahren für die Bestimmung von Emissionen aus Hardcopygeräten im Rahmen der Umweltzeichenvergabe für Bürogeräte nach RAL-UZ 62, 85 und 114 (A test method for the determination of emissions from hardcopy devices as part of ecolabel award for office devices according to RAL-UZ 62, 85 and 114). www.blauer-engel.de

2 Entwicklung einer Prüfmethode und Untersuchungen zur Begrenzung von Emissionen aus Druckern und Kopiergeräten im Rahmen der Umweltzeichenvergabe (Development of a test method for investigations on emission control from printers and copiers as part of the ecolabel award). UBA Text Series 71/2003, Federal Environment Agency, Berlin, 2003

3 ECMA-Standard 328 6th edition / 2011 Detection and measurement of chemical emissions from electronic equipment, (currently being revised), www.ecma-international.org

4 DIN ISO 16000-9: Bauprodukte - Bestimmung der Emission von flüchtigen organischen Verbindungen (VOC) - Teil 1: Emissionsprüfkammer-Verfahren (Building products - Determination of emissions of volatile organic compounds (VOCs) - Part 1: Emission test chamber method).

5 DIN ISO 16000-6: Innenraumluftverunreinigungen. Teil 6: Bestimmung von VOC in der Innenraumluft und in Prüfkammern. Probenahme auf TENAX TA, thermische Desorption und Gaschromatographie/MSD bzw. FID (Indoor air pollution. Part 6: Determination of VOCs in indoor air and in test chambers. Sampling on TENAX TA, thermodesorption and GC/MSD or FID).

6 ISO 554, Edition: 1976-07 Normalklimate für die Konditionierung und / oder Prüfung; Anforderungen (Standard climate for conditioning and / or testing; equirements).

7 DIN EN 20287, Edition: 1994-09 Papier und Pappe - Bestimmung des Feuchtegehaltes - Wärmeschrankverfahren (ISO 287:1985); Deutsche Fassung EN 20287: 1994 (Paper and cardboard - Determination of moisture content - oven method (ISO 287:1985); German version EN 20287: 1994).

8 DIN EN 717-1, Edition: 2005-01, Holzwerkstoffe - Bestimmung der Formaldehydabgabe - Teil 1: Formaldehydabgabe nach der Prüfkammer-Methode (Wooden materials - Determination of formaldehyde emission - Part 1: Formaldehyde emission according to the test chamber method).

9 DIN 33870, Edition: 2001-01 Informationstechnik - Büro- und Datentechnik - Anforderungen und Prüfungen für die Aufbereitung von gebrauchten Tonermodulen schwarz für elektrophotographische Drucker, Kopierer und Fernkopierer (Information technology - Office machines - Requirements and test methods for the recycling of used toner cartridges for black electro-photographic printers, copiers and fax machines).

10 CIE Document No 15, Colorimetry, 2004

<u>Further Reading</u>

J. Rockstroh, O. Jann, O. Wilke, W. Horn: Development of a reliable test method for laser printers, copiers and multifunctional devices in emission test chambers, Gefahrstoffe-Reinhaltung der Luft (Hazardous substances, air pollution control), (2005), 65, p. 71 – 80.

O. Jann, J. Rockstroh, O. Wilke: Influence of emissions from hardcopy devices to indoor air quality, Proceedings of Indoor Air 2005, Beijing, Vol.2, 2123 – 2128.

S. Seeger, O. Wilke, M. Bücker, O. Jann: Time- and size-resolved characterization of particle emissions from office machines with printing function, Healthy Buildings, (2006), 2, p. 447 – 450.

O. Wilke, O.Jann, D. Brödner, U. Schneider, C. Krocker, S. Kalus, S. Seeger, M. Bücker: Prüfung von Emissionen aus Bürogeräten während der Druckphase zur Weiterentwicklung des Umweltzeichens Blauer Engel für Laserdrucker und Multifunktionsgeräte unter besonderer Berücksichtigung der Sicherung guter Innenraumluftqualität (Emission testing from office devices during the printing phase for the development of the Blue Angel ecolabel for laser printers and multifunction devices, with special consideration of ensuring good indoor air quality), Research Report 204 95 373, UBA-FB 001159, (2008), UBA Text Series 35/08. (Only available as download from http://www.umweltbundesamt.de).

T. Schripp, M. Wensing, E. Uhde, T. Salthammer, C. He, L. Morawska: Evaluation of ultrafine particle emissions from laser printers using emission test chambers, Environ. Sci. Technol., (2008), 42, p. 4338 – 4343.

M. Wensing, T. Schripp, E. Uhde, T. Salthammer: Ultra-fine particles release from hardcopy devices: Sources, real-room measurements and efficiency of filter accessories, Sci. Total Environ., (2008), 407, p. 418 – 427.

8 Explanations and examples

8.1 Test Schedule

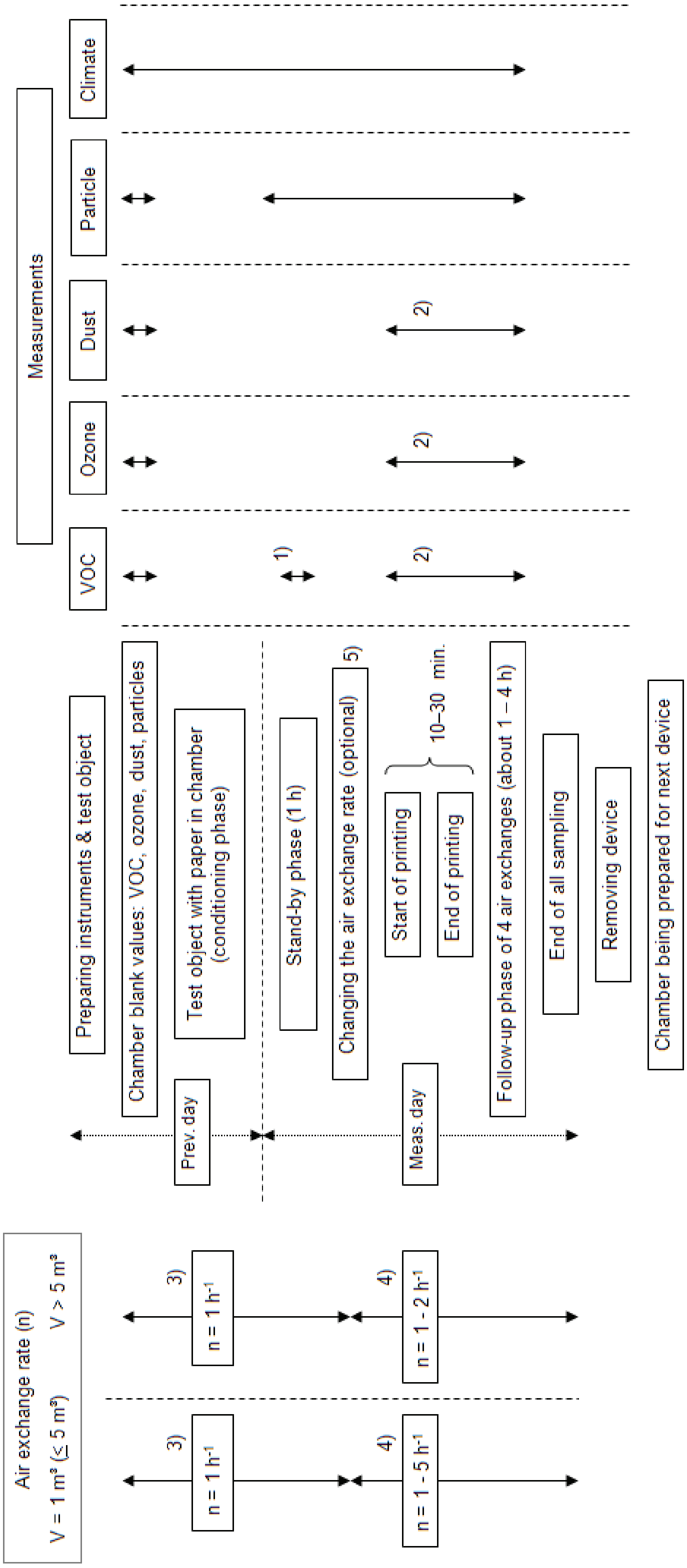

1) Sampling over last 20 minutes (100 – 200 ml/min)

2) Continuous sampling (for VOC 50 – 200 ml/min depending on sampling period)

3) Air exchange rate must be known and constant.

4) Air exchange rate depends on moisture input during printing (relative humidity of 85% must not be exceeded in the chamber); if necessary: add dry supply air (< 10 % RH), air exchange rate must be known and constant.

5) If the air exchange rate has been changed, printing must be delayed for at least one air exchange.

8.2 Setup for test devices

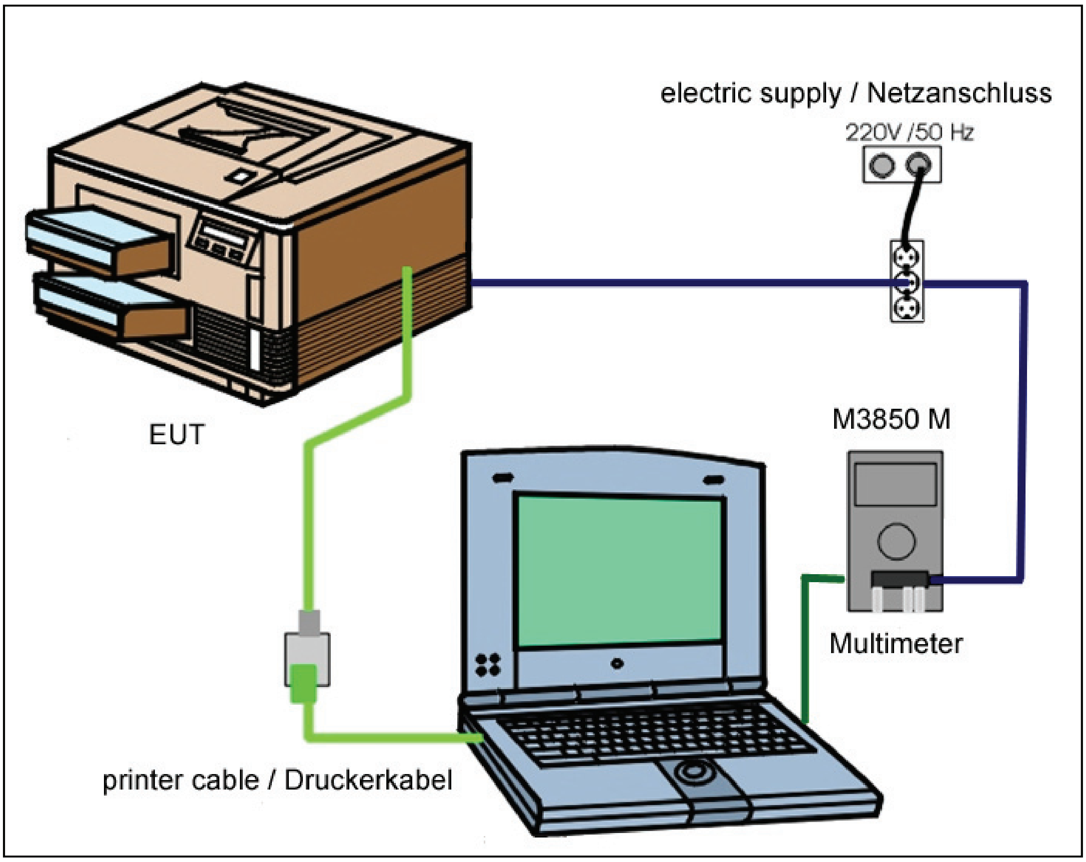

8.3 Template for 5 % coverage, black (see DIN 33870 [9])

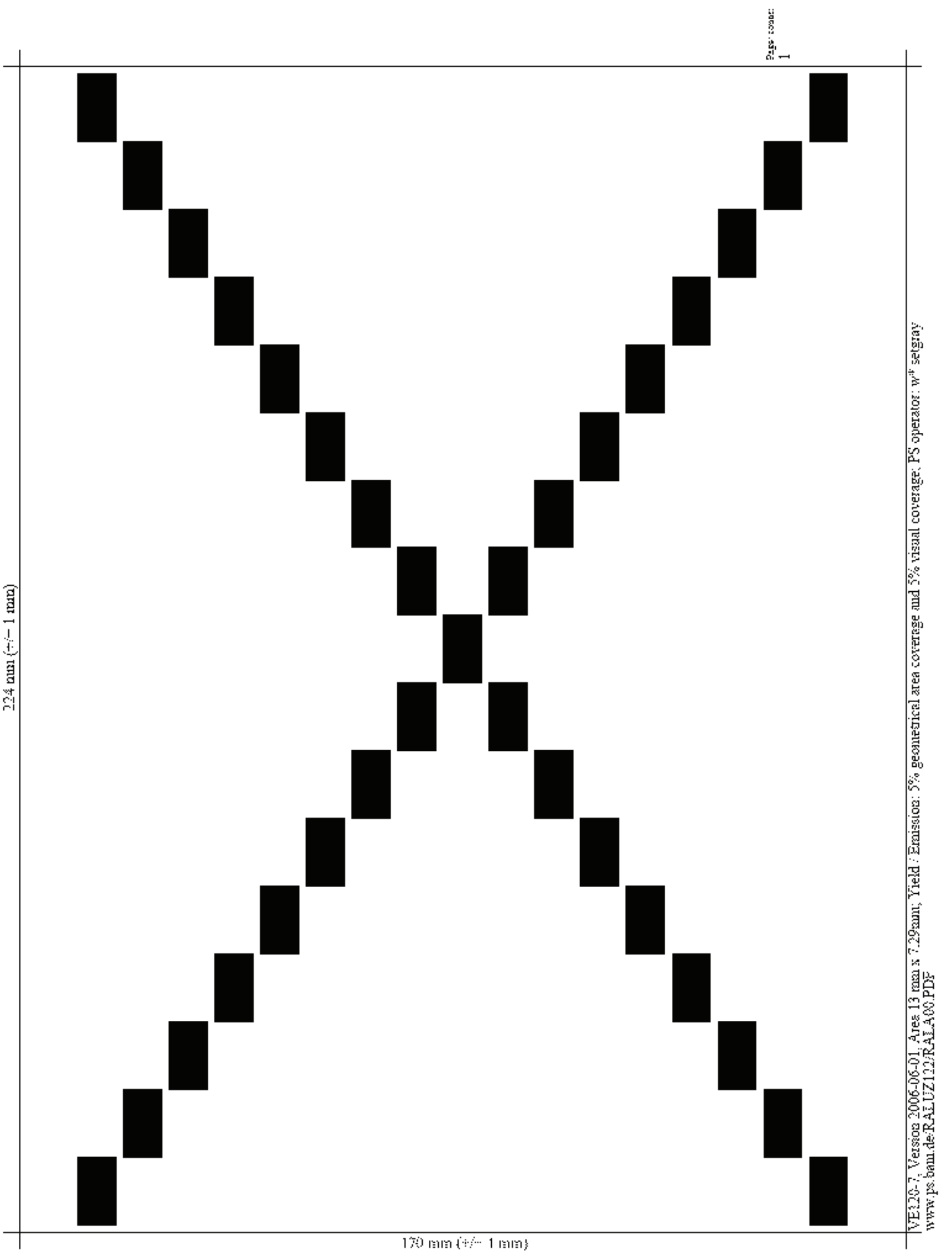

The template can be downloaded at http://www.ps.bam.de/RALUZ122.

8.4 Template for testing colour devices, 20 % coverage

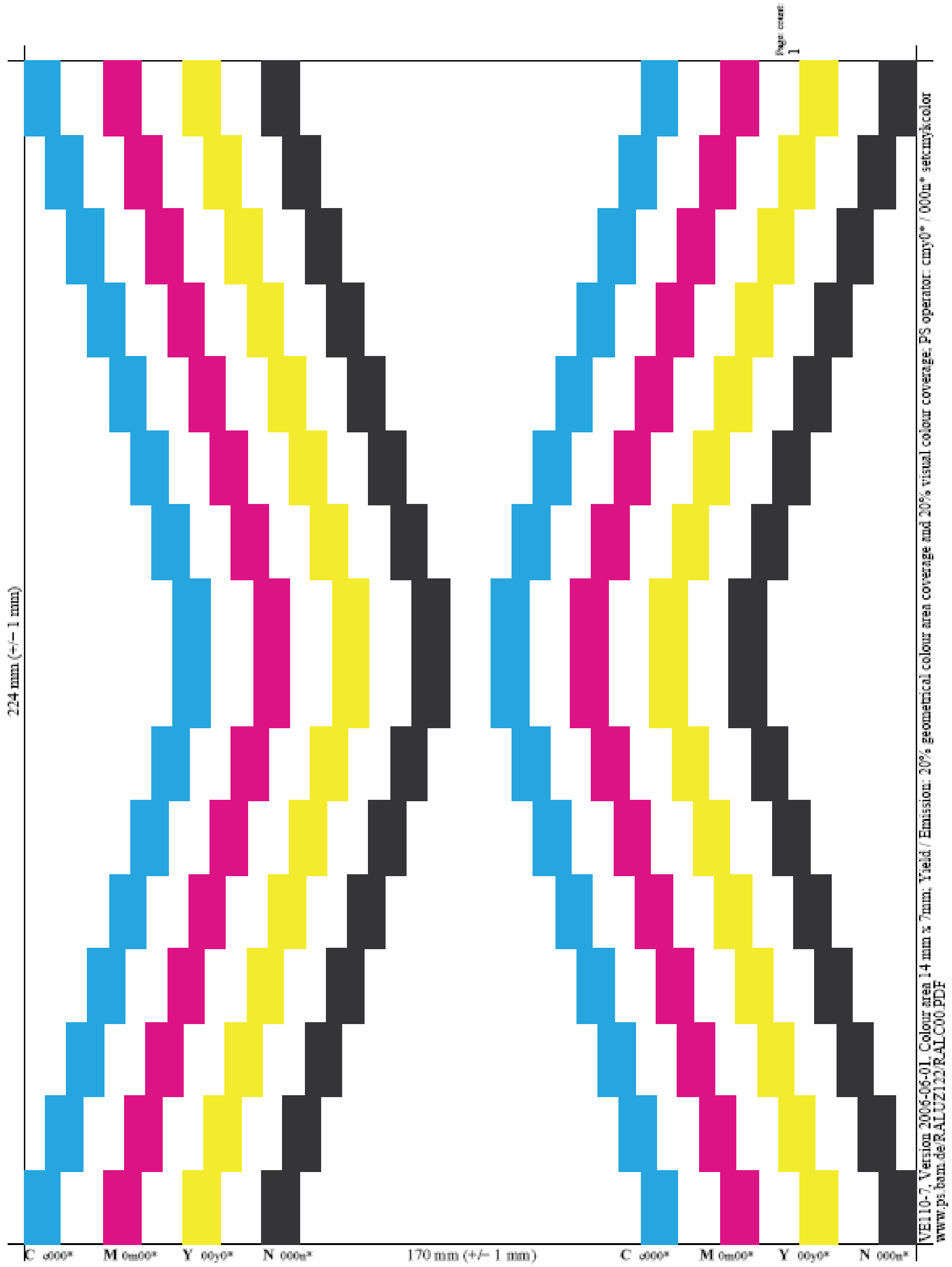

The template can be downloaded at http://www.ps.bam.de/RALUZ122.

8.5 Example for climate, current consumption and ozone concentration during a test

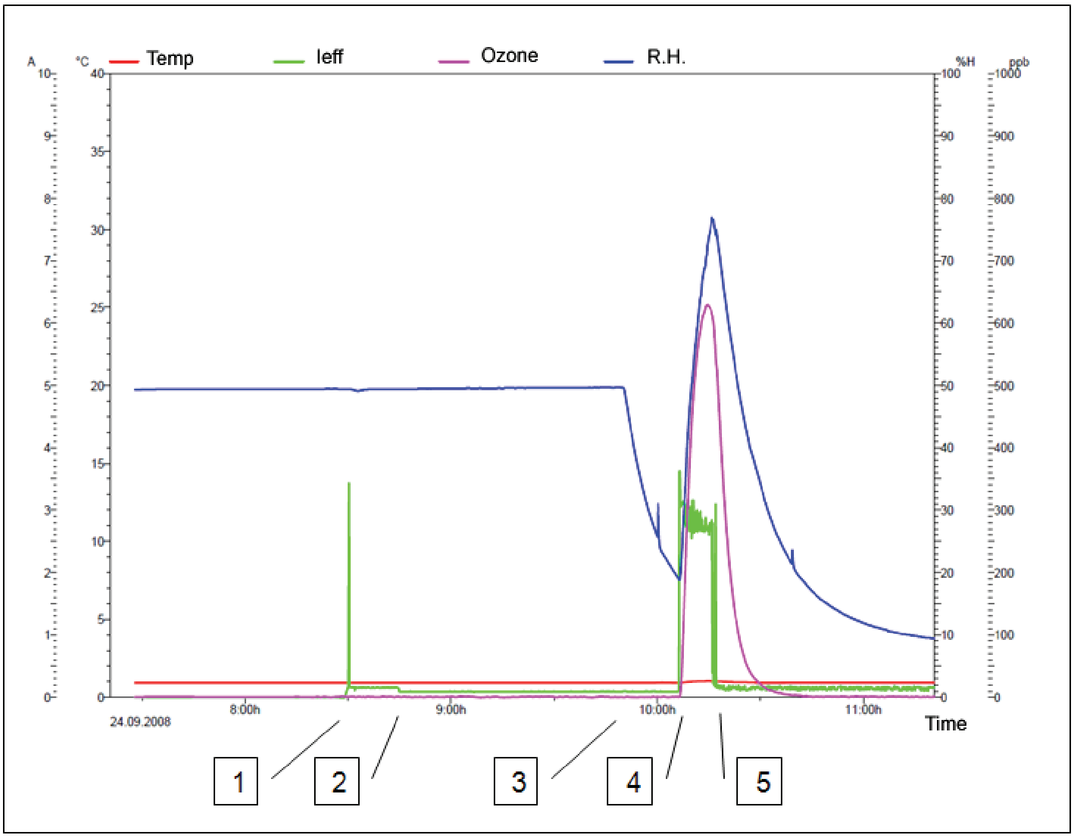

Loading on the previous day is not indicated!

1 Start of standby phase (8:30 hours)

2 Energy saving mode starts

3 Air exchange altered, reducing humidity

4 Printing phase starts

5 Printing phase ends, follow-up phase starts

8.6 Example of a proven VOC test method (cf. [2], [5])

Sampling tubes: Tenax TA (tube length 178 mm, OD 6 mm, 4 mm ID, 200 mg Tenax TA (60-80 mesh) with glass wool plugs); sampling volume > 1.0 l (100 ml/min). prior to sampling, the Tenax tubes have to be spiked with the internal standard dissolved in methanol.

The calibration is carried out by drawing (spiking) the calibration substances, dissolved in methanol, onto Tenax tubes, and rinsing it with a litre of synthetic air or nitrogen (purity 5.0) to simulate a sampling while the methanol which remained on the Tenax after spiking is desorbed.

Analysis system

Thermodesorption / Gerstel TDS 2 cold feeding system / KAS-3 (programme: 40 – 280 °C with 40 K min^{-1}, keeping at 280° C for 5 min / cryofocussing at -150 °C, heating at 10 K^{-1} to 290 °C / He flow 35 ml min^{-1})

HP 5890 II GC + HP 5972 MSD (HP 1 column; 60 m, 0.25 mm, 0.25 µm, temperature programme 40 °C for 4 min, 5 K min^{-1} to 140 °C, 10 K min^{-1} to 240 °C, 25 K min^{-1} to 290 °C, keeping for 3 min / MSD: scan 25-400: 1.9 scans / sec; 300 °C, NBS - 75K - database).

Selection of occurring compounds

Acetophenone
n-Alkanes (C10-C16)
Benzaldehyde
Benzene
BHT (2,6-di-tert.-butyl-4methylphenol)
Ethyl benzene
Ethyl hexanol
Unsaturated aldehydes (C6-C10)
n-Butanol
n-Propylbenzene
Phenol
Propylene glycol
Siloxanes (e.g. D3-D6)
Styrene
Toluene
Trimethyl benzenes
Xylenes

8.7 Ozone concentration during printing at a high concentration (data in ppm)

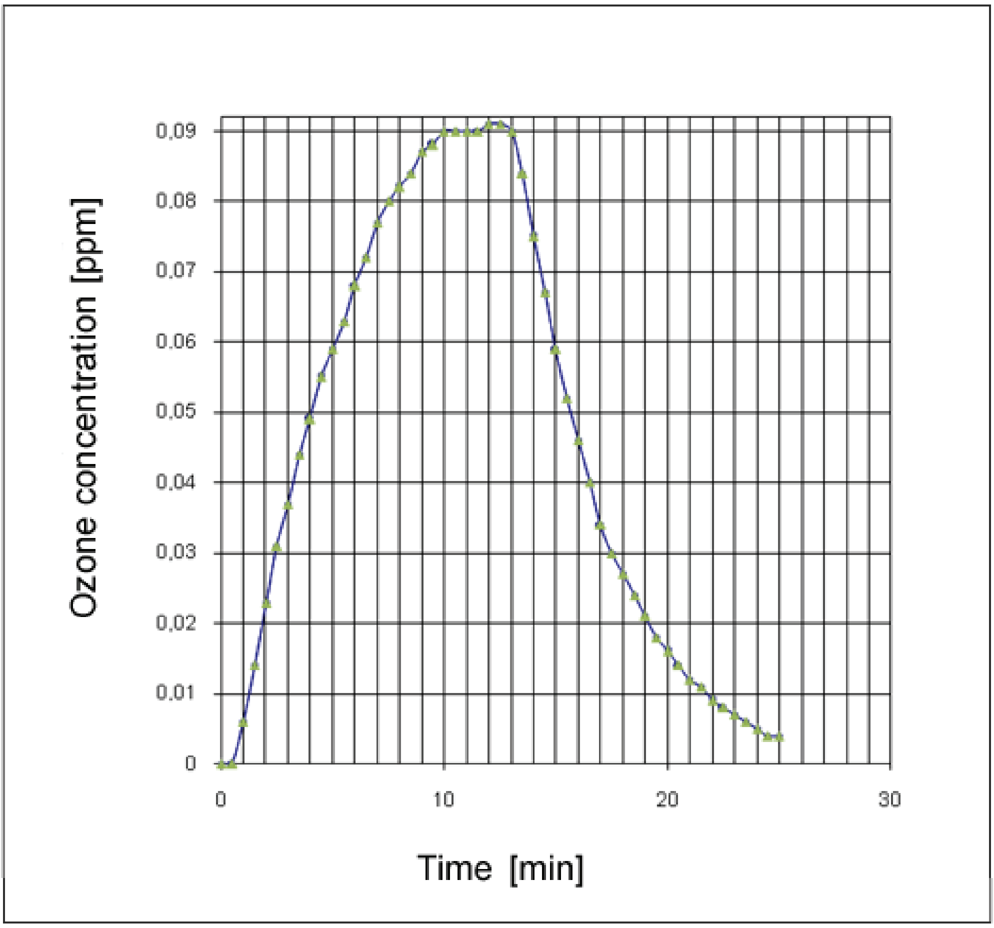

To calculate the emission rate, the ozone half-life is determined from the declining branch (after finishing the printing process) of the ozone concentration curve.

8.8 Technical information about aerosol measurement instruments

Comments on the particle size range and number concentration range

The lower detection limit of the particle size is the smallest particle diameter, where the counting efficiency of a specific aerosol measurement instrument is at 50 %.
The corresponding upper detection limit is the greatest particle diameter, where the counting efficiency of a specific aerosol measurement instrument is at 50 %.
The lower detection limit of the particle number concentration is the concentration which can be distinguished from the measured background concentration with a statistical probability of 95 % (due to the device-specific error-count rate). The error count rate is a count rate which is not caused by particles.

8.9 Measures to ensure the readiness of aerosol measurement instruments

This appendix describes the mandatory measures to ensure the readiness of aerosol measurement instruments. The measures described should be performed in addition to periodic maintenance.

8.9.1 Rapid aerosol measurement instruments

Setting up the instrument

1. The aerosol measurement instrument and the connecting hoses are checked for cleanliness.
2. The aerosol measurement instrument is placed so that the connection with the emission test has a maximum length of 3 m and is as straight as possible.
3. Time and date of the aerosol measurement instrument, software and laboratory clock are synchronised when the data provided differ by more than 1 second from each other.

8.9.1.1 Zero measurement

The zero measurement should be carried out at a maximum of one day (e.g. overnight) prior to the EUT test procedure. To ensure the stability of the aerosol measurement instrument, it should not be switched off between zero measurement and EUT test procedure.

1. A HEPA filter (filter efficiency ≥ 99.99 %) is connected to the aerosol inlet of the aerosol measurement instrument.
2. The aerosol measurement instrument is turned on and a warm-up period of at least 20 minutes is ensured.

3. All operating parameters (air temperature, voltage, and internal pressure and flow rates) are checked.
4. A reset (zeroing) according to the manufacturer's instructions will be carried out. Subsequently, whether the offset and RMS values are within the range specified by the manufacturer is checked.
5. The zero measurement is started with an attached HEPA filter in the particle number concentration mode with a time resolution of 1 s. The zero measurement has a minimum duration of 2 hours. The recorded spectra are checked for errors and artefacts.
6. The observed particle number concentration [dN] in each particle size channel shall not exceed the appropriate manufacturer's instructions for error-count rate by more than 500 cm-3. The spectra should be devoid of sudden changes in the particle concentration (e.g. increase/decrease of the concentration values by more than a factor of 2 within a period of 10 s).

8.9.1.2 Preparation for measurement

The following steps should be executed in sequence:

1. All operating parameters (air temperature, voltage, internal pressure and flow rates) are checked.
2. A reset (zeroing) is performed according to the manufacturer's instructions and ensured that the offset and RMS values of electric meter currents are within the manufacturer's specified range.
3. After another period of 30 minutes, step 2 is repeated and checked whether the obtained offset values of the electrometer current differs by no more than ± 10 fA.
4. The HEPA filter is removed from the aerosol inlet of the aerosol measurement instrument.
5. The sampling flow rate of the aerosol measurement instrument is checked. An internal flow meter should preferably be used for this. Otherwise, an externally calibrated flow meter shall be used. The measured flow rate of the aerosol measurement instrument shall not deviate by more than ± 10 % of the specified set point in the calibration certificate.
6. The aerosol measurement instrument is connected to the sampling port of the emission test chamber.
7. The particulate background concentration is measured in the emission test chamber. The background concentration shall not exceed the specified values under 4.1.

8.9.2 CPCs

For the measurement of total particle number concentration, only those CPCs are used which use isopropanol or butanol as a working fluid. The following steps should be performed before a measurement.

Preparation for measurement

1. The aerosol measurement instrument is turned on and the reservoir is filled with the appropriate operating fluid to a specified level (note the manufacturer's precautions regarding moving the filled CPCs).
2. If the CPC were dried for transportation or storage, the device will be restored to an operable condition in accordance with the manufacturer's instructions.
3. If necessary, the excess reservoir of the CPCs shall be emptied.
4. The warm-up phase of the CPC is maintained according to the manufacturer's instructions.
5. The sampling flow rate of the aerosol measurement instrument is checked. An internal flow meter should preferably be used for this. Otherwise, an externally calibrated flow meter shall be used. The measured flow rate of the aerosol measurement instrument shall not deviate by more than ± 10 % of the set point specified in the calibration certificate.
6. To check the operational readiness, the room/laboratory air is measured. The measured room air particle number concentration should be at least about 1000 cm-3. The values are usually higher. Other aerosol sources with sufficiently high particle number concentration can optionally be used for this test. A zero reading indicates a device fault.
7. Whether or not the particle number concentration is near the lower detection limit is checked if a HEPA filter (filter efficiency ≥ 99.99 %) is connected. If concentrations > 1 cm-3 are observed within a period of 1 min after any leaks between the HEPA filter and aerosol inlet were eliminated, there is a defect.
8. The CPC is connected to the sampling port of the emission test chamber via a conductive material (e.g. conductive silicone tube, stainless steel) with a maximum length of 3 m.
9. The particulate background concentration in the emission test chamber is measured. The background concentration shall not exceed the specified values under 4.1.